AD_____

GRANT NUMBER DAMD17-94-J-4427

TITLE: Effect of Estrogen on Progression of Human Proliferative
Breast Cancer Disease in a Xenograft Model

PRINCIPAL INVESTIGATOR: P.V. Malathy Shekhar, Ph.D.

CONTRACTING ORGANIZATION: Barbara Ann Karmanos Cancer Institute
Detroit, Michigan 48201

REPORT DATE: September 1997

TYPE OF REPORT: Annual

PREPARED FOR: Commander
U.S. Army Medical Research and Materiel Command
Fort Detrick, Frederick, Maryland 21702-5012

DISTRIBUTION STATEMENT: Approved for public release;
distribution unlimited

The views, opinions and/or findings contained in this report are
those of the author(s) and should not be construed as an official
Department of the Army position, policy or decision unless so
designated by other documentation.

19980226 018

[DTIC QUALITY INSPECTED 3

REPORT DOCUMENTATION PAGE

1. AGENCY USE ONLY (Leave blank)	2. REPORT DATE September 1997	3. REPORT TYPE AND DATES COVERED Annual (1 Aug 96 – 31 Jul 97)

4. TITLE AND SUBTITLE

Effect of Estrogen on Progression of Human Proliferative Breast Cancer Disease in a Xenograft Model

5. FUNDING NUMBERS

DAMD17-94-J-4427

6. AUTHOR(S)

P.V. Malathy Shekhar, Ph.D.

7. PERFORMING ORGANIZATION NAME(S) AND ADDRESS(ES)

Barbara Ann Karmanos Cancer Institute
Detroit, Michigan 48201

8. PERFORMING ORGANIZATION REPORT NUMBER

9. SPONSORING/MONITORING AGENCY NAME(S) AND ADDRESS(ES)

Commander
U.S. Army Medical Research and Materiel Command
Fort Detrick, Frederick, Maryland 21702-5012

10. SPONSORING/MONITORING AGENCY REPORT NUMBER

11. SUPPLEMENTARY NOTES

12a. DISTRIBUTION / AVAILABILITY STATEMENT

Approved for public release; distribution unlimited

12b. DISTRIBUTION CODE

13. ABSTRACT (Maximum 200

We have utilized the T24-Ha-ras transfected MCF10A xenograft model of early human breast cancer progression to a) determine whether the observed epidemiologic link between estrogen and increased risk of breast cancer indeed reflect a direct growth promoting effect of estradiol (E_2) on estrogen receptor positive (ER+) HBEC, and b) specify genetic and cellular changes that accompany (or characterize) the progression observed in successive transplant generations. The effects of E_2 on neoplastic progression of HBEC were evaluated by examining the effects of E_2 supplementation on progression of MCF10AneoT and its derivatives from the orthotopic site in ovariectomized female nude mice. Results indicate that E_2 supplementation enhances conversion of lesions from grades 0/1 (simple/moderate hyperplasia) to grades 3/4/5 (atypical hyperplasia/carcinoma in situ/invasive carcinoma), speeds the process of transformation, increases size of lesions, and promotes angiogenesis. Our data also indicate that alterations in expression of Bcl-2, cyclin D1, c-erbB-2 and pS2 are valid correlative markers for progression. Our data show the presence of at least two pathways of wild-type p53 functional inactivation in MCF10AT xenografts: one via a functionally inactive conformation and other via association of native wild type p53 with mdm-2.

14. SUBJECT TERMS

Breast Cancer

15. NUMBER OF PAGES

131

16. PRICE CODE

17. SECURITY CLASSIFICATION OF REPORT	18. SECURITY CLASSIFICATION OF THIS PAGE	19. SECURITY CLASSIFICATION OF ABSTRACT	20. LIMITATION OF ABSTRACT
Unclassified	Unclassified	Unclassified	Unlimited

FOREWORD

Opinions, interpretations, conclusions and recommendations are those of the author and are not necessarily endorsed by the U.S. Army.

_____ Where copyrighted material is quoted, permission has been obtained to use such material.

_____ Where material from documents designated for limited distribution is quoted, permission has been obtained to use the material.

_____ Citations of commercial organizations and trade names in this report do not constitute an official Department of Army endorsement or approval of the products or services of these organizations.

✓ In conducting research using animals, the investigator(s) adhered to the "Guide for the Care and Use of Laboratory Animals," prepared by the Committee on Care and Use of Laboratory Animals of the Institute of Laboratory Resources, National Research Council (NIH Publication No. 86-23, Revised 1985).

_____ For the protection of human subjects, the investigator(s) adhered to policies of applicable Federal Law 45 CFR 46.
✓

_____ In conducting research utilizing recombinant DNA technology, the investigator(s) adhered to current guidelines promulgated by the National Institutes of Health.

_____ In the conduct of research utilizing recombinant DNA, the investigator(s) adhered to the NIH Guidelines for Research Involving Recombinant DNA Molecules.

_____ In the conduct of research involving hazardous organisms, the investigator(s) adhered to the CDC-NIH Guide for Biosafety in Microbiological and Biomedical Laboratories.

_____   9/29/97
PI - Signature   Date

TABLE OF CONTENTS

PROGRESS REPORT OF WORK ACCOMPLISHED BY P.I. IN YEAR THREE AT KARMANOS CANCER INSTITUTE AND PLANS FOR YEAR FOUR

BACKGROUND

Strategies for breast cancer prevention require understanding of the molecular events leading to transformation or progression of human breast epithelial cells (HBEC). Although little is known about risk factors for breast cancer, much of the evidence suggests that a major determinant is total cumulative exposure to estrogen. We have utilized the T24-Ha-ras transfected MCF10A xenograft model of early human breast cancer progression to a) determine whether the observed epidemiologic link between estrogen and increased risk of breast cancer indeed reflect a direct growth promoting effect of estradiol (E_2) on estrogen receptor positive (ER+) HBEC, and b) specify genetic and cellular changes that accompany (or characterize) the progression observed in successive transplant generations.

We have previously shown that the activated endogenous estrogen receptor (ER) protein in T24-Ha-ras transfected MCF10A cells is functionally active based on its ability to mediate E_2-regulated increase of transcription from both exogenous (ERE-TKCAT), and endogenous E_2 regulated genes, progesterone receptor (1) and pS2 (2).

BODY OF THE REPORT

In year 2 of the study, we showed that although the p53 transcripts expressed in the MCF10AT xenografts are wild type, unlike in parental MCF10A cells, the p53 protein predominantly exists in a conformationally altered state that is defective in both binding to its response elements in the WAF1 promoter and in its ability to function as a transcription factor. To determine whether this loss of P53 function resulted from differences in structural modifications and/or cellular distribution, we examined the phosphorylation status of p53 protein by ^{32}P labeling studies and cellular distribution of P53 by confocal microscopy.

MCF10AT3B cells were chosen since they represented the most advanced serial xenograft passage of MCF10AT system cells, and previous studies have shown these cells to express significant amounts of conformationally altered P53 with very minimal ability to support P53-mediated transcription activating function.

Alteration in phosphorylation status of p53 in MCF10AT xenografts: Subconfluent cultures of parental MCF10A and MCF10AT3B cells plated in DMEM/F-12 supplemented medium were preincubated in phosphate deficient media for 4 h, following which the media were replaced with fresh phosphate-free media and 1 mCi of inorganic [32]P. Cells were labeled with the isotope for 1 h, washed in cold phosphate buffered saline and lysed on ice in 150 mM NaCl/ 10 mM Tris-HCl, pH 7.5/1% Triton X-100, containing vanadyl phosphate, inorganic pyrophosphate and a cocktail of protease inhibitors (PMSF, aprotonin, pepstatin and leupeptin). Cell lysates were clarified by centrifugation at 10,000 x g for 10 min, and aliquots of cell lysates containing equivalent number (10^7 cpm) of TCA precipitable radioactivity were used immediately for immunoprecipitation with two p53 monoclonal antibodies: pAb421, reactive to an epitope in C-terminus of P53 (3), and pAb240, reactive to an epitope that is commonly exposed in mutant P53 or in

conformationally altered (denatured) form of wild type P53 (4). The immunoprecipitates were pelleted by incubation with Protein G Sepharose, washed, and electrophoresed on 10% SDS-polyacrylamide gels. Following electrophoresis, the proteins were transferred on to Immobilon P membranes, and subjected to autoradiography.

Results: As shown in **Fig. 1A**, equivalent amounts of ^{32}P-labeled P53 were immunoprecipitated from parental MCF10A cells with both pAb240 or pAb421 antibodies. In contrast, no ^{32}P-labeled P53 was immunoprecipitated with pAb421 from MCF10AT3B cells, whereas ^{32}P-labeled P53 immunoprecipitated with pAb240 was associated with several high molecular weight phosphorylated proteins. That the absence of radiolabeled p53 with pAb421 in MCF10AT3B cells reflected the presence of unphosphorylated native P53 and not an experimental error was confirmed by probing the filter with pAb1801, a P53 antibody that recognizes an epitope in the NH$_2$ terminus of p53. **Fig. 1B** shows the presence of pAb421-reactive unphosphorylated P53 in MCF10AT3B cells. The absence of phosphorylated native P53 in MCF10AT xenografts may explain for loss of p53 function. Although phosphorylation at the C-terminus is not a prerequisite for conferring DNA binding capacity, it represents the most physiologically relevant mechanism by which the conformation of P53 may be altered to confer DNA binding activity. In fact, mutation of a C-terminal serine residue of murine p53 has been shown to eliminate its tumor suppressor function in mammalian cells, suggesting that phosphorylation of this residue is required for activation of P53 tumor suppressor activity (5). The unique association of several higher molecular weight proteins with the pAb240-reactive form of P53 from MCF10AT3B cells (and not parental MCF10A cells that has functionally active P53) suggest the presence of factors in the cellular milieu that may be responsible for stabilization of wild type P53 in a conformationally altered state that has a "mutant" immunological phenotype.

Interaction of MDM-2 with P53: In many tumor types, wild type p53 protein is functionally inactivated by mechanisms that include binding to the cellular MDM-2 oncoprotein (6). In order to determine whether P53 from parental MCF10A and MCF10AT xenografts existed as complex with MDM-2, we stripped the filters from Figs. 1A and 1B and incubated with anti-MDM-2 antibody. Interestingly, MDM-2 reactivity was observed only in a) MCF10AT3B cells and b) only in the lane that contained pAb421-reactive P53. No MDM-2 coprecipitated with P53 from parental MCF10A cells (Fig. 2). Similarly, although MCF10AT3B cells contained high levels of conformationally altered P53 (pAb240-reactive), this form of P53 does not appear to bind to MDM-2 (**Fig. 2**).

In summary, major differences in P53 function between parental MCF10A and MCF10AT xenografts appear to correlate with: 1) absence of phosphorylated native p53 in MCF10AT xenografts, 2) presence of high levels of conformationally altered P53 in MCF10AT xenografts, 3) specific interaction of conformationally altered P53 with high molecular weight proteins in MCF10AT xenografts, 4) interaction of native wild type P53 with MDM-2 possibly resulting in functional inactivation in MCF10AT xenografts. Our results also show that while MDM-2 associates with a subset of wild type P53 (probably the native form), it clearly does not form complexes with conformationally altered P53. At least two mechanisms may account for loss of P53 function in MCF10AT xenografts: a) predominant existence of P53 in a conformationally altered state and b) binding of native wild type P53 with MDM-2.

6

Cellular localization of P53 in MCF10AT xenografts. MCF10AT3B cells were plated on coverslips, and after 2-3 days of culture when the cells reached confluence, the slides were rinsed twice with phosphate buffered saline and fixed in methanol:acetone. Cells were preincubated with pAb421 or pAb240 following incubation in blocking solution (7). Coverslips were washed and incubated in fluorescein-conjugated goat anti-mouse IgG antibody. Coverslips were washed, mounted and viewed using a confocal microscope equipped with an Argon/Krypton laser model. Negative controls were incubated with normal mouse IgG substituted for pAb421 and pAb240. Results: Results from immunofluorescence microscopy confirmed the abundant presence of pAb240-reactive P53 in >95% of MCF10AT3B cells (Fig. 3B). Staining is often associated with large distinct aggregates in both the nuclear and cytoplasmic compartments. Similar accumulation of pAb240-reactive P53 has been reported in MCF-7 cells, suggesting a correlation between increasing accumulation of conformationally altered P53 and increasing potential for tumorigenicity (8). In contrast to pAb240 reactivity, pAb421 reactive protein is exclusively present in the nuclei of confluent MCF10AT3B cells; >90% of nuclei show punctate or granular staining (Fig, 3A). These results are in concurrence with those obtained from immunoprecipitation studies of P53 discussed above (Fig. 1), viz., that pAb421 reactive P53 in MCF10AT3B cells represents a subset of P53 (probably the native wild type in nuclear compartment), whereas the pAb240 reactive P53 represents a major pool of P53 that is associated with large distinct aggregates in cytoplasm and nuclear compartments.

Effect of estrogen on progression in early stages of breast cancer. In this study we sought to determine whether a relationship exists in vivo between estrogen exposure and morphological progression of preneoplastic lesions, and to define the step(s) in the morphological sequence at which estrogen may act. Previous studies have shown that MCF10AT cells grow in immunodeficient mice, where over a period of several months, they undergo a sequence of progressive histological changes mimicking those seen in breasts of women at high risk of breast cancer that culminate in a significant proportion of grafts with frankly invasive cancer (9). In the absence of estrogen supplementation, proliferative lesions develop but progress sporadically to high risk lesions within intervals ranging from 7-56 weeks (10). These data suggest that in hormonally unsupplemented animals, additional promotional events may be required for the eventual development of neoplasia.

The effect of estradiol on neoplastic progression of ER+ MCF10AT cells were examined in E_2-supplemented ovariectomized female nude mice. The following cells were used: ER+ MCF10AneoT, ER+ MCF10AT1 and a clone of MCF10AT3c (MCF10AT3c.cl4) that responded to estrogen stimulation with increased anchorage independent growth, i.e., increased colony forming efficiency and colony growth (**Fig. 4**). MCF10ANeoT and MCF10AT1 cells were chosen since they represent unpassaged and first transplant generation (first passage in vivo), respectively; as these cells have undergone none or minimal in vivo selection.
Method: 10^7 cells were suspended in Matrigel (Collaborative Research) and inoculated subcutaneously into the mammary fatpad region of ovariectomized nude mice that received sc implants of 1.7 mg/60 day release E_2 (13 mice each cell line) or placebo (control; 5 mice each cell line) pellets (Innovative Research). Animals were observed twice a week and palpated for

lesion formation once a week after 5 weeks of injection of MCF10AneoT, MCF10AT1 or MCF10AT3c.cl4 cells. Pellets were replaced at seven weeks, and all mice sacrificed at 10 weeks post injection by cervical dislocation. NIH guidelines for proper and humane use of animals were observed. Lesions were removed, weighed and portions of lesions were: fixed in neutral buffered formalin for paraffin embedding, frozen for cryostat sectioning, and digested with collagenase/hyaluronidase enzyme mixtures for recovery of cells for further in vitro analysis and preparation of stock cultures. Histological grading of lesions were done as described previously (10). These were done in collaboration with Dr. Daniel Visscher, Associate Professor, Department of Pathology, Wayne State University School of Medicine. The histological grades were, 0 = simple epithelium; 1 = mild hyperplasia; 2 = moderate hyperplasia; 3 = atypical hyperplasia; 4 = carcinoma in situ (CIS); 5 = invasive carcinoma. Each lesion was graded according to the most advanced (deviant from normal) morphological pattern.

Results from MCF10AT1 and MCF10AT3c.cl4 lesions were similar (**Fig. 5**). Histological analysis of lesions derived from estrogen-treated mice revealed that 92% of lesions displayed histological features of atypical hyperplasia (grade 3; 5/13), carcinoma in situ (grade 4; 5/13) and invasive carcinoma (grade 5; 2/13) whereas only 1/13 (8%) lesion exhibited features of moderate hyperplasia (grade 2). These lesions exhibited extensive areas of histologically papillary growth as opposed to cribriform as well as adenosis-like areas, often with noticeable eosinophilic intraluminal secretion. In contrast, 3 out of 5 MCF10AT1 lesions (60%) and 4 out of 5 MCF10AT3c.cl4 lesions (80%)) derived from control groups at 10 weeks exhibited features of grades 0/1 (simple epithelium/mild hyperplasia); one lesion exhibited features of atypical hyperplasia in both cases (20%), and remaining MCF10AT1 lesion had no epithelium (Fig. 5).

Results from MCF10AneoT lesions are shown in **Fig. 5**. While none of the 5 MCF10AneoT lesions from control group had epithelium, 75% of MCF10AneoT lesions from estrogen-exposed mice had progressed to invasive carcinoma at 10 weeks. Histologically, the lesions from MCF10AneoT group differed from those obtained from MCF10AT1 and MCF10AT3c.cl4 cells in that the MCF10AneoT lesions exhibited histological characteristics of squamous carcinoma unlike glandular type (adenocarcinoma) observed in MCF10AT1 and MCF10AT3c.cl4 lesions, although estrogen clearly advanced progression in all cases. Estrogen-exposed xenografts from all three cell lines differed from controls of our study and from previous studies (10) by virtue of demonstrating prominent host inflammatory infiltration and angiogenesis. These results suggest that estrogen exerts a growth promoting effect on benign or premalignant ducts by enhancing a) the frequency of lesion formation, b) size of lesions, c) the speed of transformation from grades 0/1 to grades 3 and higher, d) the degree of dysplasia, and e) the degree of angiogenesis. Estrogen-induced effects on lesion growth and progression are shown in **Figs.6-10** .

Immunohistochemical staining and correlation of specific breast cancer genes with lesion dysplasia: Results obtained for staining of bcl-2, cyclin D1, c-erbB-2 and pS2 from paraffin embedded sections of MCF10AT1 lesions recovered from estrogen-exposed mice are shown in **Figs. 11-15**. These markers were selected since their expression levels have been correlated to ER status of human breast cancer cell lines. Bcl-2 protein levels are downregulated in MCF-7

8

cells that are starved of estrogen, resulting in increased bax/bcl-2 ratio and induction of apoptosis. However, restimulation of estrogen-dependent MCF-7 cells with estrogen results in elevated expression of bcl-2 with a concomitant decrease in bax expression (11,12). Cyclin D1 has been recently shown to form functional complexes with ER in the absence of estrogen (13). This interaction results in transcriptional activation of ER-regulated genes. Cyclin D1/ER interaction is inhibited by antiestrogens, and this interaction is independent of cdk4/cdk6 (13). Expression of high levels of c-erbB-2 has been correlated with poor prognosis (14). Expression of pS2 was examined as it is an estrogen-regulated gene, the expression of which requires a functional ER (15).

Results: Bcl-2 staining was observed primarily in simple glandular regions and focally in nonatypical hyperplasia (**Fig. 11**), whereas c-erbB-2 protein is absent in simple glands but its expression is increased in higher grades of dysplasia, viz., hyperplasia with atypia, carcinoma in situ and invasive carcinoma (**Fig. 12**). Cyclin D1 protein expression is negative in all grades except in regions of lesions showing invasive carcinoma where intense nuclear staining of cyclin D1 was observed (**Figs.13 and 14**). pS2 staining was observed in simple and hyperplastic ducts (**Fig. 15**). Although statistical analysis of these data remains to be completed, the expression patterns of these breast cancer susceptibility markers indicate good molecular correlation with degree of dysplasia since within the same lesion, areas of simple, atypical and nonatypical hyperplasia, CIS and invasive carcinoma are seen. Thus, the specificity, reproducibility and significance of a particular gene product as a molecular correlate for breast cancer progression can be assessed with greater confidence in MCF10AT lesions as they exhibit considerable structural heterogeneity.

We have not been successful in obtaining staining for ER in these lesions. It is possible that since these lesions were derived from mice exposed to elevated levels of estradiol that ER may be downregulated. We have also been unable to demonstrate ER staining in tumors derived from estrogen-supplemented mice injected with MCF-7 cells. However, the ER in these lesions appear to be functionally active as very intense cytoplasmic staining of pS2 protein is observed in simple and hyperplastic ducts (Fig. 15). We are currently standardizing staining protocols for staining frozen sections for ER, pS2, PgR, P53 and MDM-2.

In vitro analysis of lesion-derived cells. Portions of lesions derived from MCF10AneoT, MCF10AT1 and MCF10AT3c.cl4 lesions were enzymatically digested with collagenase/hyaluronidase and placed in culture. Microscopic examination of the lesion digests revealed the presence of an abundance of ductular glands that are tightly wrapped with interstitial type IV collagen bundles (**Fig. 16**). Histological analysis of paraffin embedded organoids showed that these glands were hyperplastic with atypia (**Fig. 17**). After approximately 10 days in culture, majority of the ducts were freed from collagen bundles, attached to plastic dish, and started to grow as monolayers. Interestingly, although the cells derived from estrogen-treated lesions start as monolayers on plastic, they possess the ability to form ball like structures resembling cysts that are extremely proliferative (**Figs. 18 and 19**). Pinching off these structures from the basal monolayer results in it attaching to a new and empty spot on the dish and continuation of the

9

whole process (**Fig. 18**). During the formation of these proliferative cyst like structures, the cells reorganize, exhibit intense secretory activity (observed by the presence of secretory granules and vacuoles; **Fig. 18**), and express high levels of mucin and vimentin (data not shown). In contrast to cells derived from MCF10AT1 and MCF10AT3c.cl4 lesions of estrogen-treated mice, the control lesions contained very few ductular glands upon dissociation with the enzymes. Cells from these lesions grew as monolayers and failed to exhibit the characteristic features observed from lesions of estrogen-exposed mice. We have not been successful at propagating cells derived from lesions of MCF10AneoT cells. In vivo experiments with MCF10AneoT cells will be repeated to determine whether the progression of MCF10AneoT lesions to invasive squamous carcinoma in estrogen-supplemented mice is reproducible. Evaluation of molecular correlates with pathological grading of MCF10AneoT lesions may provide valuable information for the understanding of a small subset of patients who have squamous carcinoma of the breast.
In vitro growth and development of cyst-like structures are shown in Figs. **16-19**.

Three-dimensional growth in Matrigel-coated slides: Single cell suspensions were prepared by trypsinization of monolayers/cyst-like structures (derived from estrogen-exposed MCF10AT1 lesions) and 10^5 cells were plated on top of Matrigel-coated chamber slides. Matrigel was used to maintain consistency as it was also used for preparing cell suspensions for the in vivo assays. Cells were treated with 1 nM E_2, 1 nM E_2 plus 1 μM ICI 182,780 (pure antiestrogen), or 1 μM ICI 182,780 alone. Control cultures received only the vehicle (0.01% ethanol). Treatment with ICI 182,780 was done to determine whether the culture media contained estrogenic activity. Within 3 h of plating, microscopic examination showed the cells to polarize and reorganize. Within 12 h, the cells had completed organization into duct like structures in all cases: control, ICI alone and E_2-treated cultures. By 2 days of culture, differences between estrogen-treated and control cultures became more obvious. Estrogen-treated cultures exhibited pronounced tube thickening (several layers thick), formation of papillary bridges resembling those seen in human breast tumor specimens and formation of new ducts, whereas control cultures showed tubes that were only a few layers thick, with no papillary bridges or new ducts (**Fig. 20**). Inclusion of ICI 182,780 in cultures resulted in further thinning of the tubes indicating the presence of small amounts of estrogen in the culture media. Addition of ICI 182,780 to cultures containing E_2 caused inhibition of papillary bridge formation, formation of new ducts, and significant thinning of tubes (**Fig.20**).
Histological analysis of paraffin embedded sections of these ductular structures from Matrigel confirmed the above morphological analysis. It revealed the presence of multilayered ductal epithelia exhibiting characteristics of atypical hyperplasia in cultures exposed to E_2 (data not shown). These results are significant in that we are not only able to reproduce in vitro morphological and histological characteristics of atypia, an important transitional event in conversion to invasive carcinoma, but also because we can reduce in vitro the time required for development and progression of preneoplastic ducts from 10 weeks in vivo to ~5 days in vitro. It must be noted that similar three dimensional growth of tumorigenic MCF-7 cells in Matrigel produce balls of cells that do not differentiate or organize into ducts, and fail to form papillary bridges. We are currently optimizing procedures for better paraffin embedding of cells grown in Matrigel. Once these are standardized, we will stain these sections for the breast cancer

10

susceptibility markers as described above.

Time course of duct formation in vitro: Cells were plated as described above for Fig. , and at various times (6, 24, 48, 72, 96 and 120 h) the cultures were fixed in buffered formalin, paraffin embedded and sections analyzed for histology. Our preliminary data indicated increased growth and tube thickening within 24 h of estrogen treatment when compared to untreated control cultures. Estrogen treated cultures showed a steady increase in proliferative capacity throughout the culture period as evidenced by the presence of several mitotic nuclei. These data are preliminary and hence the figures are not shown.

Conclusions

1. From the studies carried out in year 3 using the MCF10AT xenograft model for progression of human proliferative breast disease, we conclude that E_2 increases the risk of breast cancer development by exerting a direct growth promoting effect on benign or premalignant ducts by enhancing a) the frequency of lesion formation, b) size of lesions, c) the speed of transformation from grades 0/1 to grades 3 and higher, d) the degree of dysplasia, and e) the degree of angiogenesis.
2. Expression patterns of bcl-2, cyclin D1 and c-erbB-2 show good correlation with the degree of ductal dysplasia, and concur with results obtained from human breast cancer specimens. These data strongly validate the utility of MCF10AT xenograft model for study of human breast disease..
3. There at least two pathways of P53 inactivation in MCF10AT xenografts: one via a functionally inactive altered conformation and other via association of native wild type P53 with mdm-2. Conformationally altered wild type P53 does not interact with mdm-2. Stabilized existence of P53 in a conformationally altered "mutant" immunological phenotype in MCF10AT xenografts appear to result from its interaction with several high molecular weight proteins present in the milieu of MCF10AT cells.

Future Plans for year 4.

1. We will characterize p53 protein isoforms in MCF10A/MCF10AT xenografts, and from cells derived from MCF10AT1/MCF10AT3c.cl4 lesions of estrogen-exposed mice. Isoforms of P53 radiolabeled with ^{35}S-methionine or ^{32}Pi immunoprecipitated with pAb421 or pAb240 from cytoplasmic and nuclear compartments of MCF10A/MCF10AT xenografts will be resolved by 2D-PAGE and differences in subcellular localization of one or more isoforms, phosphorylation status and interaction of specific isoforms with MDM-2 will be examined.
2. In vivo experiment will be repeated with MCF10AneoT cells with estrogen supplementation to determine if progression to invasive squamous carcinoma is reproducible. Lesions and cells derived from them will be analyzed for p53, ER, PgR, bcl-2, cyclin D1, c-erbB-2 and pS2 expression.
4. In vivo assay will be carried out with MCF10AT1 cells using estrogen pellets that will release

physiological concentrations of E_2 (100-200 pg/ml). Experiments will be done with tamoxifen administration to determine its effects on estrogen-induced progression of lesions. All lesions will be examined for histological grading and expression of breast cancer susceptibility markers. Cells will be expanded from these as before and used for analysis.

5. Cells derived from these lesions will also be plated for three dimensional growth in Matrigel coated plates, and evaluated for grading and expression of breast cancer markers.

Experiments will not be done with ER-negative MCF10AT xenografts as previously proposed as we have not been successful at cloning MCF10AT cells that are ER-negative.

REFERENCES

1. Expression of functional estrogen receptor in MCF10AT, a model for early human breast cancer. P.V.M. Shekhar, M.L.-Chen, J. Werdell, G.H. Heppner, F.R. Miller, and J.K. Christman. Manuscript submitted after revision.
2. Environmental estrogen stimulation of growth and estrogen receptor function in preneoplastic and human breast cancer cell lines. P.V.M. Shekhar, J. Werdell and V.S. Basrur. J. Natl Cancer Inst., In press.
3. Harlow E, Crawford LV, Pim DC and Williamson NM. Monoclonal antibodies specific for simian virus 40 tumor antigens. J. Virol 39;861-869, 1981.
4. Gannon JV, Greaves R, Iggo R and Lane DP. Activating mutations in p53 produce a common conformational effect: a monoclonal antibody specific for the mutant form. EMBO J. 9;1595-1608, 1990.
5. Milne DM, Palmer RH and Meek DW. Mutation of the casein kinase II phosphorylatin site abolishes the antiproliferative activity of p53. Nucleic Acids Res. 20:5565-5570, 1992.
6. Momand J, Zambetti Gp, Olson DC, George DL, and Levine AJ. The mdm2 oncogene product forms a complex with the p53 protein and inhibits p53-mediated transactivation. Cell 69:1237-1245, 1992.
7. Altered P53 conformation: A novel mechanism of wild-type p53 functional inactivation in a model for early human breast cancer. P.V.M. Shekhar, R. Welte, J.K. Christman, H. Wang and J. Werdell. Int. J. Oncol., In press.
8. Bartek J, Iggo R, Gannon J and Lane DP. Genetic and immunochemical analysis of mutant p53 in human breast cancer cell lines. Oncogene 5:893-899, 1990.
9. Miller, F.R., Soule H.D., Tait, L., Pauley R.J., Wolman S.R., Dawson, P.J., Heppner, G.H (1993). Xenograft model of human proliferative breast disease. J. Nat. Cancer Inst. 85:1725-1732.
10. Dawson PJ, Wolman SR, Tait L, Heppner GH and FR Miller. MCF10AT: A model for the evolution of cancer from proliferative breast disease. Am. J Pathol 148:313-319, 1996.
11. Huang Y, Ray S, Reed JC, Ibrado AM, Tand C, Nawabi A, and Bhalla K. Estrogen increases intracellular p26Bcl-2 to Bax ratios and inhibits taxol-induced apoptosis of human breast cancer cells. Breast Cancer Res Treat 42:73-81, 1997.
12. Visscher DW, Sarkar F, Tabaczka P and Crissman J. Clinicopathologic analysis of bcl-2 immunostaining in breast carcinoma. Mod Pathol 9:642-646, 1996.

13. Neuman E, Ladha MH, Lin N, Upton TM, Miller SJ, DiRenzo J, Pestell RG, Hinds PW, Dowdy SF, Brown SF and Ewen ME. Cyclin D1 stimulation of estrogen receptor transcriptional activity independent of cdk4. Mol Cell Biol 17:5338-5347, 1997.
14. Parkes HC Lillycrop K, Howell A and London UK. C-erbB2 mRNA expression in human breast tumors: comparison with c-erbB2 DNA amplification and correlation with prognosis. Br J Cancer 61:39-45, 1990.
15. Ioakim-Liossi A, Karakitsos P, Markopoulos C, Aroni K, Delivelioti K, Gogas J and Kyrkou K. Expression of pS2 protein and estrogen and progesterone receptor status in breast cancer. Acta Cytol 41:713-716, 1997.

WORK ACCOMPLISHED IN YEAR THREE BY CO-P.I. (SUBCONTRACT: UNIVERSITY OF NEBRASKA)

1. Genomic Instability:

We have continued our studies of genomic instability using frequency of spontaneous appearance of drug (PALA) resistant variants as a marker [1]. Analysis of three additional isolates, MCF10AT20, MCF10AT4CCC and MCF10AT4DDD from lesions with a phenotype of carcinoma (MCF10AT20 and MCF10AT4CCC) and hyperplasia (MCF10AT4DDD) indicated that all had a similar frequency of resistance to PALA at 9 X LD_{50}. When added to the previously submitted data, this strengthens the hypothesis that 'genomic instability' is <u>inversely</u> related to passage number through nude mice and unrelated to the phenotype of the lesion from which the lines are derived.

We are now trying to sift through the possible causes for a diminished ability of MCF10AT cells to generate PALA resistant colonies after serial xenograft passage. The three most likely possibilities are: 1) that some factor related to growth in the immune suppressed host provides a strong selective advantage to cells that maintain a near normal genotype; 2) that re-establishment of cells in culture provides a strong selective advantage to cells that maintain a near normal genotype or; 3) that there is no correlation between ability to develop drug resistance and the ability to form progressive xenograft lesion in this model of human breast proliferative disease.

The possibility that human breast epithelial cells with a normal genotype have a growth advantage in xenograft lesions is supported by published observations. First, it has already been reported that normal rat mammary epithelium is easily transplanted and grows well in athymic nude mice. However, both rat and human mammary cancers resist transplantation and grow poorly in athymic nude mice [2]. Second, the karyotype of MCF10AT cells appears to be extremely stable during the process of serial transplantation. MCF10AT cells carry an additional chromosome 9 [47xx,t(3;9),t(9;9;5),6p+,t(3;17),9+], a karyotype present in a minor population of MCF10A cells. This karyotype has not changed during serial transplantation and is present in all MCF10ATn lines that have been examined. Third, MCF10AT cells seem to have the characteristics of a stem cell line that gives rise to both myoepithelial and epithelial cells with "a wide range of differentiation potential"[3].

13

This pattern of growth does not change with passage. Even cells derived from fourth transplant generation lesion recapitulate a pattern of lesion growth that starts with simple ductular elements that develop focal areas of progression. In addition, all lesions, even those containing areas with the morphology of invasive carcinoma are slow growing and non-metastatic. Thus, it can be argued that the only cells in the lesions that maintain unlimited growth potential *in vivo* are stem cells with a minimally altered karyotype. This would be consistent with the observed loss of capacity for FPRC with serial passage but does not rule out an effect of *in vitro* selection.

The large variation in colony number observed when MCF10AT system cells are exposed to PALA at 3 and 6 x LD_{50} may provide a clue to the mechanism(s) involved. The initial outgrowth of resistant colonies at 6 x LD_{50} occurs with frequencies $> 10^{-5}$ in almost all of the MCF10AT lines, even some from the fourth transplant generation, yet none of the resistant colonies contains cells with a potential for unlimited growth. Analysis of CAD gene copy number in these cells indicated 5-9 fold amplification of CAD genes, much greater than that found in late passage MCF10A or MCF10AT cells (1.5-2 fold). Fig. 1 shows the actual levels of aspartyl transcarbamylase in these cells. The highest level, ~5 fold increase over control, was found in cells that have an initial outgrowth of resistant colonies with limited growth potential (MCF10AT4D). This suggests that all of the MCFAT derived lines have a relatively high frequency of cells with capacity for gene amplification linked to a commensurate increase in aspartate transcarbamylase but that these cells do not survive prolonged passage. It would appear that P53's role in mediating G1 arrest or inhibiting apoptosis is temporarily abrogated in these cells but can be reactivated, perhaps by accumulation of DNA damage during multiple rounds of DNA synthesis.

Work to be accomplished in year 4: During the coming year we will determine the nature of the amplification of the CAD gene in the initially resistant cells: i.e. whether they undergo the tandem array amplification of CAD DNA characteristic of cells with damaged chromosome 2 and/or loss of functional P53.

A manuscript describing this work is in the final stages of preparation.

2. Analysis of P53 in MCF10A and MCF10ATn cells by immunostaining.

We completed an extensive analysis of P53 protein both by FACS and immunostaining. FACS analysis was primarily aimed at determining whether any cell cycle dependence could be observed for accumulation of P53 in either conformationally altered or native form. Cells were sorted for propidium iodide binding and for binding of anti-P53 antibody 1801 (recognizes both native and conformationally altered P53) or 240 (recognizes conformationally altered P53). No cell cycle dependence was found for expression of either epitope. We also determined the effect of culture cycle on P53 expression. The distribution of P53 in nuclei and cytoplasm of MCF10A, MCF10AT and MCF10AT system cells was analyzed using pAb1801 and pAb240. Neither Ab detected nuclear P53 in subconfluent

14

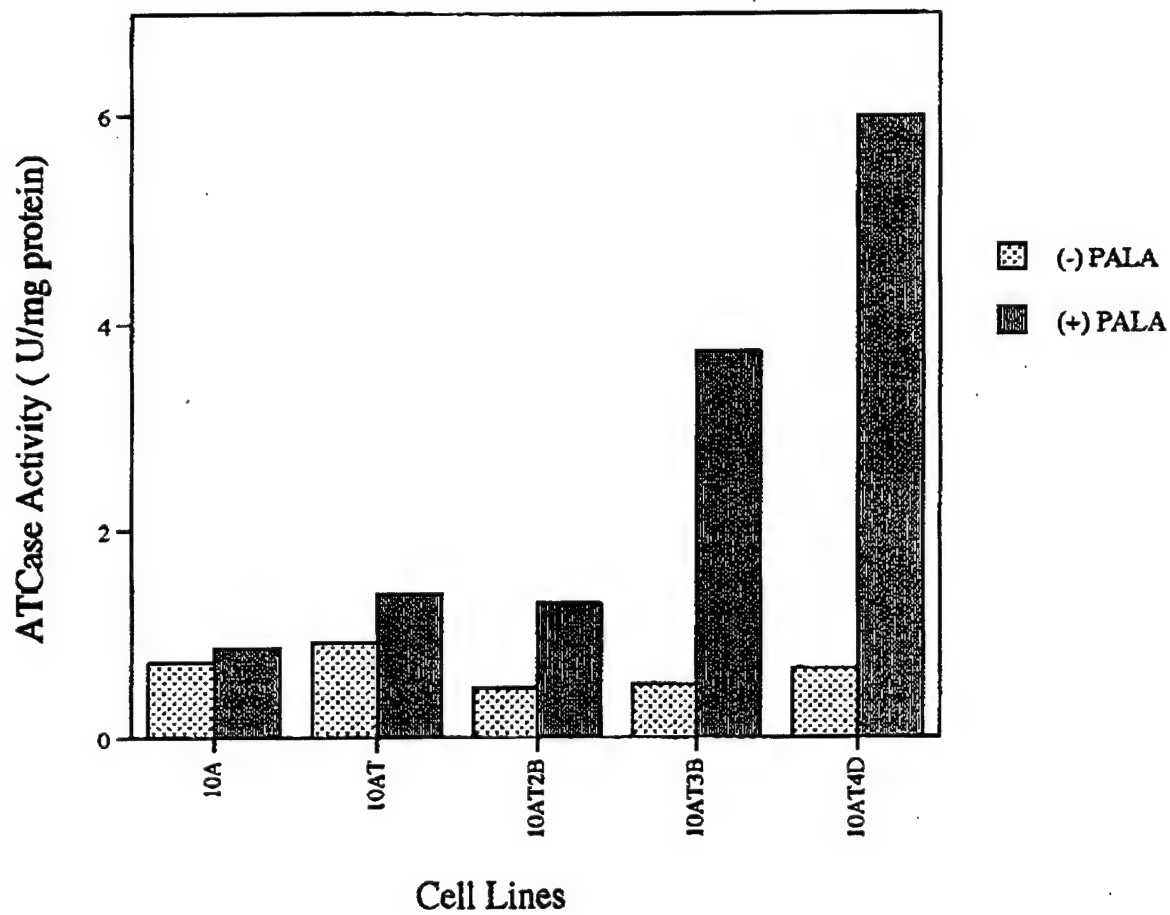# Aspartate transcarbamylase activity in different MCF10A cell lines

Figure 1A

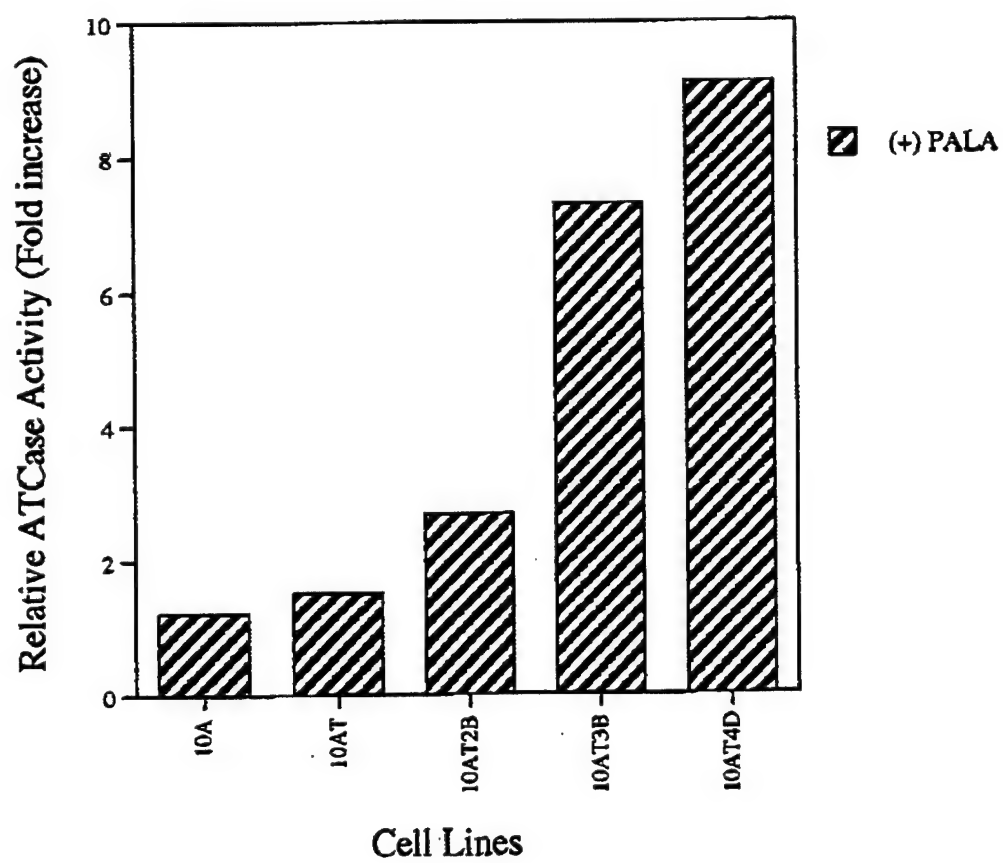Relative ATCase activity in PALA resistant MCF10A cell lines

Figure 1B

cultures of MCF10A or any of the MCF10AT lines. However, cytoplasmic or perinuclear staining was noted with both anti-P53 antibodies. MCF10A cells had barely detectable levels of cytoplasmic P53 reactive with mAb1801 but no P53 reactive with mAb240. MCF10AT cells also had low levels of cytoplasmic P53 reactive with pAb1801, but significant levels of protein reactive with pAb240. The distribution of P53 detected by these mAbs was quite different; faint and disperse cytoplasmic staining with pAb1801 and a mixture of uniform diffuse cytoplasmic staining and highly concentrated perinuclear staining with pAb240. MCF10AT3B and 3C cells had higher levels of cytoplasmic staining for P53 reactive with both Abs relative to MCF10A and MCF10AT cells. The pattern of cytoplasmic P53 staining was also more varied than in MCF10AT cells, with some P53 concentrated in distinct perinuclear structures. These structures were most evident in MCF-7 cells, suggesting a correlation between increasing accumulation of both conformationally altered and normal P53 in the cytoplasm of exponentially growing cells and increasing potential for tumorigenicity.

When grown to confluence, cells from all of the tested lines including MCF10A and MCF-7 displayed high levels of nuclear P53 in 20-40% of cells in addition to increased levels of cytoplasmic P53. The percentage of nuclei exhibiting uniform dark staining with both pAb240 and 1801 were similar in MCF10A and all MCF10AT system cells. The only major difference noted between cell lines was an increased occurrence of intense nuclear staining in a 'stippled' pattern with pAb240 in MCF10AT3 and AT4 cells relative to MCF10A and MCF10AT cells. The pattern of staining of confluent MCF-7 cells obtained with pAb240 in our assays is similar to that reported by Bartek et al[4], 5-15% of cells with intense staining of nuclear P53 reactive with pAb240 with most other cells having faint stippled nuclear staining. The cytoplasmic structures noted in subconfluent cells were no longer present. This may be a contributing factor to inactivation of P53 in exponentially growing MCF10AT derived cell lines, since our immunohistochemical studies indicate no abnormal accumulation of nuclear P53 but rather an increase in both native and conformationally altered P53 in cytoplasm.

SUMMARY:

Distribution of P53 in Confluent and Subconfluent MCF7 and MCF10AT cells							
Confluent				Subconfluent			
mAb	1801		240		1801		240	
Cell Type	N	P	N	P	N	P	N	P
MCF10A	++	-	+++	-	-	-	-	-
MCF10AT	++	-	+++	-	-	-	-	+*

Distribution of P53 in Confluent and Subconfluent MCF7 and MCF10AT cells							
MCF10AT1	++	-	+++	-	-	-	-	+*
MCF10AT3B	++	-	+++†	-	-	+	-	+*
MCF10ATC3	++	-	+++†	-	-	+	-	+**
MCF7	++	-	+++†	-	-	++	-	++**

N=nuclear; P=perinuclear *=surrounds nucleus **=accumulated on one side of nucleus; †=stippled.

<u>Work to be accomplished in year 4:</u> To compare distribution of conformationally altered and native P53 in areas of MCF10AT lesions at morphologically distinct stages of progression with those seen in cycling and stationary cell cultures from the lesions. These will be lesions from both estrogen supplemented and normal female hosts.

3. <u>Role of DNA Methylation Changes in ER expression:</u>

A complete analysis of methylation in the proximal promoter region and exon one has been completed using bisulfite sequencing. This is summarized in Figs. 2 and 3. Exon 1 is unmethylated in ER+ MCF7 cells and sporadically methylated in MCF10A cells. Methylation at the NotI site occurs in approximately 40% of DNA strands analyzed, approximately what would be predicted from the NotI digests reported previously. No significant methylation is noted in the proximal promoter region from either cell type. No significant change was observed in the exon 1 pattern of methylation in MCF10ATn lines. This would suggest that, unlike breast tumor cells [5], silencing of ER expression is not accompanied by extensive exon 1 methylation in the near normal MCF10A lines and that its reactivation does not depend on complete loss of methylation in exon 1. However, the possibility still exists that cells with the more methylated ER exon 1 are less active in expressing ER than those with less methylated exon 1. Thus, during the past year, we attempted to subclone a pure populations of ER+ and ER- MCF10AT3B cells by FACS sorting. This was to be accomplished by making MCF10AT3B transfectants stably expressing an ER-regulated green fluorescent protein (GFP) gene . Although we were able to get transient expression of GFP that was responsive to estrogen treatment, this property was lost with G418 selection making it impossible to carry out sorting.

<u>Work to be accomplished in year 4:</u> To determine whether 5-azaC treatment increases ER production in MCF10A3B cells as would be predicted if lower exon 1 methylation is associated with increased expression of ER in MCF10A3B cells. Exon 1 methylation will be examined in the treated cells to determine if it is altered. In addition, nuclear extracts from MCF10A, MCF10AT3B and 5-azaC treated MCF10AT3B cells will be examined for presence of transacting factors that interact with the ER promoter regions.

METHYLATION OF THE EXON I CpG ISLAND IN EXON I

                                                                       1   **2**

3051 TCAGATCCAA GGGAAC**G**AGC TGGAGCCCCT GAACCGTCCG
CAGCTCAAGA

                        3   **4**   **5**

3101 TCCCCCTGGA GCGGCCCCTG GGCGAGGTGT ACCTGGACAG
CAGCAAGCCC

        6   **7**   **8** **9**   **10**

3151 GCCGTGTACA ACTACCCCGA GGGCGCCGCC TACGAGTTCA
ACGCC**GCGGC**
  11   **12,13**

       14 **15**   **16 17**   **18**   **19**

3201 *CGC*CGCCAAC GCGCAGGTCT ACGGTCAGAC CGGCCTCCCC
TACGGCCCCG
  20   **21**

                          22 **23** **24**   **25**

3251 GGTCTGAGGC TGCGGCGTTC GGCTCCAACG GCCTGGGGGG

MCF-7   No methylation over region 7-20 (4 clones).   Three have single 5meC at sites 6 or 21.

MCF 10A   Four of 9 clones with methylation over region 7-20 including Not I site (Italics).
       Four clones with no methylation over region.
       One clone with single 5meC at site 1.

MCF10AT   Seven of 9 clones with methylation over region 7-20 including 4 at Not I site.
       Two with no methylation over region.

METHYLATION OF THE CpG ISLAND IN THE PROXIMAL ER PROMOTER

                                                                                1

2651   CTGGAGTGAT GTTTAAGCCA ATGTCAGGGC AAGGCAACAG TCCCTGGCCG

                                                                       2

2701   TCCTCCAGCA CCTTTGTAAT GCATATGAGC TCGGGAGACC AGTACTTAAA

```
              3                    4         5   6
2751   GTTGGAGGCC CGGGAGCCCA GGAGCTGGCG GAGGGCGTTC GTCCTGGGAC


              7  8    9   10        11     12         13
2801   TGCACTTGCT CCCGTCGGGT CGCCCGGCTT CACCGGACCC GCAGGCTCCC


              14        15,16   17,18        19   20
2851   GGGGCAGGGC CGGGGCCAGA GCTCGCGTGT CGGCGGGACA TGCGCTGCGT


       21        22                        23  24
2901   CGCCTCTAAC CTCGGGCTGT GCTCTTTTTC CAGGTGGCCC GCCGGTTTCT


                 26        27             28 29    30
2951   GAGCCTTCTG CCCTGCGGGG ACACGGTCTG CACCCTGCCC GCGGCCACGG
```

MCF-7   No methylation over region (3 clones)

MCF-10A   No methylation over region (5 clones, 2 with
    individual methyl group at 10 or 11)

MCF-10ANeoT No methylation over region (4 clones)

  TGs:2b Methylation at 2,18 (1 clone)
      3c No methylation over region (2 clones)
   Methylation at 4-6 and 8-22 (1 clone).

REFERENCES

1. **Tlsty, T.D.,** Normal diploid human and rodent cells lack a detectable frequency of gene amplification, *Proc. Natl. Acad. Sci. USA*, 87, 3132, 1990.
2. **Welsch, C.W., O'Connor, D.H., Aylsworth, C.F. and Sheffield, L.G.,** Normal but not carcinomatous primary rat mammary epithelium: readily transplanted to and maintained in the athymic nude mouse, *J. Natl. Cancer Inst.*, 78, 557, 1987.
3. **Miller, F.R.,** Models of progression spanning preneoplasia and metastasis: The human MCF10AneoT.TGn series and a panel of mouse mammary tumor subpopulations., in *MAMMARY TUMOR CELL CYCLE, DIFFERENTIATION AND METASTASIS*, Dickson, R. and Lippman, M., Eds., Kluwer Academic Publishers, 1996, 243.
4. **Bartek, J., Iggo, R., Gannon, J. and Lane, D.P.,** Genetic and immunochemical analysis of mutant p53 in human breast cancer cell lines, *Oncogene*, 5, 893, 1990.
5. **Ottaviano, Y.L., Issa, J.P., Parl, F.F., Smith, H.S., Baylin, S.B. and Davidson, N.E.,** Methylation of the estrogen receptor gene CpG island marks loss of estrogen receptor expression in human breast cancer cells, *Cancer Res.*, 54, 2552, 1994.
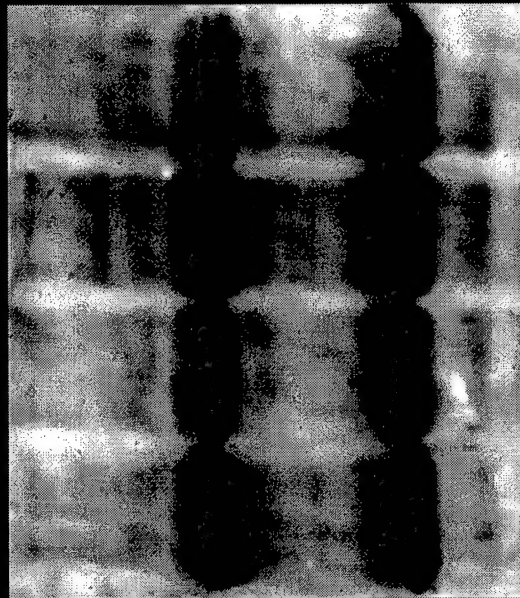
P53 PROTEIN-ASSOCIATED MDM2 IN MCF10A/MCF10AT SYSTEM CELLS
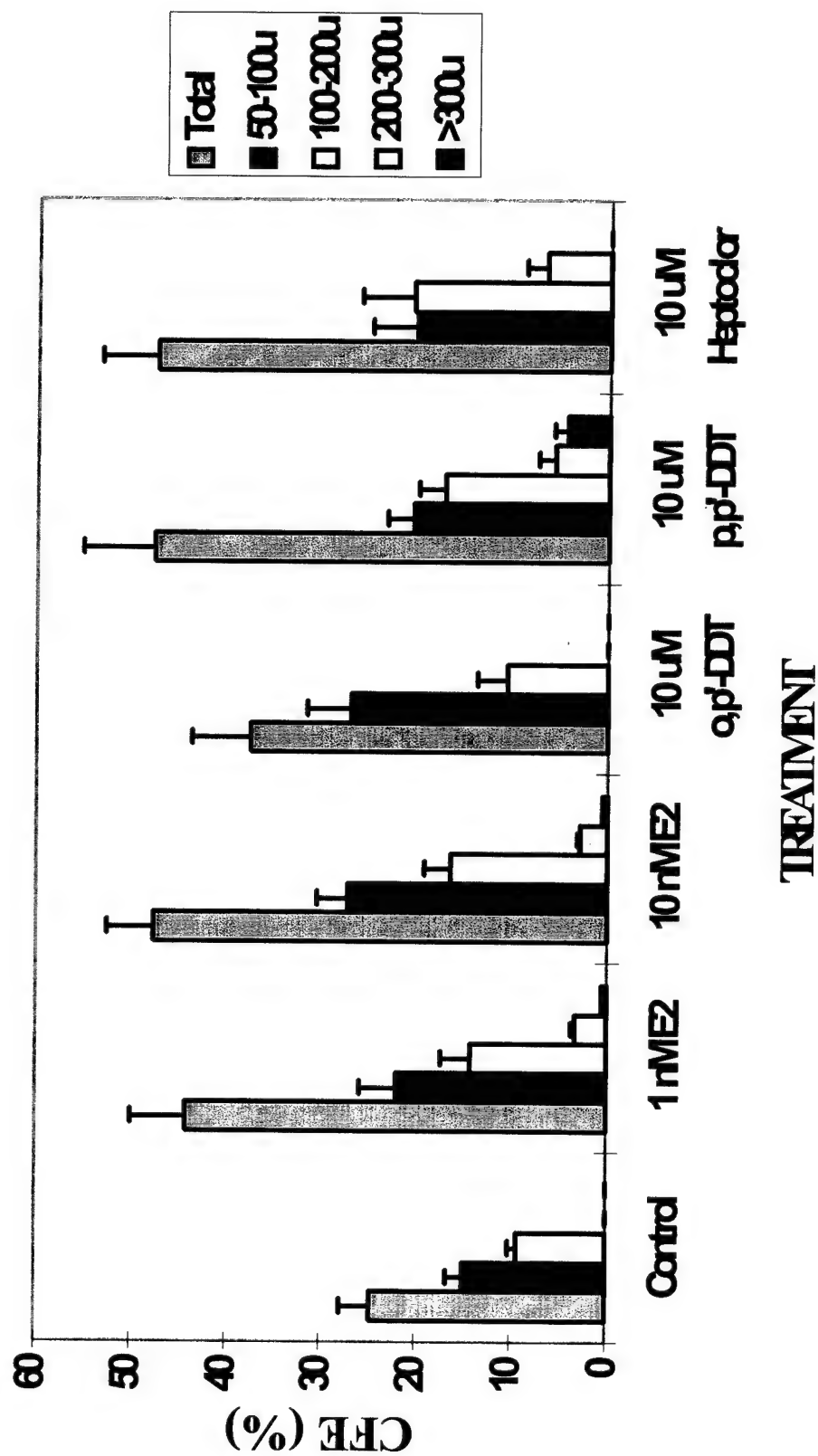

Figure 2

B

pAb240

A
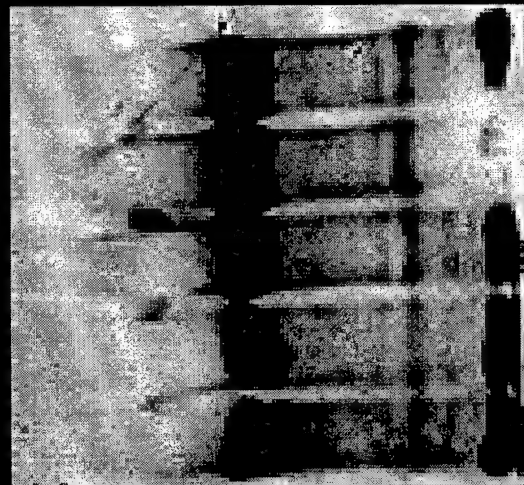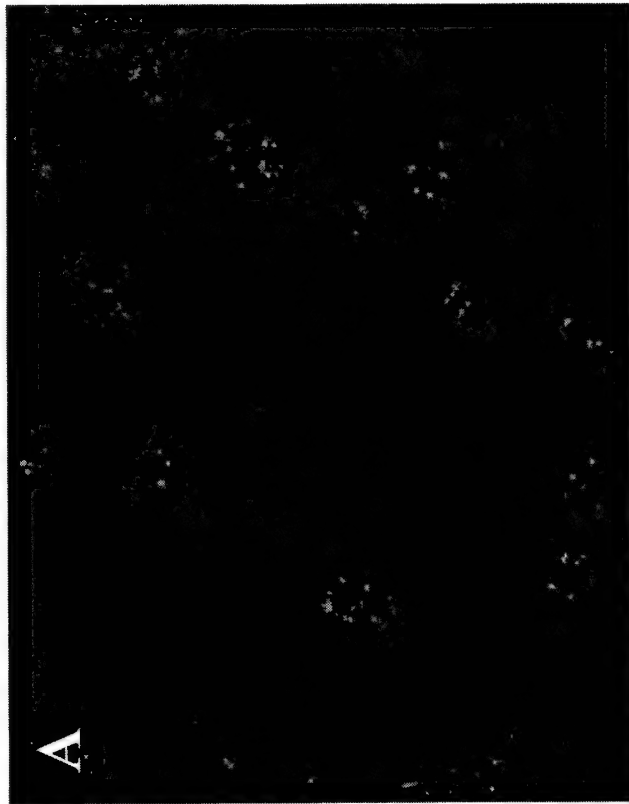
pAb421

MCF10AT3B

FIG. 3

Figure 4

EFFECT OF ESTRADIOL ON PROGRESSION OF MCF10ANEOT AND MCF10AT1 XENOGRAFTS

MCF10AT1 / MCFlbAT3Cd4

MCF10ANEOT

Control

5 xenografts

None
100%

5 xenografts

None
20%
0
60%
3
20%

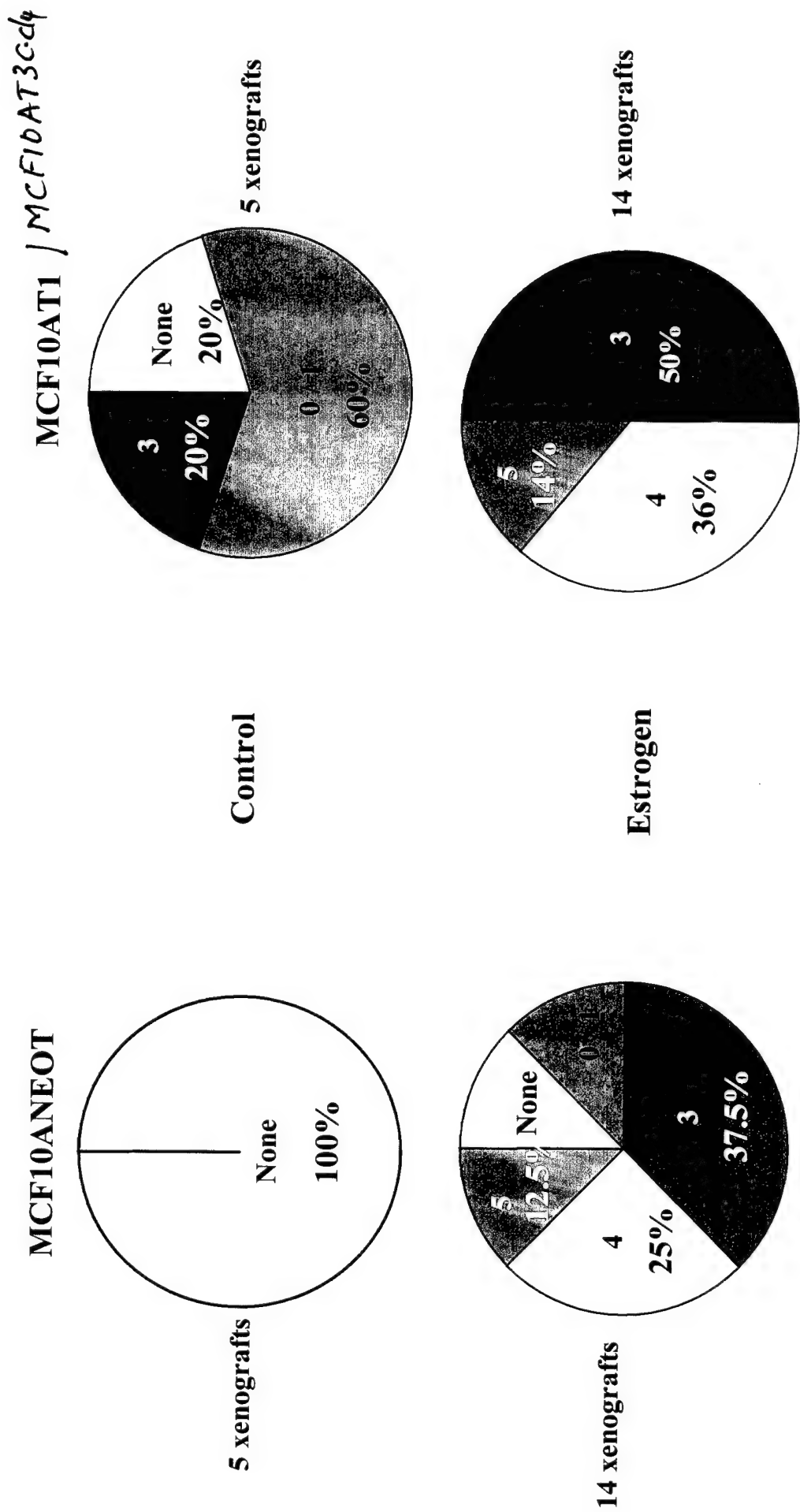**Estrogen**
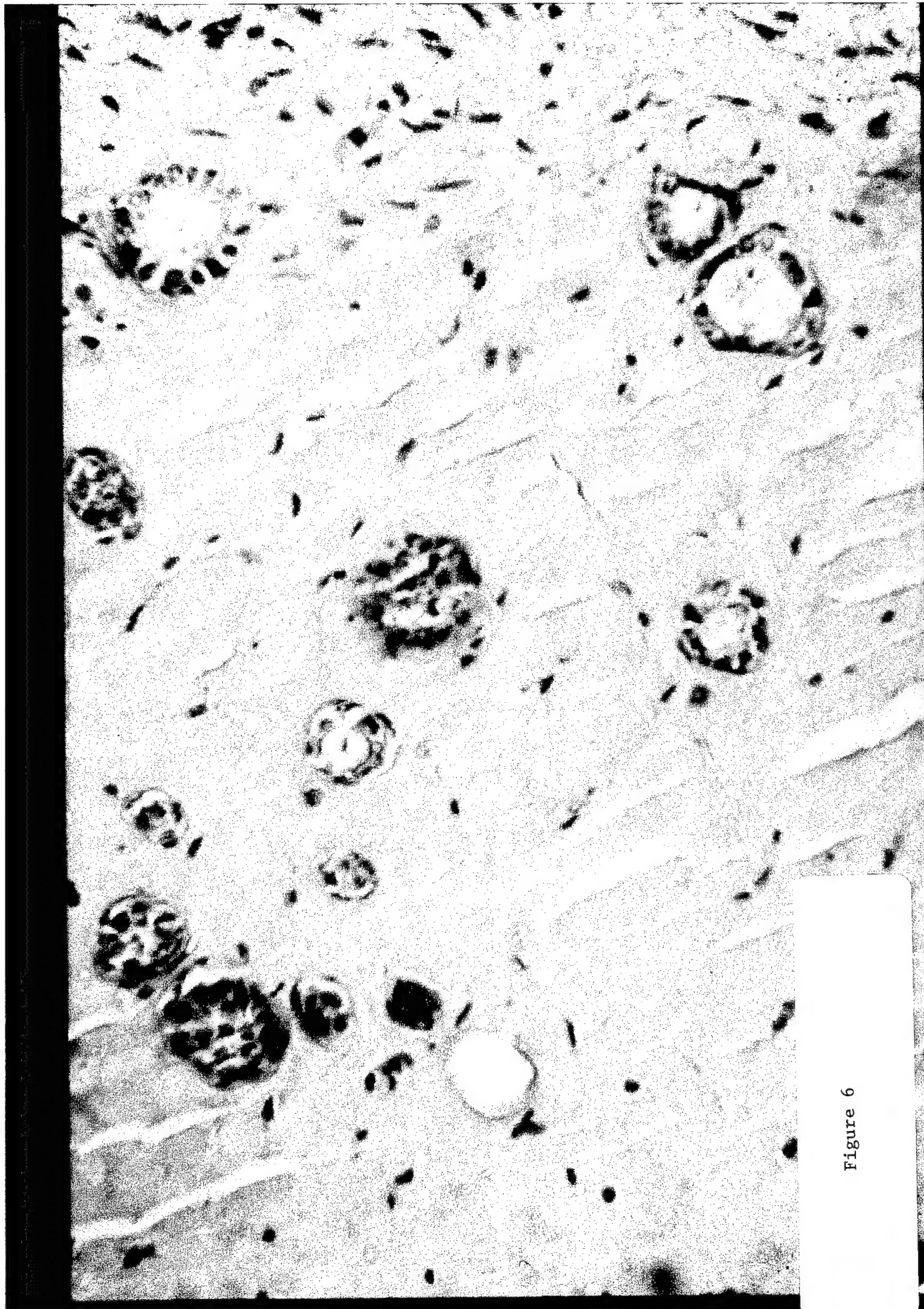
14 xenografts
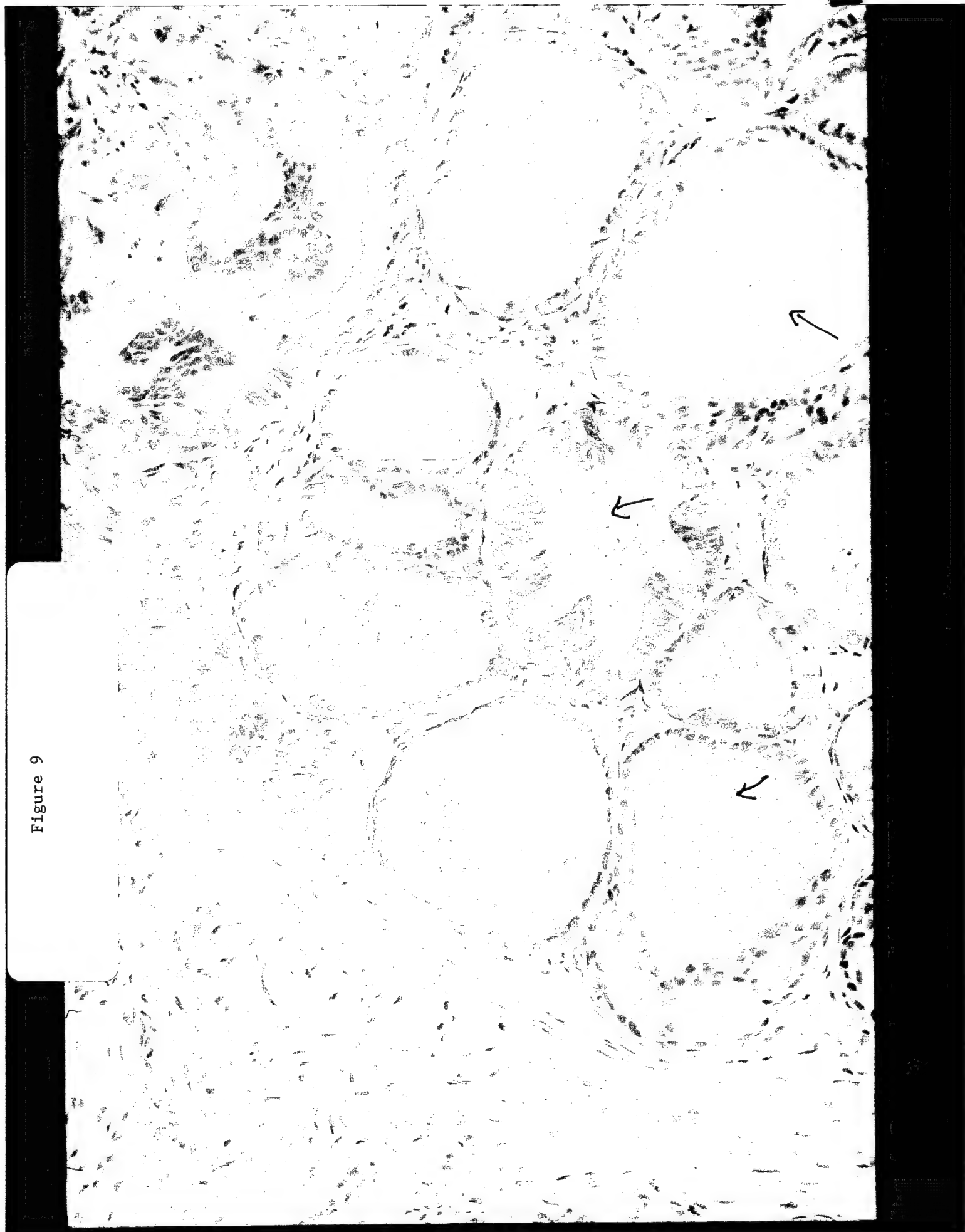
0
None
4
25%
5
12.5%
3
37.5%

14 xenografts

3
50%
5
14%
4
36%

Figure 5

Figure 6

Figure 7

Figure 8

Figure 9
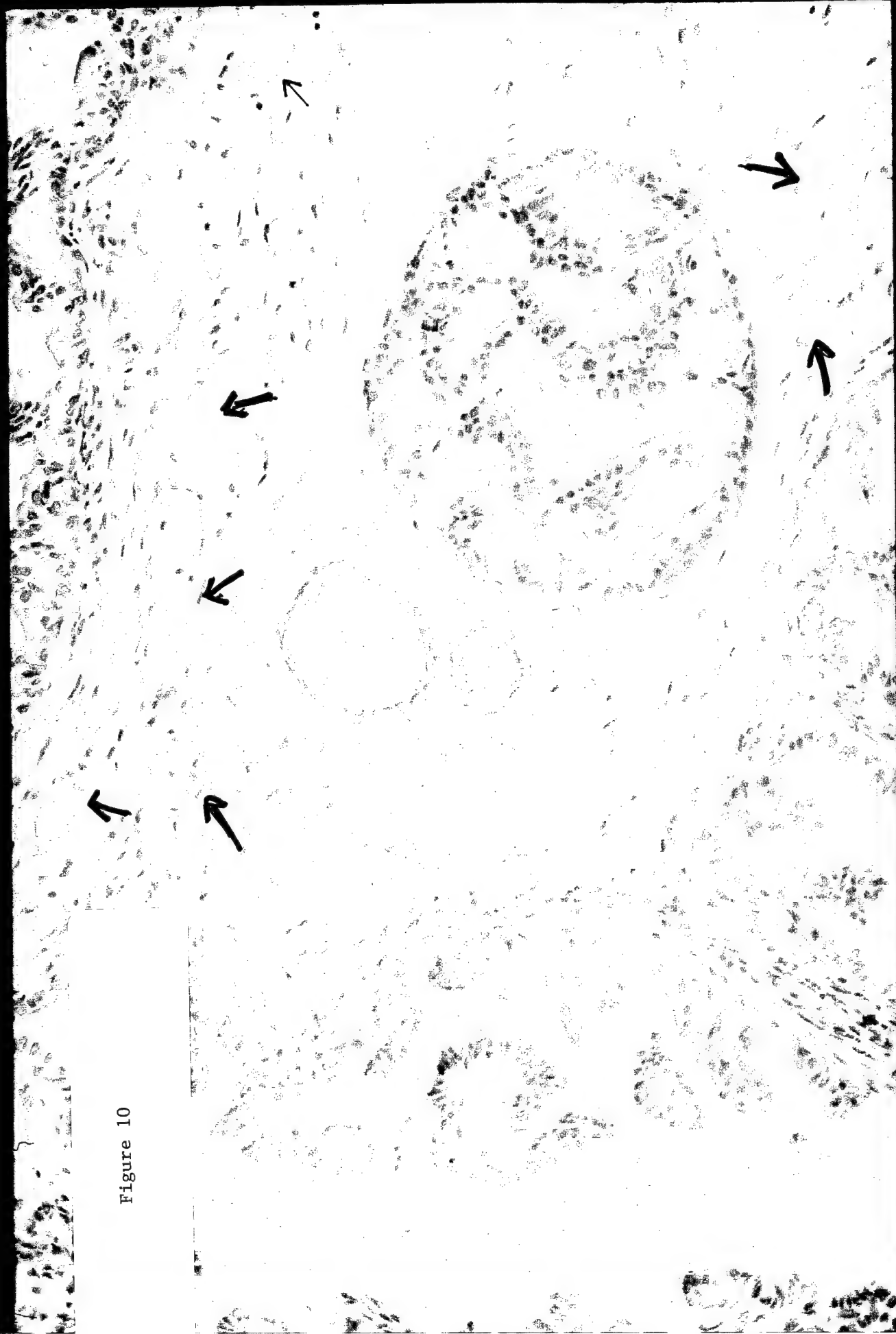
Figure 10

Bcl-2
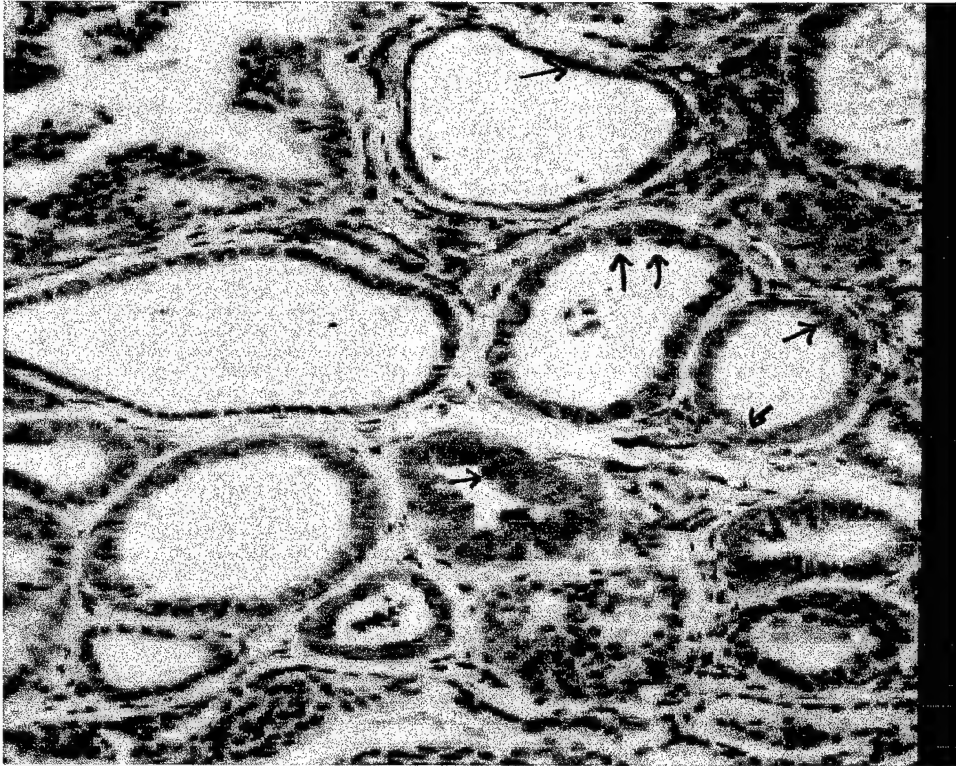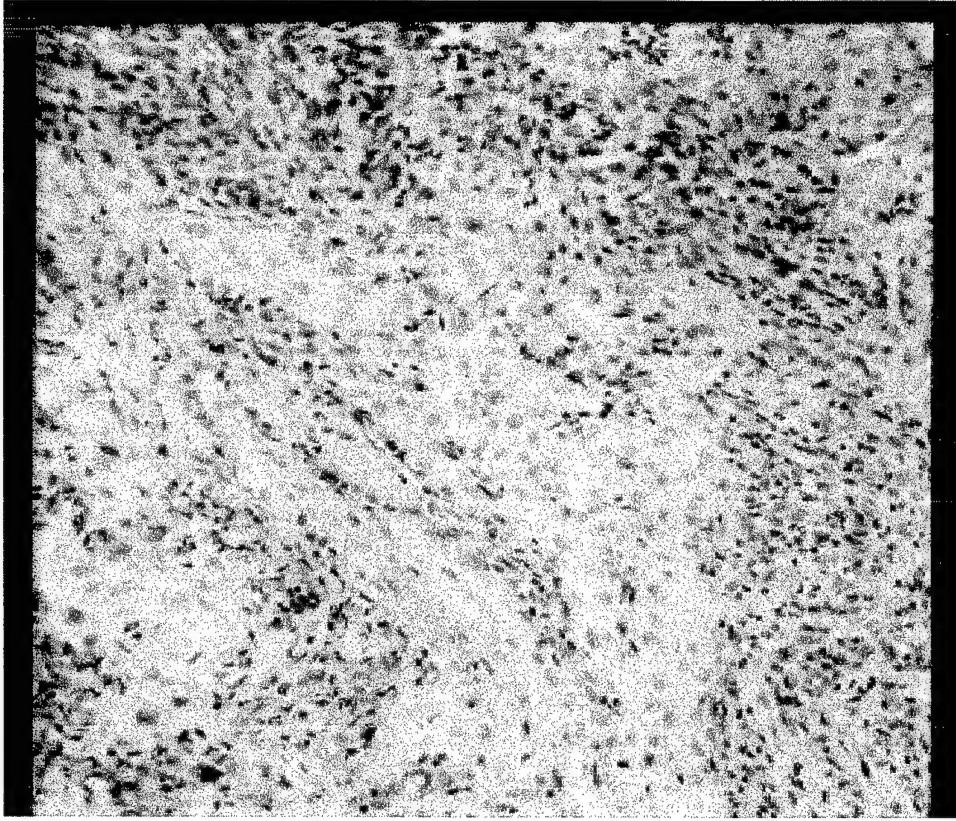
Invasive
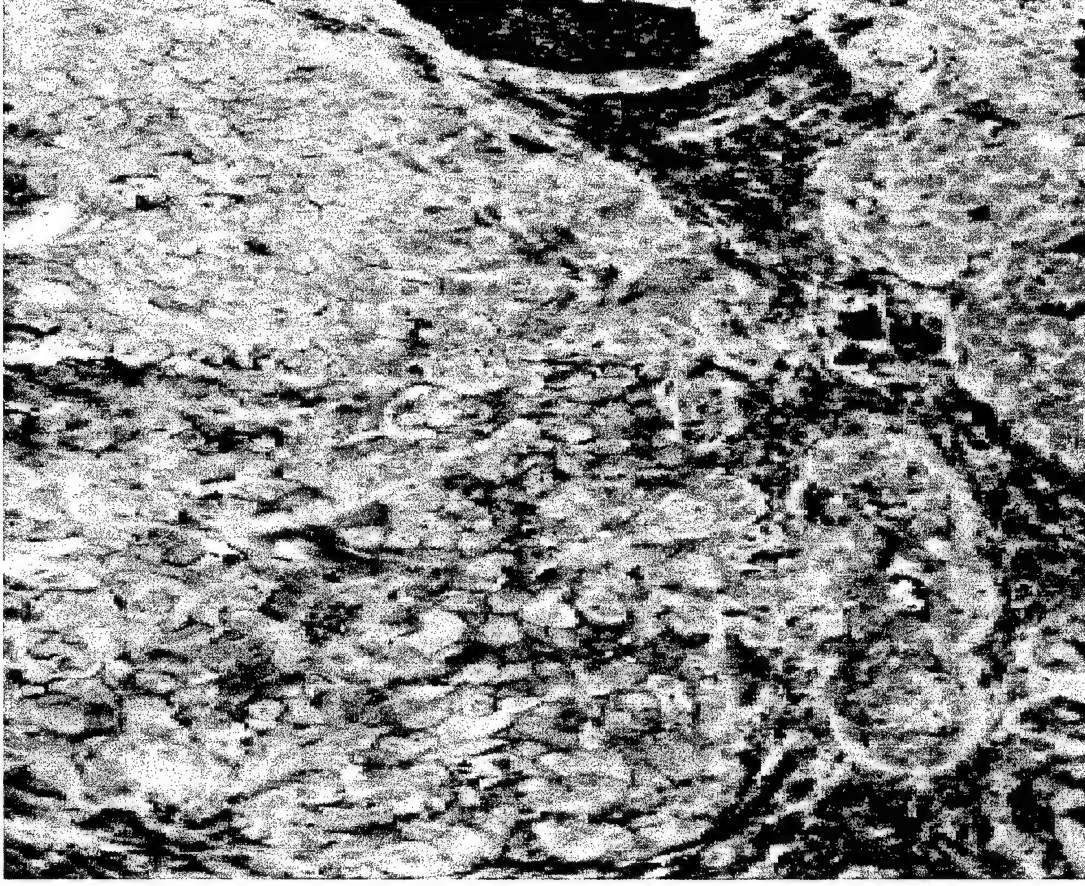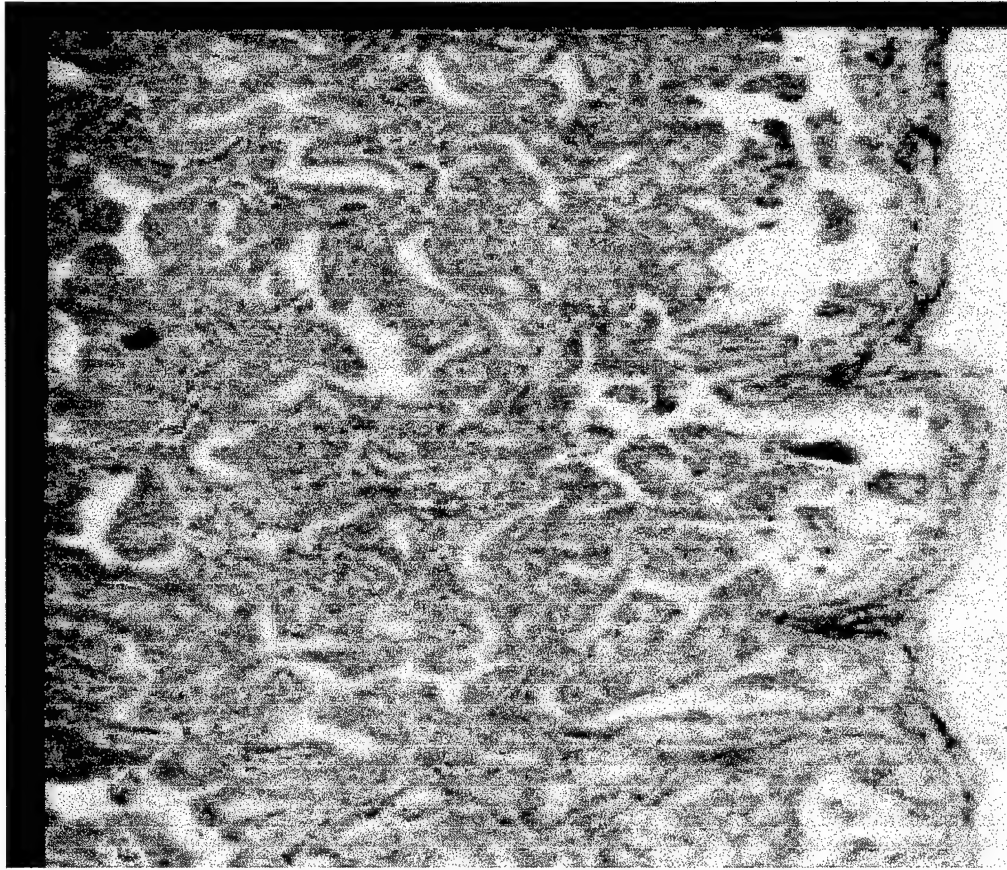
Benign

Figure 11

c-erbB-2
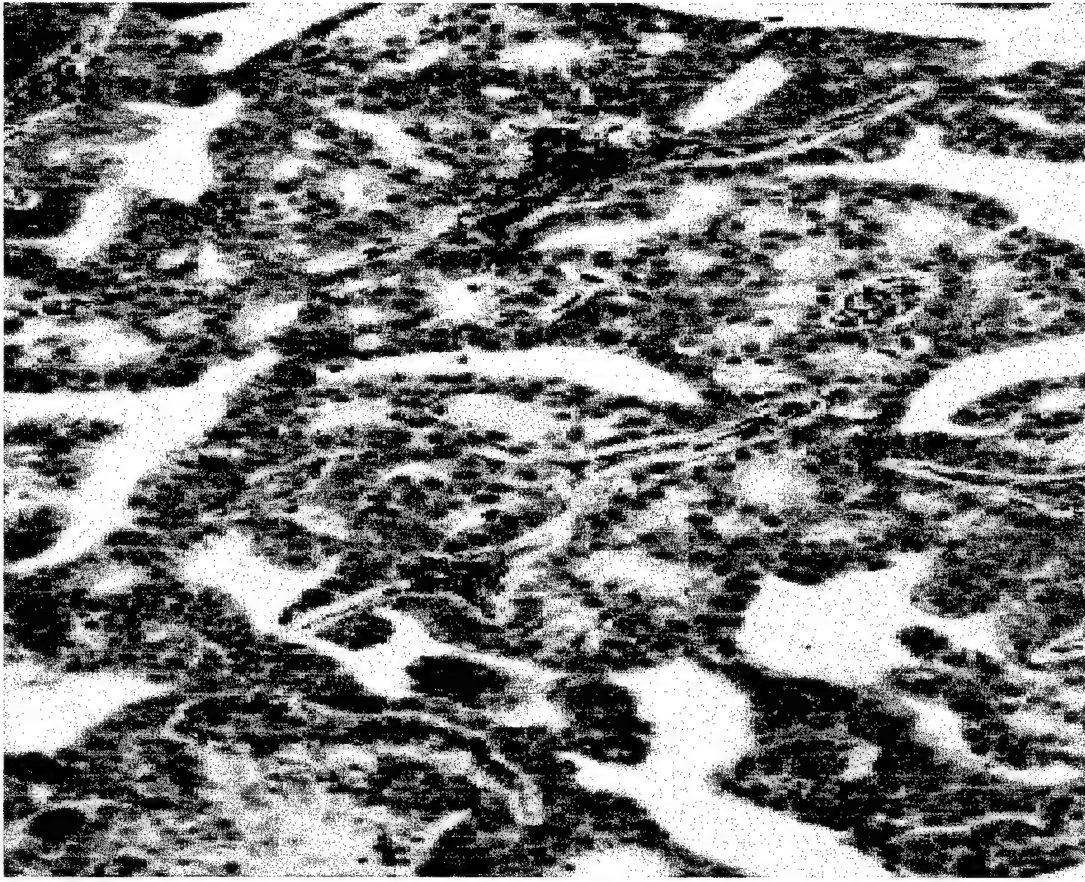
Carcinoma in situ

invasive carcinoma

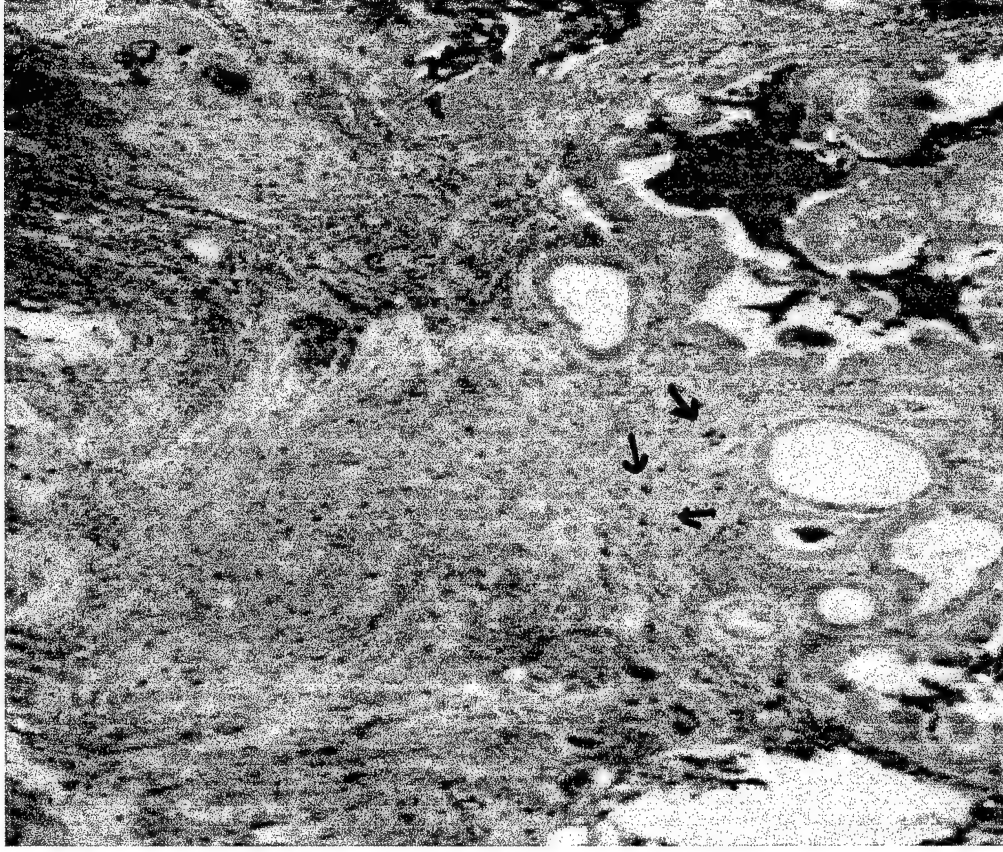Figure 12

cyclin D1
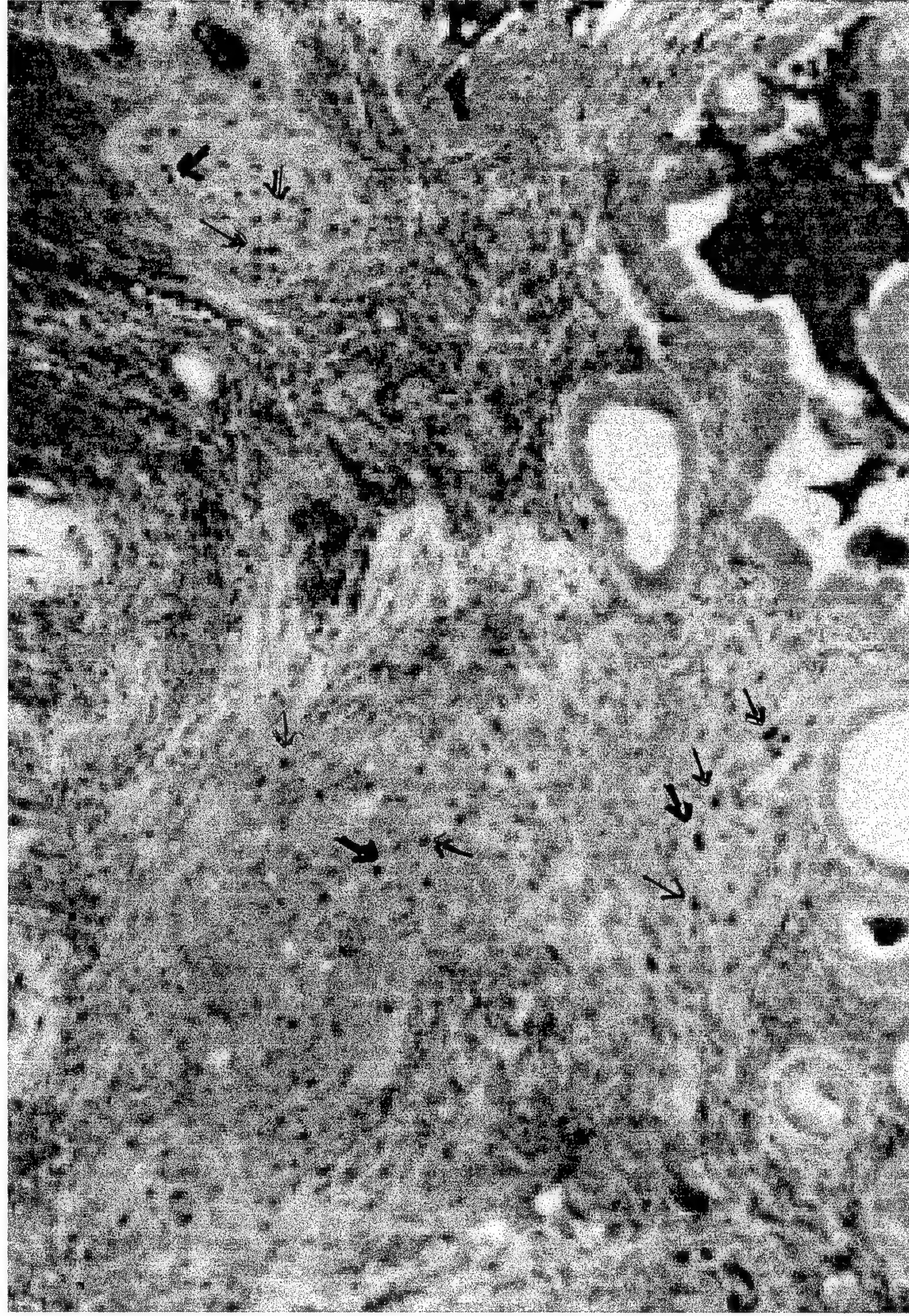
grade 5

grade 3

Figure 13

Cyclin D1

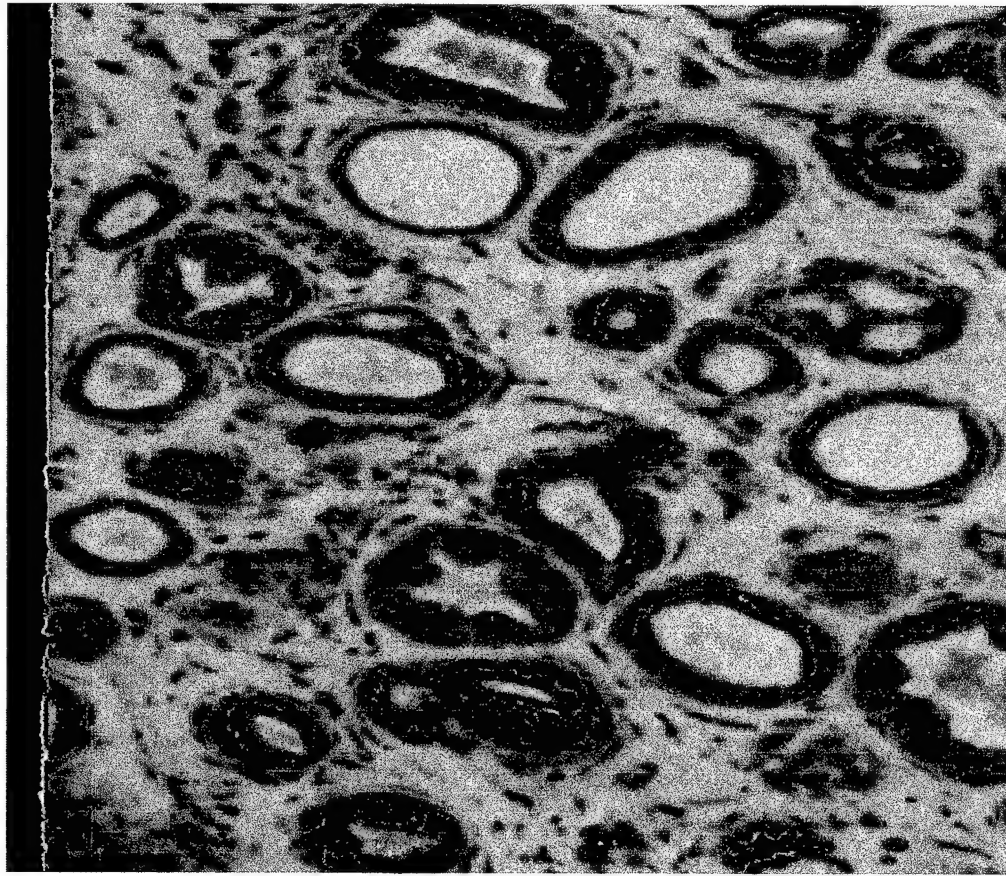

invasive carcinoma

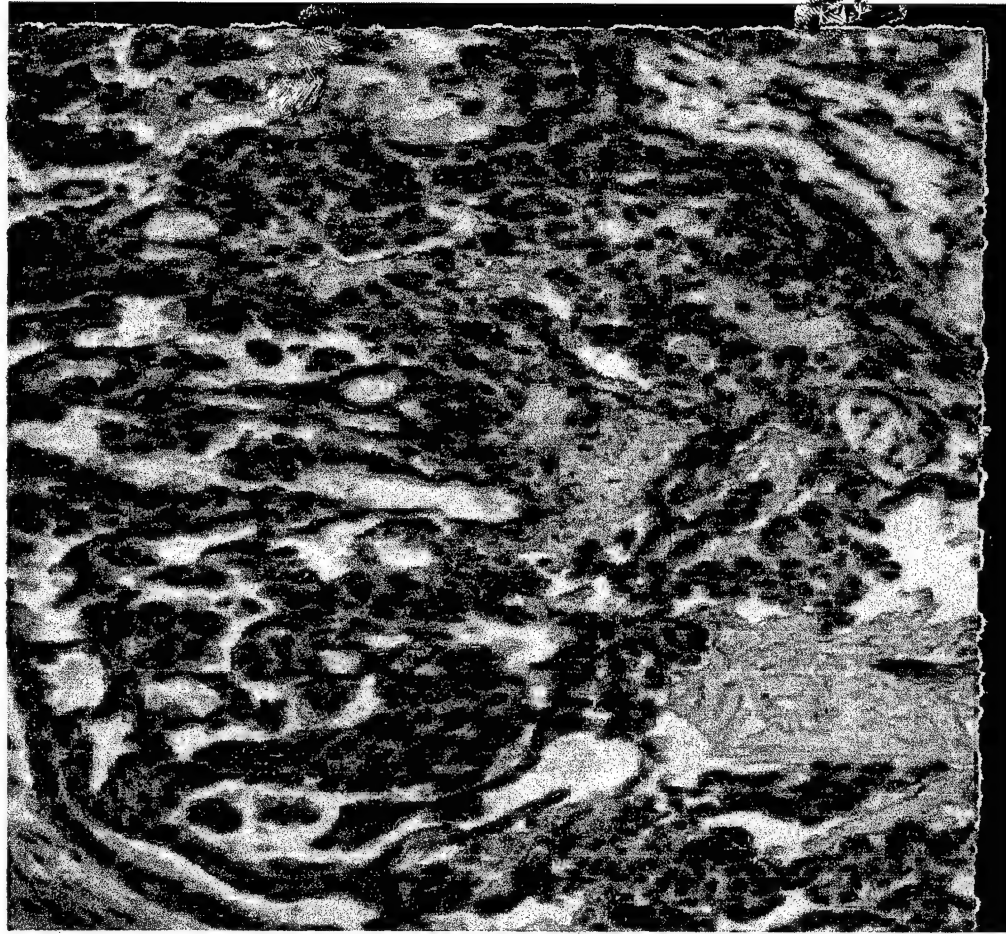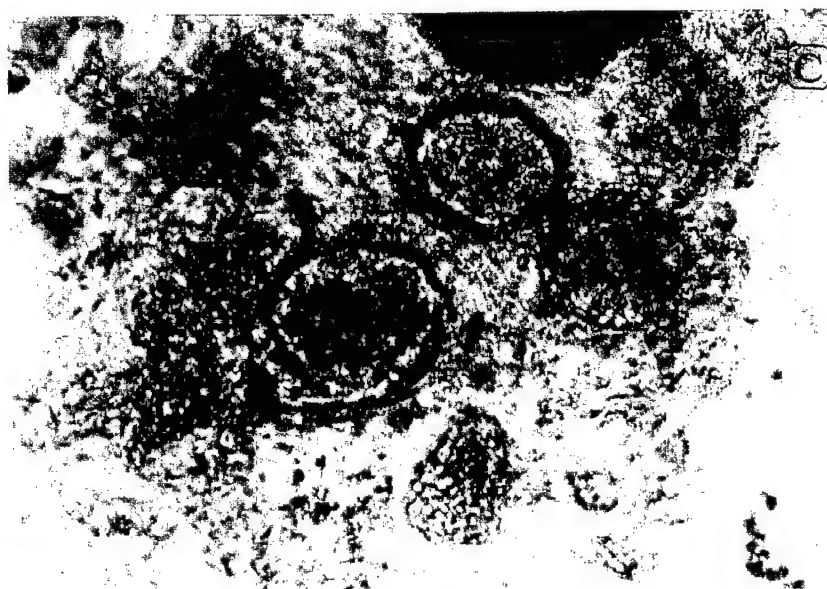Figure 14

pS2

Carcinoma in situ

Simple (benign)

Figure 15

Figure 16

Figure 17

A

B

cyst-
like
ductular
structures
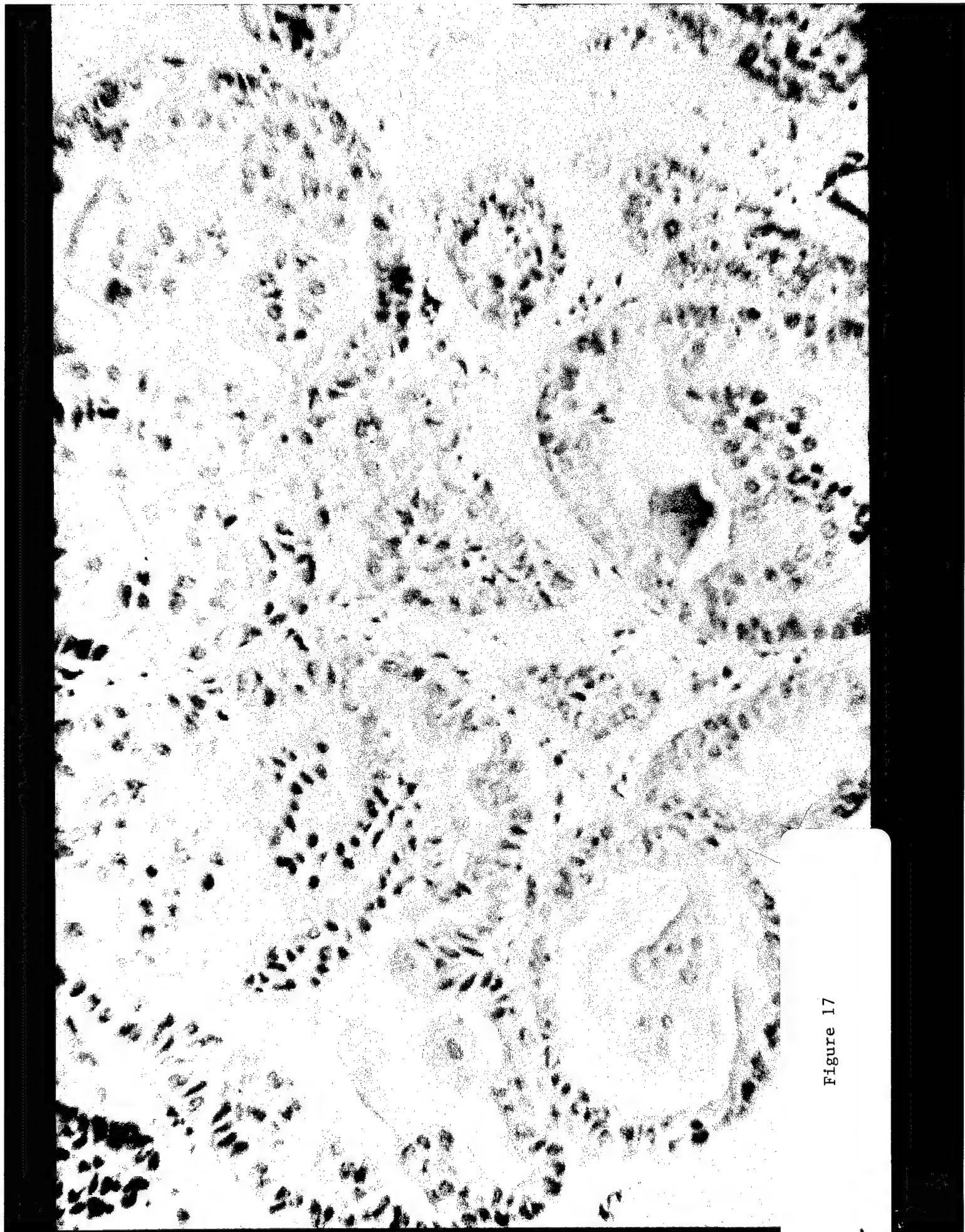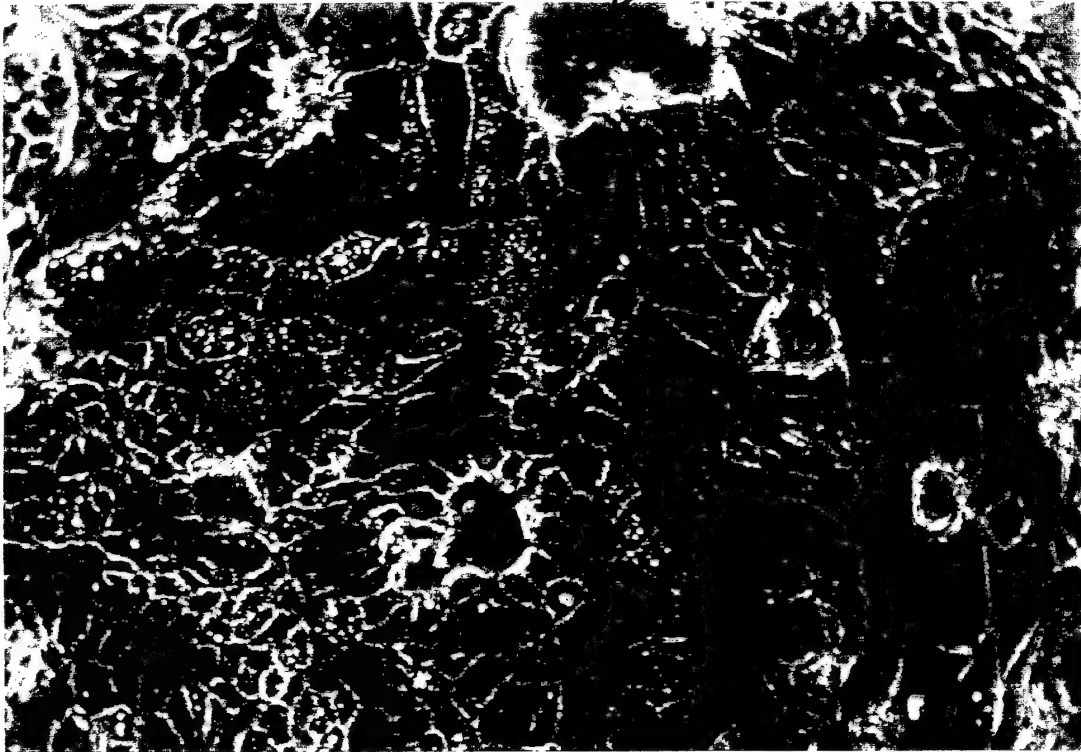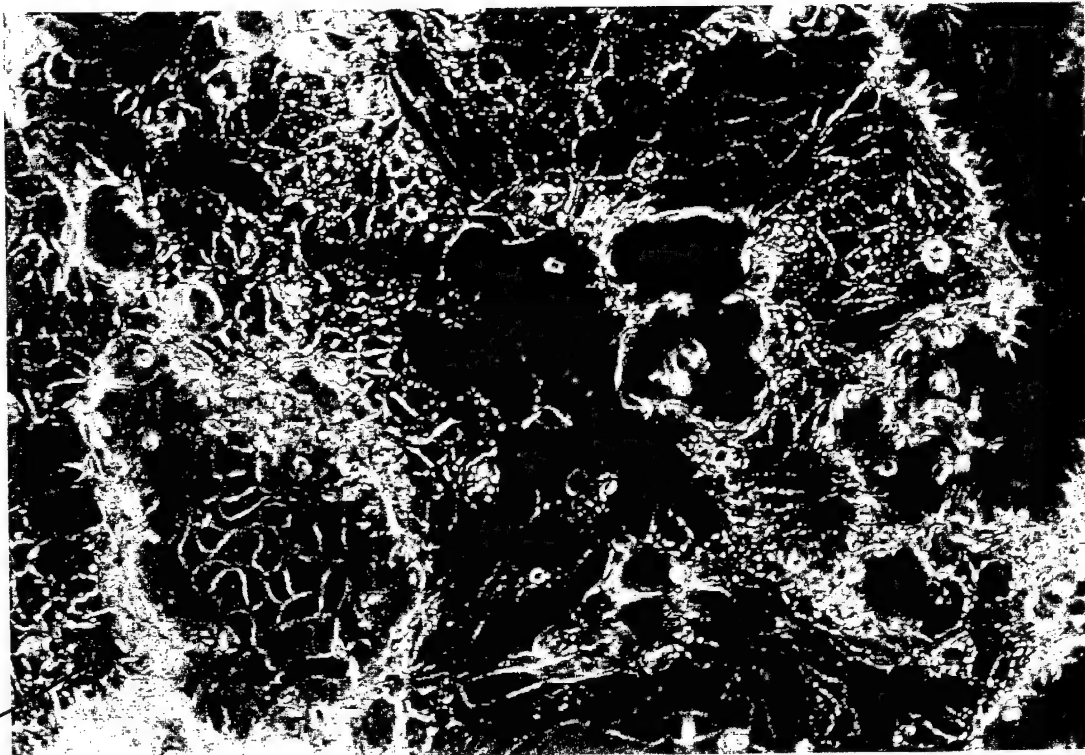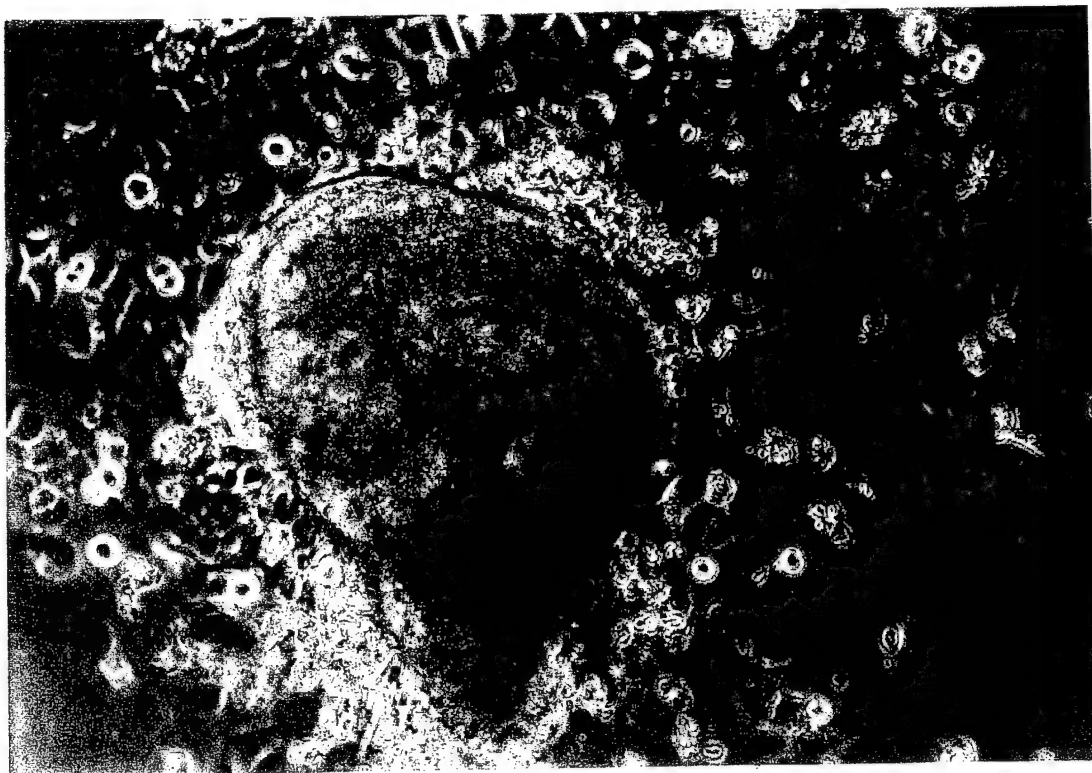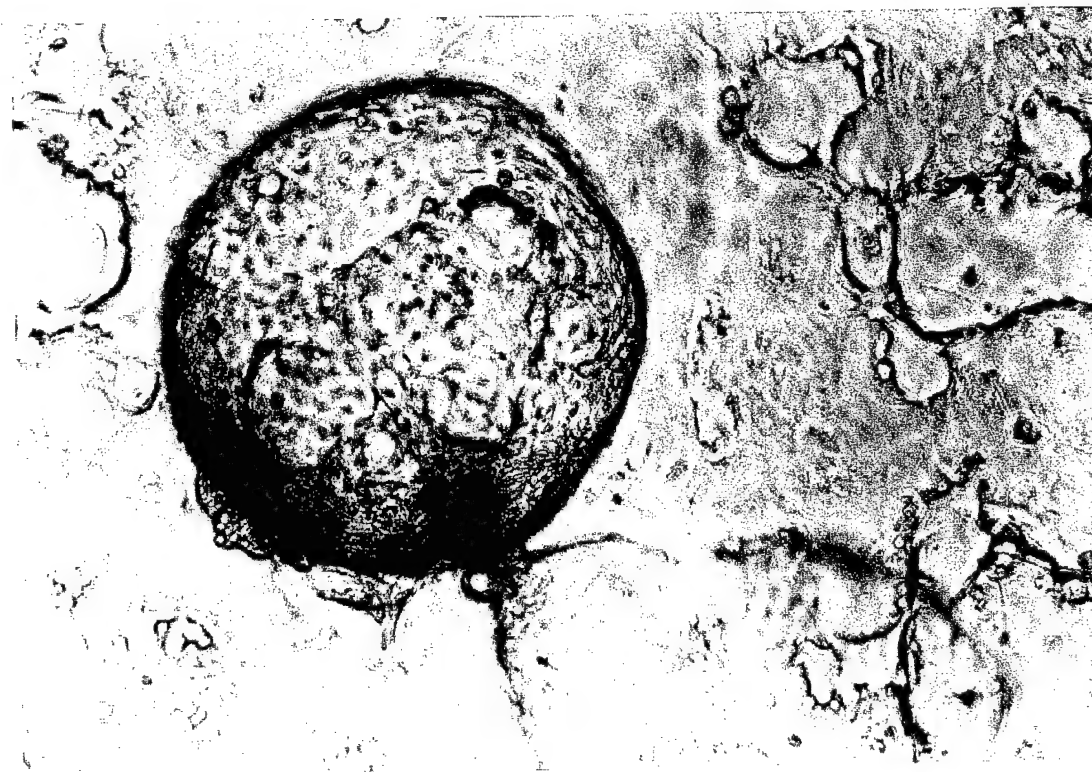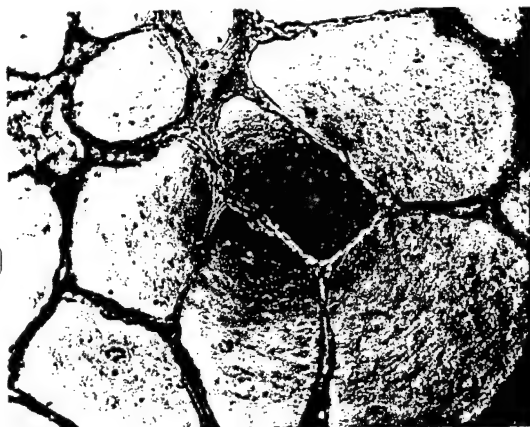
Figure 18

Figure 19

CONTROL

ICI
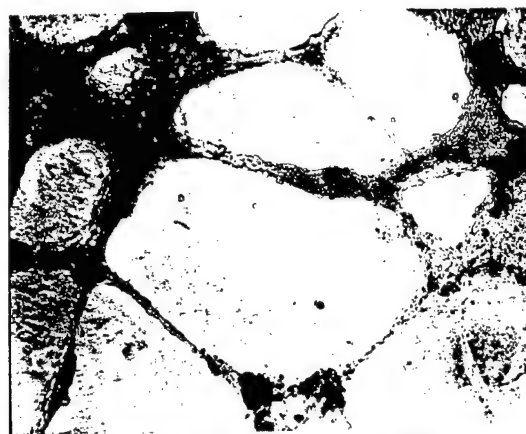
E2

E2 and ICI

E2
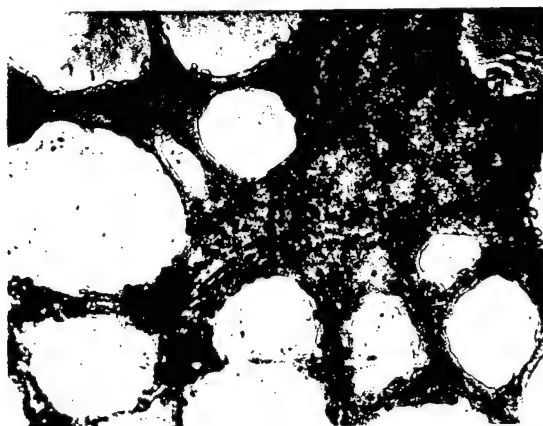
Figure20

Figure legends.

Fig. 1. Phosphorylation status of P53 in MCF10A and MCF10AT3B cells. Cells were radiolabeled with ^{32}Pi, and aliquots of cell lysates containing equivalent amounts of TCA precipitable radioactivity were used for immunoprecipitation with pAb421 or pAb240 antibodies. Proteins were separated by SDS-PAGE and subjected to Western blot analysis.
A: Autoradiograph of blot. Note the absence of labeled P53 in lane immunoprecipitated with pAb421 in MCF10AT3B cells. Also, note the presence of several coprecipitating proteins only in pAb240 lane of MCF10AT3B cells.
B: Western blot of above filter with pAb1801, a P53 monoclonal antibody that recognizes an epitope in the amino terminus of P53. Note the presence of P53 in pAb421 lane of MCF10AT3B cells (indicated by an arrow) indicating the presence of unphosphorylated pAb421-reactive P53.

Fig. 2. Interaction of P53 with MDM-2.
A. Total levels of MDM-2 in cell lysates of MCF10A and MCF10AT xenografts detected by Western blot analysis with MDM-2 antibody.
B. The filter from Fig, 1 was stripped and reprobed with anti-MDM-2 antibody. Note the presence of MDM-2 coprecipitated only in pAb421-immunoprecipitated lane of MCF10AT3B cells (indicated by an arrow).

Fig. 3. Cellular localization of P53 by confocal microscopy.
A. Note the presence of focal or punctate staining of pAb421-reactive P53 only in the nuclei of MCF10AT3B cells. **B**. Note staining of pAb240-reactive P53 is associated with large aggregates in both cytoplasmic and nuclear compartments of MCF10AT3B cells.

Fig. 4. Effect of estrogen on anchorage independent growth of an estrogen-responsive clone of MCF10AT3c cells, MCF10AT3c.cl4. Both colony forming efficiency (CFE) and colony size are increased by estradiol.

Fig. 5. Effect of estradiol on progression of MCF10AT cells in nude mice.
None = no epithelium; grade 0/1 = simple/mild hyperplasia; grade 2 = moderate hyperplasia; grade 3 = atypical hyperplasia; grade 4 = carcinoma in situ; grade 5 = invasive carcinoma.

Fig. 6. Histologic analysis of a lesion derived from control mice injected with MCF10AT1 cells at 10 weeks. Note that majority of the glands have only simple epithelium. The highest grade seen is grade 2. The background represents the matrigel milieu in which the cells were injected.

Fig. 7. A lesion harvested at 35 days of injection of MCF10AT1 cells from an estrogen-supplemented animal. The evolution of simple ducts into higher grades is obvious. Note that majority of the ducts have already progressed to atypical hyperplasia.

Fig. 8. Estrogen-exposed MCF10AT1 lesion showing papillary hyperplasia.

Fig. 9. Adenosis induced by estrogen in MCF10AT1-derived lesions. Note the apocrine secretions from these ducts (marked by arrows).

Fig. 10. Angiogenesis induced by estrogen in MCF10AT1-lesion. Note the presence of several blood vessels, indicated by arrows.

Fig. 11. Immunocytochemical staining of bcl-2 in benign and invasive regions of a MCF10AT1 lesion from estrogen-treated animal. Focal staining is observed only in simple glandular epithelia. No staining observed in invasive carcinoma.

Fig. 12. C-erbB2 staining observed in plasma membrane of MCF10AT1 cells in both CIS and invasive areas of the lesions. Staining is more intence in areas of lesions that have progressed to invasive carcinoma.

Fig. 13. Cyclin D1 staining. Nuclear staining observed only in invasive areas of MCF10AT1 lesions. Areas of lesion that are of lower grades do not stain for cyclin D1.

Fig. 14. An enlarged image of cyclin D1 staining in invasive areas of MCF10AT1 lesion (indicated by arrows).

Fig. 15. pS2 staining in benign and CIS areas of MCF10AT1 lesion. Intense cytoplasmic staining observed in simple glandular epithelia. No staining observed in grades 4 and 5 of MCF10AT1 lesion. This is difficult to discern from a black and white copy of the image.

Fig. 16. Morphology of lesions digested with collagenase and hyaluronidase. Note the tight wrapping of ducts even after digestion for 48 h with the enzymes.

Fig. 17. Histologic analysis of paraffin embedded lesion after digestion with collagenase and hyaluronidase. Note that the ducts seen in Fig. 16 are of grades 3 and higher.

Fig. 18. Formation of cyst like structures from single cell suspensions of MCF10AT1 lesions. Note the organization of cells into cyst like structures, intense secretory activity and vacuole formation.

Fig. 19. A fully formed cyst like structure is shown in Fig. 19 B. Note that these cysts are very proliferative as they are able to reattach to plastic (Fig, 19A).

Fig. 20. 3-dimensional growth of MCF10AT1-lesion derived cells in matrigel. Note the organization of cells into glandular structures. In the presence of E_2, note that the tubes are multilayered (higher contrast); there are also several new papillary bridges and new ducts. Addition of ICI 184,780 to these cultures causes inhibition of the estrogen-induced effects on ductal growth and proliferation. Note that the tubes arte extremely thin in control cultures to which ICI is added, indicating the presence of estrogenic activity in culture media.

Publications:

1. Altered P53 conformation: A novel mechanism of wild-type p53 functional inactivation in a model for early human breast cancer. P.V.M. Shekhar, R. Welte, J.K. Christman, H. Wang and J. Werdell. Int. J. Oncol., 11: In press.

2. Expression of functional estrogen receptor in MCF10AT, a model for early human breast cancer. P.V.M. Shekhar, M.L.-Chen, J. Werdell, G.H. Heppner, F.R. Miller, and J.K. Christman. Manuscript submitted after revision.

3. Direct action of estrogen on sequence of progression of human preneoplastic breast disease. P.V.M. Shekhar, P. Nangia-Makker, L. Tait, G.H. Heppner, and D.W. Visscher. Manuscript submitted.

4. Environmental estrogen stimulation of growth and estrogen receptor function in preneoplastic and human breast cancer cell lines. P.V.M. Shekhar, J. Werdell and V.S. Basrur. J. Natl Cancer Inst. In press.

5. An in vitro model for human preneoplastic breast disease. P.V.M. Shekhar and S.R. Wolman. Manuscript in preparation.

6. Serial xenograft passage is associated with decreased frequency of N-(phosphonoacetyl)-L-aspartate resistant variants in MCF10AneoT cells.Kurumboor S, Shekhar PVM, Christman JK. Manuscript in preparation.

Expression of Functional Estrogen Receptor in a Model for Early Breast Cancer

P.V. M. Shekhar[1,2,6], Mei-Ling Chen[3], Jill Werdell[1], Gloria H. Heppner[1,4], Fred R. Miller[1,2], and

Judith K. Christman[3,5]

[1]Breast Cancer Program, Karmanos Cancer Institute; Departments of [2]Pathology and [4]Internal

Medicine, Wayne State University, Detroit, MI 48201; and [3]Department of Biochemistry and

Molecular Biology, [5]Eppley Institute for Cancer Research and UNMC/Eppley Cancer Center,

University of Nebraska Medical Center, Omaha, NE 68198.

Running Title: Activation of endogenous estrogen receptor expression.

[6]To whom correspondence should be addressed:

P.V.M. Shekhar
Breast Cancer Program
Karmanos Cancer Institute
110 E. Warren Ave.
Detroit, MI 48201

Tel: (313) 833-0715, Ex. 2326/2259
Fax: (313) 831-7518

1

Summary

The long-term goal of our investigations is to elucidate the molecular mechanisms that account for the observed link between estrogen (E_2) exposure and risk of breast cancer development utilizing the MCF10AT xenograft model for progression of human proliferative breast disease. In these studies, reverse transcriptase-polymerase chain reaction (RT-PCR) was used to determine the transcriptional activity of the endogenous estrogen receptor (ER) gene in a number of cell lines of the MCF10AT system. ER transcripts were undetectable in the parental MCF10A cells and in MCF10A cells transfected with normal c-Ha-ras or vector. However, MCF10AneoT and other cells of the MCF10AT system, all of which stably express a transfected mutated T24 Ha-ras gene, also express the endogenous ER genes. The transcripts contain a normal full-length ER coding region and direct synthesis of a normally sized ER protein. The protein is functional based on its ability to mediate E_2-induced increases of transcription from both an endogenous (progesterone receptor, PgR) and a transfected (ERE-TKCAT) E_2-regulated gene. Transcriptional activation of the endogenous ER gene does not appear to be related to a change in methylation status of the gene since a diagnostic CpG site in exon 1 that is methylated in ER^- breast tumors and completely unmethylated in normal breast tissues and ER^+ breast tumors is hypomethylated to the same extent in ER^- MCF10A cells and ER^+ MCF10AT cells.

Finally, while E_2 had no significant effect on monolayer growth of MCF10AT system cells or on soft-agar colony formation by MCF10AneoT cells, it increased both the number and size of soft-agar colonies formed by MCF10AT3c cells, a line from a third generation MCF10AT

2

xenograft lesion. This suggests that xenograft passage has selected for growth regulatory pathways that are E_2- responsive and that identification of these pathways and their role in progression will aid in determining how E_2 acts to increase risk of breast cancer.

Key words: Estrogen receptor, MCF10A, T24 Ha-ras, xenograft model, breast cancer progression, preneoplasia.

Introduction

Breast cancer is the most common malignancy among women in North America. Although very little is known about the molecular events underlying the development of mammary tumors in humans, much evidence indicates that the presence of ER is generally a favorable prognostic marker because ER^+ tumor cells are usually more differentiated and have lower metastatic potential than ER^- tumor cells. Only 6-10% of normal human breast epithelial cells are ER^+ (1,2), yet more than 60% of primary human breast tumors are ER^+ and initially depend on E_2 for growth (3-5).

We have utilized the MCF10AT xenograft model of early human breast cancer progression (6). MCF10AneoT cells are a T24 Ha-ras transformed line derived from MCF10A preneoplastic human breast epithelial cells (7). MCF10A cells form lesions in nu/nu Beige mice that regress within five weeks, In contrast, MCF10AneoT cells form persistent lesions (6). MCF10AneoT and lines derived by alternating in vivo transplantation and in vitro culture (MCF10ATn) are collectively known as the MCF10AT system (8). The lesions formed by lines of the MCF10AT system are composed of a heterogeneous spectrum of ductular tissues with a range of morphology that includes mild hyperplasia, atypical hyperplasia, carcinoma in situ (CIS), moderately differentiated carcinoma, and undifferentiated carcinoma, as well as histologically normal ducts (6,8). Thus, the MCF10AT system provides a transplantable, xenograft model of human proliferative breast disease with proven neoplastic potential. Approximately 62% of lesions produced in mice injected with MCF10AneoT cells are comprised of simple to mildly hyperplastic epithelia while the remaining 38% contain elements of invasive carcinoma

4

irrespective of whether the host is male or female (8). In contrast, MCF10AT1 cells, a line derived from an MCF10AneoT lesion containing elements of squamous carcinoma, not only form lesions with a wider range of morphology than those formed by MCF10AneoT (8) but, to date, have formed lesions with invasive carcinoma only in female mice (F. Miller, unpublished observation). This suggested to us that ER-mediated processes might play a role in MCF10AT progression after initial selection for the capacity to form persistent lesions. However, MCF10A cells, from which the cell lines of the MCF10AT system are derived, are ER⁻ at both the protein and mRNA level (9,10). Here, we present evidence that the endogenous ER genes in MCF10A cells have been activated in MCF10AT cells leading to expression of functional ER protein. The implications of this event for progression of MCF10AT system xenografts are discussed.

Materials and methods

Cell lines and cell culture

These studies utilized parental MCF10A, MCF10Aneo (vector transfected), MCF10AneoN (normal Ha-ras-transfected), and the following lines from the MCF10AT system: MCF10AneoT, MCF10AT1, 2b and 3c. Cells from all of these lines were maintained in phenol red-free DMEM/F-12 medium with 0.1 μg/ml cholera toxin, 10 μg/ml insulin, 0.5 μg/ml hydrocortisone, 0.02 μg/ml epidermal growth factor, 100 i.u./ml penicillin, 100 μg/ml streptomycin, and 2.5% horse serum [DMEM/F12^sup]. Charcoal-stripped serum was not used since it reduces the proliferative capacity and/or viability of MCF10A cells, possibly due to removal of essential growth factors (11). The only sera used routinely were those which were unable to support

growth of the ER$^+$ cell line, MCF-7, indicating absence of biologically significant levels of E$_2$ or other estrogenic compounds. MCF-7 cells, which were used as a positive control for ER expression, were grown in Eagle's minimal essential medium with Hank's balanced salt solution, 2.5 mM L-glutamine, and 25 mM HEPES, supplemented with 0.1 mM nonessential amino acids, 1 mM sodium pyruvate, 5 µg/ml gentamicin and 5% donor calf serum. T47D cells were used as a positive control for PgR expression and were grown in Eagle's MEM supplemented with 0.1 mM nonessential amino acids, 2 mM L-glutamine, 5% fetal calf serum and 6 ng/ml of insulin. To induce PgR, MCF10AneoT and MCF10AT3c cells were treated for 3 days with 0.1-10 nM E$_2$ dissolved in ethanol (0.01% final concentration). Controls were treated with ethanol alone.

RT/PCR

Two µg of RNA were denatured at 65°C for 5 min and reverse transcribed in the presence of 1 mM dATP, 1 mM dCTP, 1 mM dTTP, 1 mM dGTP, 5 mM dithiothreitol, 1 unit/µl RNase inhibitor, 20 µM random primers (Pharmacia, Pistcataway, NJ), reverse transcriptase buffer and 5 units/µl reverse transcriptase (Seikagaku, Japan) for 20 min at room temperature and 1 h at 42°C followed by 10 min at 95°C. PCR was performed using 500 nM concentrations of each primer and 0.5 unit Taq polymerase (Promega, Madison, WI) in a total volume of 100 µl. PCR products were further characterized by restriction mapping, Southern blot analysis and DNA sequencing.

Detection of ER mRNA expression

Total RNA was reverse transcribed as described above. An oligonucleotide primer set [sense 5'-GCCCGCGGCCACGGACCATGACCAT-3', and antisense, 5'-TGACCATCTGGTCGGCCGTC-3'] flanking the human ER cDNA sequence from base -17 to 950 was used for amplification by PCR yielding a 967 bp fragment that includes exons 1-6 of ER (12). The identity of the 967 bp ER cDNA fragment amplified from MCF10AneoT and derivatives was confirmed by Southern blot hybridization analysis with a full-length human ER cDNA probe. Full length ER cDNAs were amplified from MCF10AneoT and MCF10AT3c by RT-PCR using primer sets flanking base -17 to 1735 (12) and cloned into TA-cloning vector (Invitrogen, San Diego, CA). Both strands were sequenced using ER specific primers.

Analysis of c-Ha-ras mRNA expression

PCR amplifications of reverse transcribed Ha-ras mRNAs were carried out with an oligonucleotide primer set flanking the c-Ha-ras sequence from base 18 to 556 of the human Ha-ras cDNA [sense, 5'- CGATGACGGAATATAAGCTGGTGGTGGT-3', and antisense, 5'-GGGGCCACTCTCATCAGGAGGGTTCAGCTT-3']. This includes bases 1661-3317 of the human c-Ha-ras gene (13). PCR products were cleaved with NaeI. All single base ras-activating substitutions at codon 12 eliminate a NaeI site (GCC/GGC) and give a novel 179 bp fragment under these conditions. NaeI-restricted cDNAs were analyzed by electrophoresis through 2% agarose gels.

7

Analysis of ER expression

Immunodetection of ER

MCF10Aneo, MCF10AneoT, MCF10AT3c and MCF-7 cells that had been grown to near confluence were rinsed in phosphate buffered saline (PBS), harvested by trypsinization, pelleted and resuspended in a high salt buffer containing 10 mM $NaMoO_4$, 10 mM Tris, 1 mM EDTA, 1 mM DTT and 0.6 M KCl, pH 7.5. Lysates were centrifuged at 100,000 x g for 30 min and the supernatant (cytosolic) fractions incubated with human anti-ER monoclonal antibody (mAb), D547 (gift from Dr. Geoffrey Greene), followed by the addition of Protein A Sepharose. Bound ER was extracted from the Sepharose resin by boiling in Laemmli's buffer and separated on a 7.5% SDS-polyacrylamide gel (14). Proteins were electroblotted onto Immobilon- P membranes, incubated sequentially with anti-ER mAb D547 and ^{125}I-labeled anti-rat IgG. Following four washes with buffer containing 50 mM Tris-HCl/ 0.3 M NaCl/ 1% Triton X-100/ 1 mM PMSF, pH 7.5, the membrane strips were dried and exposed to Kodak XAR film at -70°C for 1-3 days. The relative amounts of ER expressed were quantitated with a densitometer (Molecular Dynamics, Model 300A).

Immunofluorescence Microscopy

MCF10AT3c and MCF-7 cells were grown to near confluence on Lab-Tek chamber slides (Nunc, Naperville, IL). The cells were fixed and immunostained with rat monoclonal antibody to human ER, mAb H222 following directions provided by the supplier of the ER mAb. Controls were similarly treated with normal rat IgG or buffer alone. The cells were washed with PBS and

incubated for 30 min with FITC-conjugated goat anti-rat IgG (Zymed Laboratories, Inc., San

Francisco, CA) and rinsed with PBS. Slides were viewed with a 63X oil objective using a Nikon

Optiphot microscope with epifluorescence.

Determination of endogenous ER function

Reporter plasmid construct

Construction of the ERETKCAT vector, JA-12, is described in Ref. 15. JA-12 contains tandem

EREs (one consensus and one mutated) between the XbaI site and the TATA box of

p-37TKCAT (16).

Cell culture and transfection

MCF10AneoT cells (500,000/60 mm dish) were plated in phenol red-free DMEM/F12^{sup} medium

and maintained for 18 h prior to transfection with 10 μg of JA-12 plasmid DNA using the

calcium phosphate method (17). Six hours after transfection, cells were shocked using a 3 min

incubation with 15% glycerol, washed and cultured in phenol red-free DMEM/F12^{sup} medium

containing E_2 and/or ICI 164,384 or vehicle (ethanol) at indicated concentrations for 36-42 h.

Chloramphenicol acetyl transferase (CAT) assay

Transfected cells were lysed with four cycles of freezing and thawing in 0.25 M Tris-HCl, pH

7.5. CAT assays were carried out as described by Gorman et al (18) with reaction mixtures

containing 100 μg of supernatant protein and 0.1 μCi of ^{14}C-chloramphenicol (40-60 mCi/mmol,

ICN Radiochemicals, Irvine, CA). The assay tubes were incubated for 4 h at 37°C. Acetylated

chloramphenicol was separated by thin layer chromatography and quantitated by liquid

scintillation counting. Protein concentrations were determined by the Bradford method (19). The

lacZ reporter plasmid pCH110 (Pharmacia, Piscataway, NJ) was cotransfected in some

experiments to monitor transfection efficiency and assayed according to the manufacturer's

protocol. β-galactoside standard and o-nitrophenyl β-galactoside were purchased from

Boehringer Mannheim (Indianapolis, IN).

Analysis of progesterone receptor (PgR) expression

Cell lysates prepared from MCF10AneoT and MCF10AT3c cells cultured in phenol red-free

DMEM/F12^{sup} medium with or without added E_2 (10^{-9} M) were incubated with anti-human PgR

mouse mAb (Oncogene Science, Cambridge, MA) overnight at 4°C. Immune complexes were

pelleted with Protein G Sepharose, solubilized by boiling in SDS-sample buffer and subjected to

SDS-PAGE and Western blot analysis as described above. Lysates prepared from the PgR-

positive cell line, T47D and treated in the same way were used as controls. Proteins transferred

to Immobilon P (Millipore Corp., Bedford, MA) membranes were incubated sequentially with

the same anti-PgR antibody and ^{125}I-labeled goat anti-mouse IgG (ICN Radiochemicals, Irvine,

CA).

Growth in soft agar

4×10^4 MCF10AneoT or MCF10AT3c cells were seeded in 2 ml of 0.3% agar in phenol red-free

DMEM/F12^{sup}. This suspension was layered over 1 ml of 0.9% agar medium base layer in 35-

mm dishes (Costar) and overlayered with 2 ml of phenol red-free DMEM/F12^{sup} containing 10^{-8}M or 10^{-9}M E$_2$ or an equivalent concentration of vehicle (ethanol). All dishes were incubated at

37°C in 5% CO$_2$:95% O$_2$ for 4 weeks with twice-weekly media changes. All cultures were

examined 24 h after plating and cell aggregates that might bias final results were marked. Plates

with more than 10 aggregates were discarded. Colony forming efficiency (CFE) was calculated

by dividing the number of colonies larger than 50 μm (sized using a calibrated ocular grid) by the

number of cells seeded. Ten microscopic fields were counted to calculate the total number of

colonies/well for the whole well; reported values are the average count from triplicate wells. The

number of colonies in different size ranges [50-100 μm, 100-200 μm, 200-300 μm and >300 μm]

was calculated in the same manner.

Determination of methylation status of ER

Ten μg of purified genomic DNA (20) was digested with EcoRI (4 units/μg DNA) and NotI (4

units/μg DNA) for 16 h. NotI will only cleave DNA at its recognition site (GC/GGCCGC) if the

indicated C residue in this site is unmethylated on both strands (21). This means that

methylation by mammalian C-5- DNA MTase at either CpG dinucleotide in the NotI site will

prevent cleavage. The resulting DNA fragments were separated by electrophoresis on 1%

agarose gel, blotted and probed with a 0.3 kb EcoRI/PvuII fragment of the ER gene obtained

from the plasmid POR3 (ATCC-57681). Completeness of cutting was verified by determining

that cleavage was complete at a c-myc CpG island NotI site that is normally unmethylated in

11

<u>vivo</u> (22).

Results

Analysis of ER expression in the MCF10AT system

To determine whether ER is expressed in MCF10AT system cells, RT-PCR with ER-specific

primers was used to detect ER mRNA expression. A 967 bp ER fragment amplified by PCR was

detected in all cells of the MF10AT system examined (Fig. 1, lanes 4-7), whereas this fragment

was undetectable in the parental MCF10A cells and its non-lesion forming derivatives,

MCF10Aneo and MCF10AneoN (Fig. 1, lanes 1-3). The origin of the 967 bp fragment was

confirmed by Southern blot hybridization (Fig. 1) and DNA sequencing. Full length ER cDNAs

amplified from MCF10AneoT and MCF10AT3c cells were cloned into TA-cloning vectors

(Invitrogen, San Diego, CA) and sequenced to determine whether the coding regions of the

endogenous ER gene of MCF10AT cells had undergone any alterations in sequence. Of the five

ER clones derived from MCF10AneoT cell cDNA, one clone exhibited a base substitution at

codon 286 in the hinge region of the ER molecule (ATG⇨ ACG) which will lead to replacement

of methionine by threonine. The presence of this sequence alteration has been confirmed by a

second independent PCR reaction indicating that the identified mutation is not an artifact of PCR

reaction. All four ER clones derived from MCF10AT3c and the remaining four ER clones

derived from MCF10AneoT cells had sequences identical to the sequence for normal human ER

reported in GenBank (23). These results suggest that expression of the bacterial neomycin

resistance gene in MCF10Aneo and the normal <u>c-Ha-ras</u> gene in MCF10AneoN cells are not

capable of activating the ER gene in MCF10A cells, but that expression of mutated (T24) c-Ha-ras may play a role. Steady-state levels of ER transcription in MCF10AT system cells are low since we have not been successful in demonstrating ER expression by Northern blot analysis, even when loading was increased to 10 μg of poly A$^+$ RNA.

Analysis of Ha-ras expression in the MCF10AT system

RT-PCR with c-Ha-ras-specific primers was used to determine if the transfected T24 Ha-ras oncogene present in MCF10AneoT cells was expressed as mRNA in other lines of the MCF10AT system. Amplified PCR products were subjected to NaeI digestion to distinguish between cDNA fragments derived from transcripts of the T24 Ha-ras gene in the vector pHO6T1 and those derived from endogenous genes. The 179 bp T24 Ha-ras-specific fragment diagnostic for the activating GCC--> GTC substitution in codon 12 was only present in PCR amplified cDNA from MCF10AT and its derivatives (Fig. 2, lanes 4-6). This fragment was readily distinguishable from the 144 bp NaeI fragment of normal Ha-ras cDNA which was present in amplified cDNA from MCF10A, MCF10AneoT and their derivatives (Fig. 2, lanes 1-3, and lower bands in lanes 4-6). Although it does not prove a causal relationship, this result demonstrates that the only MCF10A derived lines that express ER are those that also express T24 Ha-ras.

Detection of ER protein

Sequence analysis indicated that MCF10AT cells should be capable of synthesizing normal ER.

To confirm that ER protein was present in MCF10AT system cells, proteins obtained by immunoprecipitation with anti human ER rat mAb D547 were analyzed. Lysates from both MCF10AT3c and MCF10AneoT cells (Fig. 3, lanes 2 and 3) contained a single molecular size species of ER protein. This ~67 kDa protein had the same electrophoretic mobility as ER from MCF-7 cells (Fig. 3, lane 1). Quantitation by densitometry indicated that the levels of ER protein were at least 5 to 10-fold lower in MCF10AT3c and MCF10AneoT cells, respectively, than in the positive control, MCF-7 cells. As expected, no ER protein was detected in lysates from MCF10Aneo cells (Fig. 3, lane 4). Although ER was detected in MCF10AneoT cells by Western blotting (Fig. 3) and flow cytometry (data not shown), we have not been able to detect it reproducibly by immunocytochemical staining with anti-human ER rat mAb H222 even though the same antibody can detect ER in MCF10AT3c cells (Fig. 4). The intensity of fluorescent staining was lower in MCF10AT3c nuclei than in MCF-7 nuclei. However, under optimal conditions of active growth to near confluence, nuclear ER was detectable in approximately 40% of MCF10AT3c cells compared to >80% of MCF-7 cells (Fig. 4).

Functional Status of Endogenous ER in MCF10AT cells

Although our results demonstrated that cells of the MCF10AT system were capable of synthesizing ER that localized to the nucleus, it was still necessary to establish that this ER could mediate transcriptional activation. This was assessed by measuring the effect of E_2 on transient expression of the bacterial CAT reporter gene in JA12, a plasmid with CAT expression regulated by tandem EREs upstream of a minimal TK promoter (15) and by determining the effect of E_2

14

on expression of the endogenous PgR genes in MCF10AT cells.

CAT expression

A typical assay of CAT activities obtained after transfection of MCF10AneoT cells with JA-12 is illustrated, and results of three independent transfections are summarized in Fig. 5. Extracts from MCF10AneoT cells transfected with JA-12 and grown in the absence of E_2 had approximately 2-fold higher levels of CAT activity than those transfected with control, enhancerless minimal promoter construct p-37TKCAT (16). Induction of CAT expression was observed in MCF10AneoT cells cultured in the presence of as little as 10^{-10} M E_2. At this concentration, the level of CAT in MCF10AneoT lysates was able to acetylate ~4% of input chloramphenicol in 4 h. Optimal induction of CAT expression (~24% conversion of input chloramphenicol in 4 h) was obtained with 10^{-9} M E_2. The level of CAT activity in lysates from MCF10AneoT cells transfected with p-37TKCAT was unaffected by exposing the cells to E_2 (data not shown). The E_2 antagonist, ICI 164,384, was used to establish the specificity of E_2-induced response in MCF10AneoT cells. ICI 164,384 at a 100-fold higher concentration than E_2 (10^{-7} vs 10^{-9} M), reduced E_2-induced CAT activity by 50% (Fig.5). Co-transfection with pCH110, which expresses β-galactosidase activity at a constant level regardless of E_2 concentration, confirmed that these results were not due to differences in transfection efficiency or cell viability (data not shown). The functional status of ER could not be reliably determined in MCF10AT3c cells because of the low level of CAT expression obtained with calcium-mediated transfection. This is most likely due to poor uptake of DNA, since low levels of CAT

and β-galactosidase expression were also obtained after transfection of these cells with pCAT and pCH110, respectively.

PgR expression

Levels of PgR protein were determined in cell lysates from MCF10AneoT, MCF10AT3c and the PgR$^+$ breast tumor cell line T47D by immunoprecipitation and Western blotting analysis. The majority of PgR protein detected in lysates from T47D cells had an electrophoretic mobility corresponding to that of the A (Mr ~83 kDa) and B (Mr ~112 kDa) forms of PgR with a trace of protein with an apparent Mr ~52 kDa (Fig. 6, lane 1). In contrast, the bulk of protein binding anti-PgR antibody from lysates of E$_2$-treated MCF10AneoT and MCF10AT3c cells had the mobility of a 52 kDa protein and contained only trace amounts of PgR protein with the mobility of A form PgR and no detectable B form. The PgR-A protein in MCF10AT3c cells migrated slightly slower than those seen in the positive control breast cancer cell line T47D and MCF10AneoT cells. This difference in mobility may be due to the difference in protein loading or may reflect a difference in the level or number of sites of phosphorylation. Alternatively, the difference in migration may be due to the presence of isoforms that may not arise from multiple phosphorylation events (24). Samples prepared from untreated MCF10AneoT and MCF10AT3c cells had barely detectable levels of the 52 kDa protein and none of the larger forms (Fig. 6, lanes 4 and 5). As the PgR epitope recognized by the monoclonal antibody used in these experiments has not been localized, the origin of the E$_2$ inducible 52 kDa protein remains to be established.

16

One possibility is that it is a recently reported 45-50 kDa C form of PgR (24).

Effect of E_2 on anchorage independent growth of MCF10AT3c cells

Monolayer growth of MCF10A cells and MCF10A cells rendered ER^+ after stable transfection

with an ER expression plasmid is not significantly enhanced by addition of E_2 to the growth

medium (10). Similarly, we have found no significant effect of E_2 on monolayer proliferation of

MCF10AneoT cells (data not shown). MCF10A cells do not form colonies in soft agar (9).

However, both transfection with T24 Ha-ras (7) and transplant passage result in enhanced

capacity for anchorage independent growth. Under the conditions of assay utilized in our

experiments, MCF10AneoT cells had a colony forming efficiency (CFE) of 10% with the

majority of the colonies smaller than 100 μm in diameter. E_2 had no significant effect on either

the CFE or the average colony size of MCF10AneoT cells (data not shown). However, E_2

treatment did lead to the rare appearance of colonies with diameters >200 μm (~1/8 x10^4

colonies). In the absence of E_2, MCF10AT3c cells had a CFE of 25% and approximately 40% of

these colonies had a diameter >100 μm; none had a diameter >200 μm. The CFE of

MCF10AT3c cells showed a dramatic increase when the cells were exposed to physiological

concentrations of E_2 (Fig. 7). E_2 treatment also enhanced the rate of growth in soft agar with ~

1/40-80 colonies larger than 200 μm.

Correlation of ER expression with the methylation status of ER gene in the MCF10AT system

The ER gene contains several CpG islands in its promoter and first exon that are rich in sites

recognized by methylation sensitive restriction endonucleases (25). There are several reports indicating that methylation of a number of these sites is correlated with silencing of ER (26,27). The methylation status of the CpG island in exon 1 was examined by Southern blot analysis of DNA digested with the methylation sensitive enzyme, NotI, and the methylation insensitive enzyme, EcoRI. The 3.1 kbp EcoRI fragment containing this CpG island has a single NotI site. NotI cleaves the 3.1 kbp fragment, releasing 1.2 and 1.9 kbp fragments if the site is completely unmethylated (22). Our results (Fig. 8) indicate that this NotI site is unmethylated in most MCF10A cells and that the proportion of methylated to unmethylated NotI sites in exon1 does not change in MCF10AneoT and its derivatives. This suggests that even though loss of methylation at this NotI site may be an indicator of a generalized lack of methylation in the CpG islands of the ER and of active ER transcription in breast tumor cells and lines (26, 27), loss of methylation at the NotI site in exon1 is not sufficient to allow activation of ER transcription in MCF10A cells.

Discussion

By examining gene expression in a number of the cell lines that comprise the MCF10AT xenograft model for progression of human proliferative breast disease, we have demonstrated that expression of endogenous ER occurs only in MCF10A-derived lines that are transfected with and expressing T24 Ha-ras. Although the steady-state levels of ER transcripts are very low, our data show that the ER protein expressed in cell lines of the MCF10AT system is readily detected by Western blots suggesting efficient translation of ER mRNAs and/or stabilization of the ER

protein in MCF10AT system cells. Our data further indicate that the ER expressed in cell lines of the MCF10AT system is functional and can mediate E_2 induced transcription of both endogenous and transfected genes as well as stimulation of CFE and growth of MCF10AT3c cells in soft agar.

Our studies also revealed that the majority of PgR-related protein isolated from MCF10AneoT and MCF10AT3c cells has a molecular size of ~52 kDa rather than the equimolar expression of PgR A and B forms observed in normal human tissues (28) and breast cancer cell lines (29; Fig. 6). Translation from an internal initiation codon AUG encoded in exon 2 (Met[595]) has been shown to lead to synthesis of a 45-50 kDa PgR termed the C receptor (24). The supposition that the 52 kDa protein we have observed is, or is similar to, the C form of the PgR is supported by the observation that anti-PgR antibodies that recognize epitopes in the amino-terminal domain encoded in exon 1 do not detect PgR in MCF10AneoT and MCF10AT3c cells (data not shown). Ongoing molecular and functional characterization of the 52 kDa protein should determine the relationship between the 52 kDa protein and the 83 kDa PgR and clarify the potential role of the 52 kDa protein in progression in the MCF10AT system. However, regardless of the outcome of these studies, our results clearly demonstrate that synthesis of both the small amount of 83 kDa PgR and the 52 kDa protein is induced by E_2 in an ER-mediated process.

Our results have not provided many clues as to the mechanism(s) by which ER transcription became activated after transfection of MCF10A cells with T24 Ha-ras. Although not all studies are in agreement (30,31), there are a number of reports indicating that the silencing of ER expression in breast tumors and breast tumor cell lines is associated with extensive methylation

19

of C residues in the exon 1 CpG island of ER (26,27,32), including those in the NotI site examined in the studies reported here. Treatment with 5-azadeoxycytidine, which is incorporated into DNA where it acts as an inhibitor of 5-C-DNA methyltransferase (33,34), results in partial loss of methylation at a number of CpG sites including the exon 1 NotI site in the ER gene of ER⁻ MDA-MB-231 breast cancer cells. It also results in expression of functional ER protein, strengthening the suggestion that methylation plays a role in silencing ER transcription (35). Our data demonstrate 1)that lack of methylation at the NotI restriction site cannot by itself be used as a direct indicator of transcriptional activation of the ER gene in breast cells and 2) that a low level of methylation at the NotI site, which is characteristic of normal breast tissue (26), is not sufficient to allow expression of ER in MCF10A cells. The low level of methylation at this NotI site is similar in both ER⁻ MCF10A cells and ER⁺ MCF10AneoT and MCF10AT3c cells. (Fig. 8). These results do not rule out the possibility that methylation of other C residues in the exon 1 region or at upstream sites in the ER promoter plays a role in regulating ER expression. We are currently evaluating this by analyzing methylation of all C residues in the promoter and exon 1 regions of MCF10A and MCF10AneoT ER genes.

An alternative mechanism for transcriptional activation of the ER gene that should be considered is that expression of a mutated Ha-ras gene leads to alterations in levels or activity of transcription factors that enhance ER transcription. Since Ha-ras mutations are rare in human breast cancer, there has been speculation that T24 Ha-ras expression mimics the effect of some more common, as yet unidentified, genetic defect that leads to development of breast cancer (6,8). However, since overexpression of normal Ha-ras is a property of both benign proliferative

and malignant human breast tissues (36), it is possible that low level expression of mutated Ha-ras is equivalent to a high level expression of normal Ha-ras in maintaining growth potential of human breast epithelial cells in vivo. Our data indicate that a certain threshold level of Ha-ras may be required for promoting neoplastic progression, and that MCF10AneoN cells probably fail to produce persistent lesions because the level of Ha-ras expression in these cells is not significantly higher than in untransfected MCF10A cells (Fig. 2 and unpublished results).

Our studies show that expression of ER in MCF10AneoT cells is not sufficient to allow an E_2 induced increase in either the potential for anchorage independent growth (CFE) or the average rate of growth of colonies. This is consistent with the finding that the sex of the host had little or no influence on the establishment or growth of MCF10AneoT lesions (F. Miller, unpublished data). However, E_2 treatment in vitro did allow detection of a small population of MCF10AneoT cells with the potential to form large (>200 μm) colonies in soft agar. In contrast, MCF10AT3c cells, which had undergone three rounds of selection for ability to form lesions in vivo, responded to E_2 treatment with a significant increase in both CFE and colony size. This result, combined with the preliminary observation that MCF10AT1 cells formed lesions with elements of invasive carcinoma only in female mice (F. Miller, unpublished data), suggests the possibility that while E_2/ER-mediated processes are not necessary for growth and/or establishment of lesions by MCF10AneoT cells, they greatly enhance the growth potential of a small subset of ER^+ cells in the MCF10AneoT population and that this population is enriched in MCF10AT lesions by xenograft passage. This leads to the predictions that 1) E_2-responsive ER^+ cells will be enriched relative to ER^- cells in the most progressed areas of MCF10AT system lesions and 2)

21

an increase in degree of progression and/or size of the most progressed areas of lesion will occur in hosts with elevated E_2 levels relative to those lacking E_2. Studies of the histology and expression of selected genes in lesions from E_2 supplemented hosts as compared to anti-estrogen treated hosts are currently underway to test these hypotheses.

In summary, although much work remains to be done to dissect the underlying mechanisms of ER activation in MCF10AneoT cells and the role of RAS in development of human breast tumors, the studies reported here indicate that the presence of a functionally active ER in MCF10AT system cells will make the MCF10AT xenograft model extremely useful to study molecular alterations in early breast cancer and the role of estrogenic compounds in neoplastic progression of human breast epithelial cells.

References

1. Petersen OW, Hoyer PE, van Deurs B: Frequency and distribution of estrogen receptor-positive cells in normal, nonlactating human breast tissue. Cancer Res 47: 5748-5751, 1987

2. Jacquemier JD, Hassoun J, Torrente M, Martin PM: Distribution of estrogen and progesterone receptors in healthy tissue adjacent to breast lesions at various stages - immunohistochemical study of 107 cases. Br Cancer Res Treat 15: 109-117, 1990

3. McGuire WL, Carbone PP, Sears ME, Eschert GC: Estrogen receptors in human breast cancer: an overview. In: McGuire WL, Carbone PP, and Voller EP (eds.), Estrogen Receptors in Breast Cancer. Raven Press, New York, NY, 1975, pp 1-7

4. Lippman ME, Dickson RB: Breast Cancer: Cellular and Molecular Biology. Kluwer Academic Publishers, Boston, MA, 1988, pp 119-165

5. Wittligg JL: Steroid hormone receptors in breast cancer. Cancer (Phila.) 53: 630-643, 1984

6. Miller FR, Soule HD, Tait L, Pauley RJ, Wolman SR, Dawson PJ, Heppner GH: Xenograft model of human proliferative breast disease. J Nat Cancer Inst 85: 1725-1732, 1993

7. Basolo F, Elliott J, Tait L, Chen-XQ, Maloney T, Russo IH, Pauley R, Momiki S, Caamano J, Klein-Szanto AJ, Russo J: Transformation of human breast epithelial cells by c-Ha-ras oncogene. Mol Carcinogen 4: 25-35, 1991

8. Dawson PJ, Wolman SR, Tait L, Heppner GH, Miller FR: MCF10AT: A model for the evolution of cancer from proliferative breast disease. Am J Pathol 148: 313-319, 1996

9. Soule HD, Maloney TM, Wolman SR, Peterson WD, Brenz R, McGrath CM, Russo J,

Pauley RJ, Jones RF, Brooks SC: Isolation and characterization of a spontaneously immortalized human breast epithelial cell line, MCF-10. Cancer Res 50: 6075-6086, 1990

10. Pilat MJ, Christman JK, Brooks SC: Characaterization of the estrogen receptor transfected MCF10A breast cell line 139B6. Breast Cancer Res Treat 37: 253-266, 1996

11. Wiese TE, Kral LG, Dennis KE, Butler WB, Brooks SC: Optimization of estrogen growth response in MCF-7 cells. In Vitro Cell Dev Biol 28A: 595-602, 1992

12. Green GL, Gilna P, Waterfield M, Baker A, Hert Y, Shine J: Sequence and expression of human estrogen receptor complementary DNA. Science (Washington D.C.) 231: 1150-1154, 1986

13. Reddy EP, Reynolds RK, Santos E, Barbacid M: A point mutation is responsible for the acquisition of transforming properties by the T24 bladder carcinoma oncogene. Nature (London) 300: 149-152, 1982

14. Laemmli UK: Cleavage of structural proteins during the assembly of the head of bacteriophage T4. Nature (London) 227: 680-685, 1970

15. VanderKuur JA, Hafner MS, Christman JK, Brooks SC: Effects of estradiol-17β analogues on activation of estrogen response element regulated chloramphenicol acetyltransferase expression. Biochemistry 32: 7016-7021, 1993

16. Strahle U, Schmid W, Shutz G: Synergistic action of the glucocorticoid receptor with transcriptional factors. EMBO J 7: 3389-3395, 1988

17. Graham F, van der Eb A: A new technique for the assay of infectivity of human adenovirus 5 DNA. Virology 52: 456-467, 1973

18. Gorman CM, Moffat LF, Howard BH: Recombinant genome which express chloramphenicol acetyltransferase in mammalian cells. Mol Cell Biol 2: 1044-1051, 1982

19. Bradford MM: A rapid and sensitive method for the quantitation of microgram quantities of protein utilizing the principle of protein-dye binding. Anal Biochem 72: 248-254, 1976

20. Current Protocols in Molecular Biology, Chapter 2, Unit 2.2, John Wiley & Sons, Inc.

21. Nelson M, McClelland M: Effect of site-specific methylation on DNA modification methyltransferases and restriction endonucleases. Nucleic Acids Res 17 Suppl: 389-415, 1989

22. IssaJP, Ottaviano YL, Celano P, Hamilton SR, Davidson NE, Baylin SB: Methylation of the oestrogen receptor CpG island links ageing and neoplasa. Nature Genet 7: 536-540, 1994

23. Locus HUMERMCF, accession M12674

24. Wei LL, Gonzalez-Aller C, Wood WM, Miller LA, Horowitz KB: 5' heterogeneity in human progesterone receptor transcripts predicts a new amino terminal truncated "C"-receptor and unique A-receptor messages. Mol Endocrinol 4: 1833-1840, 1990

25. Locus HSERB5FR, accession X62462

26. Lapidus RG, Ferguson AT, Ottaviano YL, Parl FF, Smith HS, Weitzman SA, Baylin SB, Issa J-P, Davidson NE: Methylation of estrogen and progesterone receptor gene 5' CpG islands correlates with lack of estrogen and progesterone receptor gene expression in breast tumors. Clin Cancer Res 2: 805-810, 1996

27. Ottaviano YL, Issa J-P, Parl FF, Smith, HS, Baylin, SB, Davidson, NE: Methylation of the estrogen receptor gene CpG island marks loss of estrogen receptor expression in human breast cancer cells. Cancer Res 54: 2552-2555, 1994

28. Feil PD, Clarke CL, Satyaswaroop PG: Progestin mediated changes in progesterone receptor forms in the normal human endometrium. Endocrinol 123: 2506-2513, 1988

29. Lessey BA, Alexander PS, Horowitz KB: The subunit structure of human breast cancer progesterone receptors: characterization by chromatography and photoaffinity labeling. Endocrinol 112: 1267-1274, 1983

30. Falette NS, Fuqua SA, Chamness GC, Cheah MS, Greene GL, McGuire WL: Estrogen receptor gene methylation in human breast tumors. Cancer Res 50: 3974-3978, 1990

31. Kass DH, Shen M, Appel NB, Anderson DE, Saunders GF: Examination of DNA methylation of chromosomal hot spots associated with breast cancer. Anticancer Res 13: 1245-1251, 1993

32. Piva R, Rimondi AP, Hanau S, Maestri I, Alvisi A, Kumar VL, del Senno L: Different methylation of oestrogen receptor DNA in human breast carcinomas with and without oestrogen receptor. Br J Cancer 61: 270-275, 1990

33. Ferguson AT, Lapidus RG, Baylin SB, Davidson NE: Demethylation of the estrogen receptor gene in estrogen receptor-negative breast cancer cells can reactivate estrogen receptor gene expression. Cancer Res 55: 2279-2283, 1995

34. Creusot F, Acs G, Christman JK: Inhibition of DNA methyltransferase and induction of Friend erythroleukemia cell differentiation by 5-azacytidine and 5-aza-2'-deoxycytidine. J Biol Chem 257: 2041-2048, 1982

35. Taylor SM, Jones PA: Mechanism of Action of Eukaryotic DNA Methyltransferase: Use of 5-azacytosine containing DNA. J Mol Biol 162: 679-692, 1982

36. Clark GJ, Der CJ: Aberrant function of the ras signal transduction pathway in human breast

cancer. Breast Cancer Res Treat 35: 33-144, 1995

Fig. 1. Southern blot analysis of RT-PCR amplified ER cDNAs in the MCF10AT system.

Lane 1 contains ER DNA amplified from MCF10A; lane 2, MCF10Aneo; lane 3, MCF10AneoN;

lane 4, MCF10AneoT; lane 5, MCF10AT1; lane 6, MCF10AT2b, and lane 7, MCF10AT3c. Lane

8, denotes ER DNA amplified from a plasmid containing the full length human ER DNA sequence.

Amplified DNA fragments were subjected to Southern blot hybridization analysis with a full length

human ER DNA probe. Note that the 967 bp fragment amplified by RT-PCR using ER specific

primers is detectable only in cDNAs amplified from MCF10AT and other cells of the MCF10AT

system.

Fig. 2. Detection of mutated (T24) c-Ha-ras mRNA expression in cells of the MCF10AT system.

NaeI-restriced Ha-ras cDNAs from:

Lane 1, MCF10A; lane 2, MCF10Aneo; lane 3, MCF10AneoN; lane 4, MCF10AneoT; lane 5,

MCF10AT1; lane 6, MCF10AT2b; lane 7, molecular size markers. Note the novel 179 bp bands in

lanes 4-6, indicating the presence of cDNAs with a single base RAS activating substitution at codon

12. See Methods for details.

Fig. 3. Detection of ER protein by immunoprecipitation and Western blot analysis in MCF-7 and cells of MCF10A derivatives.

100 µg (MCF-7) to 200 µg (MCF10AneoT, MCF10AT3c, MCF10Aneo) of cytosolic protein was used for each immunoprecipitation with 10 µg/ml of anti-ER mAb D547. For Western blot analysis, 3 µg/ml of the same antibody was used. Lane 1, represents MCF-7; lane 2, MCF10AT3c; lane 3, MCF10AneoT and lane 4, MCF10Aneo. Note the absence of immunoreactivity with ER mAb in MCF10Aneo cells.

Fig. 4. Immunocytochemical detection of ER in MCF-7 (Panel A) and MCF10AT3c cells (Panel B). Cells were incubated with anti-human ER mAb H222 followed by fluorescein tagged rabbit anti-rat IgG following recommended procedures of the supplier (Abbot Laboratories). Note that under identical conditions of preparation, intensity of nuclear fluorescence in MCF-7.cells is stronger than in MCF10AT3c cells and that, at similar cell density, a greater percentage of MCF-7 cells have high levels of nuclear protein capable of binding the anti-ER antibody. Controls, cells incubated either without mAb-H222 or with nonimmune rat IgG, lacked any nuclear fluorescence (data not shown).

Fig.5. Functionality of ER by CAT expression from a transiently transfected ERE-TK-CAT gene in MCF10AneoT cells. Panel A: A typical autoradiogram showing CAT activity in MCF10AneoT cells transfected with the plasmid JA-12 and treated for ~ 40 h with E_2 over a concentration range of 10^{-12} - 10^{-9}M. Lane 1, cells transfected with the hormone-independent plasmid, pCAT containing SV40 promoter and enhancer sequences with the CAT gene; lane 2, p(-37)TK-CAT; lanes 3-8 represent cells transfected with the plasmid JA-12: lane 3, control (minus E_2); lane 4, 10^{-9}M E_2 plus 10^{-7} ICI 164,384; lane 5, 10^{-12}M E_2; lane 6, 10^{-11}M E_2; lane 7, 10^{-10}M E_2 and lane 8 represents cells treated with 10^{-9}M E_2. Panel B: Results obtained from three independent transfections are summarized and graphically represented. Co-transfection with pCH110 which expresses β-galactosidase activity at a constant level regardless of E_2 concentration confirmed that the results were not due to differences in transfection efficiency or cell viability (data not shown).

Fig. 6. Detection of PgR in MCF10AT system cells by immunoprecipitation and Western blot analysis.

Anti-PgR antibody at a concentration of 10 μg/ml were used for immunoprecipitation of PgR from cytosols of E_2-treated and untreated MCF10AneoT and MCF10AT3c cells, and from T47D cells, a constitutive expressor of PgR. For Western blot analysis of immunoprecipitated samples, 5 μg/ml of the same PgR antibody was used. Lane 1 represents the positive control, T47D cells; lanes 2 and 3 represent MCF10AneoT and MCF10AT3c cells treated with $10^{-9}M$ E_2; lanes 4 and 5 represent MCF10AneoT and MCF10AT3c cells without treatment with E_2.

Fig. 7. Effect of E_2 on anchorage independent growth of MCF10AT3c cells. Total number of colonies represent colonies greater than 50 µm in diameter. Colonies were counted according to their size: small, medium, large, and very large, 50-100 µm, 100-200 µm, 200-300 µm and >300 µm in diameter, respectively. Ten microscopic fields were counted to calculate the number of colonies for the whole well, and average of 3 wells for treated (10^{-9} and 10^{-8}M E_2) or untreated cells was calculated. Results are expressed mean±SD of 3 experiments.

Fig. 8. The methylation sensitive restriction enzyme NotI was used to test the methylation status of a representative site in the exon1 CpG island of the ER gene. After EcoRI , NotI cleavage, a 3.1 kbp fragment is detected by a probe specific for this region (See methods) if the NotI site is methylated. If the site is unmethylated, 1.9 and 1.2 kbp fragments result. DNA from MCF-7 cells (Lane 1); DNA from; MCF10A cells (Lane 2); MCF10Aneo cells (Lane 3); MCF10AneoT cells (Lane 4) and MCF10AT3c cells (Lane 5). Note that the proportion of unmethylated (1.9 kbp) EcoRI fragment is identical in Lane 2 (ER⁻ parental MCF10A cells) and Lanes 4,5 (ER⁺ MCF10AT system cells).

Direct Action of Estrogen on Sequence of Progression of Human Preneoplastic Breast Disease

P.V.M. Shekhar[1,3,5], P. Nangia-Makker[2,3], L. Tait[1], G.H. Heppner[1,4], and D.W. Visscher[3]. [1]Breast Cancer Program, [2]Metastasis Program, Karmanos Cancer Institute; [3]Department of Pathology; [4]Department of Internal Medicine, Wayne State University School of Medicine, Detroit, MI 48201.

Running Title: Early effect of estrogen in preneoplastic breast disease

Key words: MCF10AT xenograft model, preneoplasia, estrogen, dysplasia

[5]To whom correspondence should be addressed:

P.V.M. Shekhar
Breast Cancer Program
Karmanos Cancer Institute
110 E. Warren Ave.
Detroit, MI 48201

Tel: (313) 833-0715, Ex. 2326
Fax: (313) 831-7518

Submitted

1

The development of strategies for breast cancer prevention requires improved understanding of the molecular and cellular events that lead to transformation and neoplastic progression of human breast epithelial cells. Epidemiologic evidence suggests that breast cancer risk is related to the duration of unopposed estrogen exposure during puberty and early postmenarchial period, and during the perimenopausal period (1,2). The effects of estrogen on the proliferation of target breast cells are believed to be mediated through transactivation of specific genes which are recognized by the estradiol-estrogen receptor (E_2-ER) complex (3). This process stimulates DNA synthesis, cell division and production of biologically active proteins such as pS2, TGF-α, EGF (4) which increase cell growth and differentiation. Thus, ER-mediated enhancement of cell division could contribute to early and late stages in mammary carcinogenesis by creating cellular susceptibility to genetic errors and by propagating these errors through the enhanced replication of mutated cells (5,6). Despite wide agreement that estrogen is involved in the etiology of breast cancer, there is uncertainty as to the precise role of estrogen in the biology of breast cancer induction: viz., the transformation of high risk normal breast epithelium into cancer cells. Much of this difficulty can be ascribed to the lack of relevant model systems to understand the mechanism of early estrogen action in human mammary tumorigenesis.

In the present study we have utilized the MCF10AT xenograft model of human proliferative breast disease (7) to a) determine whether a relationship exists *in vivo* between estrogen exposure and morphological progression of preneoplastic lesions, and b) define the step(s) in the morphological sequence at which estrogen may act. Previous studies have shown that MCF10AT cells grow in immunodeficient mice, where over a period of several months, they undergo a sequence of progressive histological changes mimicking those seen in breasts of women at high

2

risk of breast cancer (i.e., atypical hyperplasia) that culminate in a significant proportion of grafts with frankly invasive cancer (7). In the absence of estrogen supplementation, proliferative lesions develop but progress sporadically to high risk or malignant lesions within intervals ranging from 7 - 56 weeks (8). These data suggest that in hormonally unsupplemented animals, additional promotional events may be required for the eventual development of neoplasia.

The effects of E_2 on neoplastic progression of ER+ MCF10AT cells were examined in E_2-supplemented ovariectomized female nude mice. 10^7 MCF10AT1 cells were suspended in Matrigel (Collaborative Research, Bedford, MA) and inoculated subcutaneously into the mammary fatpad region of ovariectomized nude mice that received sc implants of 1.7 mg/60 day release E_2 (treated; 13 mice) or placebo (control; 5 mice) pellets (Innovative Research, FL). Animals were observed twice a week and palpated for lesion formation once a week after 5 weeks of injection of MCF10AT1 cells. Pellets were replaced at seven weeks, and all mice sacrificed at 10 weeks post injection by cervical dislocation. National Institutes of Health guidelines for proper and humane use of animals were observed. Lesions were removed, weighed, and portions of lesions were fixed in neutral buffered formalin and embedded in paraffin for histological analysis. Histological grading of lesions were done as described previously (8-11). The categories were, 0 = simple epithelium; 1 = mild hyperplasia; 2 = moderate hyperplasia; 3 = atypical hyperplasia; 4 = carcinoma *in situ* (CIS); 5 = invasive carcinoma. Each lesion was graded according to the most advanced (deviant from normal) morphological pattern.

At 10 weeks, histological analysis of all lesions derived from control MCF10AT1-injected mice showed considerable structural heterogeneity (Fig. 1). The results were similar to what has

3

been reported (8). Three out of five of the control MCF10AT1 lesions displayed histological characteristics of grades 0/1; one lesion exhibited features of grade 3, and the remaining lesion had no epithelium (Fig. 1). In contrast, lesions derived at 10 weeks from E_2-supplemented MCF10AT1-injected mice were uniformly larger (~100-250 mg vs 450-550 mg) and 100% contained ductal epithelia. Histological analysis of lesions derived from estrogen supplemented group revealed that 92% of lesions (Fig. 1) displayed histological features of atypical hyperplasia (5/13), CIS (5/13) or invasive carcinoma (2/13) whereas only 8% (1/13) exhibited histological features of moderate hyperplasia. This is in contrast to lesions derived from control group in which the majority (60%) of lesions displayed features of simple or mild hyperplasia. The histopathology of lesions are shown in (Table 1). In contrast to previous studies with control xenografts (9), estrogen-exposed xenografts demonstrated extensive areas of papillary (as opposed to the "cribriform") growth as well as adenosis-like areas, often with noticeable eosinophilic intraluminal secretion. Estrogen-treated xenografts also differed from previous studies (9) by virtue of demonstrating prominent host inflammatory infiltration and angiogenesis. These results suggest that estrogen exerts a growth promoting effect on benign or premalignant ducts by enhancing a) the frequency of lesion formation, b) the size of lesions, c) the speed of transformation from grades 0/1 to grades 3 and higher, d) the degree of dysplasia, and e) the degree of angiogenesis.

In summary our results from the MCF10AT xenograft model for progressive human proliferative disease not only support the observed epidemiologic link between estrogen and increased risk of breast cancer but indicates that this link is a manifestation of a growth promoting effect of E_2 on ER+ high risk breast epithelial cells, facilitating their progression from

4

preneoplastic to neoplastic grades with atypia, a histological risk factor for the development of new or recurrent breast cancer.

The demonstration of a direct action of estrogen on sequence of neoplastic progression of ER+ MCF10AT cells provides us with an unprecedented opportunity to study the relationships between benign/ premalignant lesions and frankly invasive breast carcinoma. Furthermore, information on selective expression of relevant breast cancer susceptibility genes that correlate with specific histological indices of progression will be extremely useful in screening for agents that can effectively modulate expression of these markers at specific stages of progression.

References

(1) Apter D, Vihko R. Early menarche, a risk factor for breast cancer, indicates early onset of ovulatory cycles. J Clin Endocrinol Metab 1983;57:82-86.

(2) Russo J, Russo IH. Biological and molecular bases of mammary carcinogenesis. Lab Invest 1987;57:112-137.

(3) Pike MC, Spicer DV, Dahmoush L et al. Estrogens, progestogens, normal breast cell proliferation and breast cancer risk. Epidemiol Rev 1993;15:17-35.

(4) Adami HO, Adams G, Boyle P *et al*. Breast cancer etiology. Int J Cancer (Suppl) 1990;5:22-39.

(5) Cohen SM, Ellwein LB. Cell proliferation in carcinogenesis. Science (Washington D.C.) 1990;249:1007-1011.

(6) Russo J, Russo IH. Toward a physiological approach to breast cancer prevention. Cancer Epidemiol Biomarkers Prev 1994;3:353-364.

(7) Miller FR, Soule HD, Tait, L, Pauley RJ, Wolman, SR, Dawson, PJ, Heppner GH. Xenograft model of progressive human proliferative breast disease. J Natl Cancer Inst 1993;85:1725-1732.

(8) Dawson PJ, Wolman SR, Tait L, Heppner GH, Miller FR. MCF10AT: A model for the evolution of cancer from proliferative breast disease. Am J Pathol 1996;148:313-319.

(9) Page DL, Dupont WD, Rogers LW, Rados MS. Atypical hyperplastic lesions of the breast: a long-term follow-up study. Cancer 1985;55:2698-2708.

(10) Page DL, Anderson TJ: Diagnostic histopathology of the Breast. Edinburgh, UK, Churchill Livingstone, 1987, pp 120-145.

(11) Tavassoli FA, Norris HJ: A comparison of the results of long-term follow-up for atypical intraductal hyperplasia and intraductal hyperplasia of the breast. Cancer 1990;65:518-529.

Notes

Fig. 1. Distribution frequency of different grades of progression of MCF10AT1 lesions from the orthotopic sites of control and estrogen-supplemented mice at 10 weeks of implantation. Frequency distribution pattern represents data obtained from five control and 13 estrogen-exposed mice. Numbers indicate grade of lesion. None: no persistent epithelial lesion detected.

Pre print

Altered P53 conformation: A novel mechanism of wild-type *p53* functional inactivation in a model for early human breast cancer

P.V.M. SHEKHAR[1,2], R. WELTE[3], J.K. CHRISTMAN[4,5], H. WANG[1] and J. WERDELL[1]

[1]Breast Cancer Program and [2]Department of Pathology, Karmanos Cancer Institute and Wayne State University, School of Medicine, Detroit, MI 48201, USA; [3]Unit of Public Health, University of Ulm School of Medicine, 89081 Ulm, Germany; [4]Department of Biochemistry and Molecular Biology, [5]Eppley Institute for Cancer Research and UNMC/Eppley Cancer Center, University of Nebraska Medical Center, Omaha, NE 68198, USA

Abstract. The p53 protein is a transcription factor that is frequently mutated in human malignancies. Using the MCF10AT model for early human breast cancer we show that P53 protein is unmutated indicating that mutations are not necessary for alterations in growth and morphology that accompany preneoplastic stages of breast tumor progression. Although p53 protein is wild-type in cells of the MCF10AT model system, it exists predominantly in a conformationally altered state that is defective in its ability both to bind DNA in a sequence-specific manner and to induce transcriptional activation from the WAF-1 promoter. This contrasts with P53 from the non-tumorigenic parental MCF10A cells which is predominantly conformationally normal and functionally active. The possibility that stabilized wild-type but conformationally altered P53 plays a role in the neoplastic progression of preneoplastic MCF10AT system cells is discussed.

Introduction

Inactivation of the *p53* tumor suppressor gene is one of the most common events in neoplastic transformation. Point mutations or other genomic alterations in *p53* have been identified in more than 50% of human cancers. In many of the remaining tumor types, wild-type P53 protein is functionally inactivated by mechanisms that include binding to the cellular MDM2 oncoprotein or sequestering of P53 in the cytoplasm (1). While missense mutations of *p53* gene represent an early event in the transformation and progression of tumors of the colon (2), esophagus (3) and hematopoietic system (4), mutations of *p53* in breast cancer are less common, occurring in 20-30% of breast carcinomas examined (5).

Structurally, P53 has a typical transcription factor containing identifiable transcription activation, sequence-specific DNA binding and oligomerization domains (6). Mutational analysis has identified all three of these domains as essential for the growth suppressive properties of P53, i.e., deletion of any one of these domains inhibits the ability of P53 to act as a tumor suppressor (7). Wild-type P53 recognizes a 20 bp motif consisting of two copies of the consensus sequence 5'-PuPuPuC(T/A)(T/A)GPyPyPy-3'. When these P53-responsive elements are adjacent to a minimal promoter they stimulate gene expression in a P53-dependent fashion (8-10). Mutant P53 proteins that fail to bind DNA (8) also fail to act as transcriptional activators at P53-response elements (11-13). Muscle creatine kinase, MDM2, GADD45, WAF1/Cip1, epidermal growth factor receptor and cyclin G genes (14-19) are among the genes that contain sites with high homology to the 20 bp P53 binding site consensus motif. P53 plays a role in regulating genes involved in cell cycle (20), cell cycle arrest after DNA damage (16), and commitment of some cells to apoptosis (21-23).

We have utilized the MCF10AT model system to evaluate the importance of P53 alterations in the early stages of breast cancer. This model is comprised of an array of cell lines that undergo a sequence of progressive histological changes mimicking those seen in breasts of women at high risk for breast cancer (24-26). Here, we show that wild-type P53 protein in cells of the MCF10AT system exists predominantly in a conformationally altered state that is defective in its ability both to bind DNA in a sequence-specific manner and to induce transcriptional activation from the WAF-1 promoter. This contrasts with P53 from the non-tumorigenic parental MCF10A cells which is functionally active. The possibility that stabilized wild-type but conformationally altered P53 plays a role in the neoplastic progression of preneoplastic MCF10AT cells is discussed.

Materials and methods

Cell culture. MCF10A, MCF10Aneo (vector transfected), MCF10AneoN (normal Ha-*ras*-transfected), MCF10AneoT (T24 Ha-*ras*-transfected) (24) and cell lines derived from

---

Correspondence to: Dr P.V.M. Shekhar, Breast Cancer Program, Karmanos Cancer Institute, 110 E. Warren Avenue, Detroit, MI 48201, USA

alternating *in vivo* transplantation and *in vitro* culture (MCF10AT system cells) were maintained in DMEM/F-12 medium supplemented with 2.5% equine serum, 0.1 μg/ml cholera toxin, 10 μg/ml insulin, 0.5 μg/ml hydrocortisone, 0.02 μg/ml epidermal growth factor, 100 IU/ml penicillin and 100 μg/ml streptomycin.

Analysis of P53 protein expression
Metabolic labeling. Exponentially growing MCF10A and MCF10A-derived cells were incubated for 3 h in methionine-free DMEM with 2% dialyzed fetal bovine serum supplemented with 100 μCi of [^{35}S]-methionine (specific activity 1,083 Ci/mmol, New England Nuclear, Boston, MA). Monolayers were gently washed twice with phosphate-buffered saline (PBS) and treated with 400 μl of lysis buffer (150 mM NaCl, 10 mM Tris-HCl, pH 7.5, 1% Triton X-100, 1 mM phenyl methyl sulfonyl fluoride, PMSF) at 4°C. Cell lysates were cleared by centrifugation for 15 min at 10,000 x g and used immediately for immunoprecipitation. Aliquots of lysate containing equivalent amounts of radiolabel incorporated into trichloracetic acid insoluble material (10^7 cpm) were immuno-precipitated by incubating overnight at 4°C with 1 μg of anti-P53 monoclonal antibodies (mAbs) pAb421 (27) or pAb240 (28; Oncogene Science, Inc., Cambridge, MA) or normal mouse IgG. Protein G Sepharose beads were then added and incubation continued for 1 h at 4°C. Sepharose beads were pelleted by centrifugation and washed four times in lysis buffer. Bound proteins were resolved by sodium dodecyl sulphate (SDS)-polyacrylamide gel electrophoresis on 8.5% poly-acrylamide gels. Gels were fixed and processed for fluoro-graphy. Radiolabeled proteins were visualized by autoradio-graphy of the dried gels.

Immunofluorescence. MCF10AT3b (5×10^4) cells were plated on coverslips in media as described before, and after 2-3 days of culture when the cells reached confluence, the slides were rinsed twice with PBS and fixed in methanol:acetone (1:1) for 3 min at -20°C. Cells were incubated with pAb421 or pAb240 at 1 μg/ml following incubation in blocking solution [1% bovine serum albumin (BSA)/PBS] for 30 min. Coverslips were washed for 30 min with PBS and incubated for 45 min in fluorescein-conjugated goat anti-mouse IgG antibody (Jackson ImmunoResearch Labs, West Grove, PA) diluted 1:500 in blocking solution. Coverslips were then washed for 30 min in PBS, mounted and viewed using a confocal micro-scope equipped with an Argon/Krypton laser (model LSM 410; Carl Zeiss, Inc., Thornwood, NY). Negative controls were incubated with 1 μg/ml normal mouse IgG substituted for pAb421 and pAb240.

PCR-SSCP analysis of p53 transcripts. Total cellular RNA (2 μg/15 μl) from MCF10A and MCF10AneoT-derived cells was reverse transcribed using oligo (dT)$_{15}$ primer. An aliquot of the reaction mixture was subjected directly to PCR using primer a$^+$, 5'-GTCACTGCCATGGAGGAGCCG-3' (base 113-133) (29), and primer t$^-$, 5'-TTATGGCGGGAGGTAG ACTG-3' (base 1244-1263) (29) to amplify *p53* cDNA. As a control, the same primers were used to amplify wild-type *p53* cDNA from the plasmid, pC53-SN3 (30). PCR was performed

1 μM of each primer, 10 nM of each dNTP, 5 μCi of [α-^{32}P]-dCTP and 1X PCR buffer (Promega, Madison, WI). PCR was carried out for 35 cycles of 2 min at 95°C, 2 min at 59°C and 3 min at 68°C. A 5 μl sample of each reaction was subjected to electrophoresis on 1% agarose gel and radiolabeled products visualized by autoradiography. Individual portions of the ^{32}P-labeled PCR products were digested with restriction enzymes, AvaII, BsmAI, BsmI, MaeIII or StuI and subjected to electro-phoresis on 2.5% agarose gels.

For single strand conformation polymorphism (SSCP) analysis, the restricted PCR fragments were diluted 9-fold in denaturation solution (95% HCONH$_2$, 20 mM EDTA, pH 8.0) and heated at 95°C for 5 min. The denatured samples were electrophoresed through 6% polyacrylamide gels in 0.5X Tris-borate buffer containing 1 mM EDTA at 4°C and 25 W constant power. Following electrophoresis, gels were dried and subjected to autoradiography.

Genomic DNAs isolated from MCF10A-derived cells and normal human placenta were subjected to hot start PCR using primers e$^+$ (5'-GATGCTGTCCCCGGACGATATT-3', base 250-271) (29) and f$^-$ (5'-TTGGCTGTCCCAGAATGCAAG AA-3', base 458-480) (29). Radiolabeled PCR products were analyzed by SSCP as described above.

Analysis of DNA binding activity of P53
Preparation of cell extracts. MCF10A and MCF10AT system cells (MCF10AT1, MCF10AT2b. MCF10AT3b and MCF10AT3c) were plated on 100-mm dishes and grown to 75% confluency at 37°C. Whole cell extracts were prepared by three cycles of freezing and thawing in 0.1 ml of buffer containing 20 mM HEPES (pH 7.9), 1 mM dithiothreitol (DTT), 1 mM EDTA, 1 mM EGTA, 0.4 M KCl, 1 mM PMSF, 1 μg/ml each of leupeptin, aprotinin, and pepstatin, and 20% glycerol. Extracts were dialyzed and clarified by centrifugation at 14,000 x g for 10 min and stored at -70°C. Protein concentrations were determined by the Bradford method (31).

DNA binding assay. Oligonucleotides containing the WAF1 P53 binding site (top strand, 5'- aagtggatccGAACATGTCCC AACATGTTg-3'; bottom strand, 5'-aggaagatctcAACATGTT GG-GACATGTTC-3) (17) or the vitamin D responsive element of the human osteocalcin gene (top strand, 5'-aagtgg atccTTGGTGACTCACCGGGTGAACGGGGGCATG-3'; bottom strand, 5'-aggaagatctCAATGCCCCCGTTCACC CGGTGAGTC-3';) (32) were annealed and 5' overhangs were filled in with the Klenow fragment of *E.coli* DNA polymerase I and dATP, dGTP, dTTP and either dCTP (competitors) or [^{32}P]dCTP. Whole cell extracts were preincubated with 2 μg poly(dI-dC) and 0.5 μg mAb (pAb421 or pAb1801) for 30 min at room temperature in 20 μl of binding buffer (20 mM HEPES, pH 7.9, 1 mM DTT, 50 mM KCl, 5 mM MgCl$_2$, 10 μM ZnSO$_4$, 0.1 mg/ml BSA, 0.1% NP40, and 5% glycerol). 5 ng of [α-^{32}P]-labeled ds WAF1 P53 binding site was added and incubated for another 30 min at room temperature. Competitor oligonucleotides (either WAF1 P53 or osteocalcin vitamin D response element) were added during the preincubation step. Reaction mixtures were analyzed by electrophoresis at 160 V on 6% polyacrylamide gels (80:1, acrylamide:bisacrylamide) in 0.5 X Tris-Borate buffer

(8-10°C). Following electrophoresis, gels were dried and autoradiographed.

Analysis of transcription activation function of P53

Plasmid constructs. The ß-galactosidase reporter plasmid, pWAF1/ßgal, was constructed by cloning a 2.4 HindIII WAF1 promoter fragment from pWAF1-Luc into Blue Script/ßgal (17). The wild-type *p53* expression vector pC53-SN3 (30) has a CMV immediate early promoter upstream of the coding sequences for wild-type *p53*. The plasmid, pCMV-neo is identical to pC53-SN3 except that it lacks the *p53* coding sequences.

Transfection. MCF10A, MCF10AneoT, MCF10AT1, and MCF10AT3b cells (5x10⁵ cells per 60 mm dish) were plated 18 h prior to transfection in media as described before. To determine the functionality of endogenous P53, cells were transfected with varying amounts of pWAF1/ßgal (2.5-10 μg) using the calcium phosphate procedure (33). The effect of exogenous wild-type P53 on WAF1-induced reporter activity was determined by cotransfecting cells with 5 μg of WAF1/ßgal and varying amounts of pC53-SN3 (0.5-5 μg). Five μg of WAF1/ßgal was chosen since cells transfected with this amount of the plasmid yielded near maximal reporter activity that was still in the linear range. In both sets of transfection experiments, the control pCMVneo vector was used as carrier DNA to adjust the final concentration of DNA to 10 μg/ml. Cells were incubated with plasmid DNA for 4 h, followed by 3 min incubation with 20% glycerol. Cells were lysed 28 h following transfection and ß-gal activity assayed by ELISA (Boehringer Mannheim, Indianapolis, IN). The reporter plasmid pSVCAT (Promega, Madison, WI) was cotransfected with WAF1/ßgal into MCF10A and MCF10AT derivatives in some experiments to monitor transfection efficiency. The efficiency of wild-type P53 expression from PC53-SN3 in the transfected cells was assessed by Western blot analysis.

Results and Discussion

P53 protein expression. The levels of P53 synthesized *de novo* were examined in exponentially growing cultures by metabolic labeling with [³⁵S]-methionine and immunoprecipitation with anti-P53 antibodies. Cells were incubated with [³⁵S]-methionine for 3 h to ensure achievement of equilibrium labeling in both rapidly degraded and stable forms of P53. MAbs used to detect P53 were pAb421 which binds to an epitope near the carboxyl-terminus: residues 371-380 of human P53 and is reactive to both wild-type and mutant forms, and pAb240 which recognizes a conserved amino acid motif RHSVV, residues 213-217 in human P53. This epitope is cryptic in wild-type P53 but exposed in many oncogenic mutants (34). Normal mouse IgG, used as a control, failed to precipitate 53 kDa proteins from MCF10AT cell lysates (Fig. 1, lane 1, a representative MCF10AT2b lysate is shown). With the exception of MCF10AT1 cells, the ratio of radiolabeled P53 immuno-precipitated with pAb421 relative to total radiolabeled lysate protein was significantly higher for MCF10AT system cells than for MCF10A, MCF10Aneo and MCF10AneoN cells (Fig. 1). Densitometric analysis of the radiolabeled P53
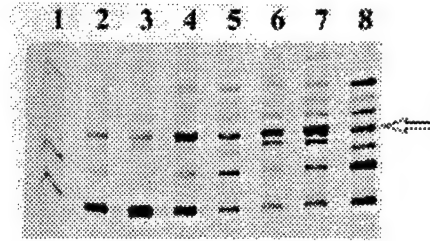
Figure 1. Synthesis of P53 in MCF10A and MCF10AT system cells. Cells were labeled with [³⁵S]-methionine for 3 h and processed for immunoprecipitation with P53-specific mAb pAb421 or normal mouse IgG. Precipitated proteins were analyzed by SDS-PAGE and visualized by fluorography. Note the appearance of enhanced labeling in the lower band of the P53 doublet in MCF10AT cells. Lane 1, MCF10AT2b immunoprecipitated with normal mouse IgG. Lanes 2-8 were immunoprecipitated with mAb pAb421. Lane 2, MCF10Aneo; lane 3, MCF10AneoN; lane 4, MCF10AneoT; lane 5, MCF10AT1; lane 6, MCF10AT2; lane 7, MCF10AT3b and lane 8, MCF10A.
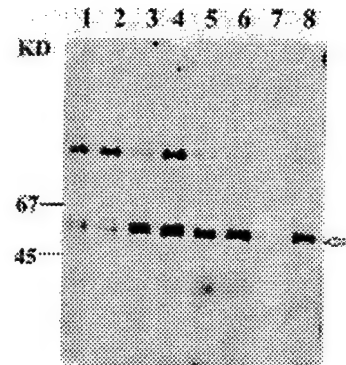
Figure 2. Synthesis and accumulation of conformationally altered P53 in MCF10AT system cells. [³⁵S]-methionine labeled proteins were immuno-precipitated with pAb240 or normal mouse IgG and precipitated proteins separated by SDS-PAGE. Lane 1, MCF10A; lane 2, MCF10AneoN; lane 3, MCF10AneoT; lane 4, MCF10AT1; lane 5, MCF10AT2b; lane 6, MCF10AT3b; lane 8, MCF10AT3c. Lane 7, labeled proteins of MCF10AT3b immunoprecipitated with normal mouse IgG.

MCF10AneoT, MCF10AT2b and MCF10AT3b cells, respectively, as compared to MCF10A, MCF10Aneo or MCF10AneoN cells. A significant portion of the increased radiolabel in pAb421 immunoprecipitable P53 was present in a form that migrated more rapidly than P53 from MCF10A, MCF10Aneo or MCF10AneoN cells. In order to determine whether the two forms of P53 represented wild-type and conformationally altered P53, the radiolabeled proteins in MCF10AT cells were immunoprecipitated with pAb240. This resulted in specific precipitation of a single species of P53 protein that was present in significantly higher amounts in MCF10AT cells than in MCF10A and MCF10AneoN cells (Fig. 2). This difference in ability to bind pAb421 and pAb240 indicates that the increase in levels of total P53 observed in MCF10AT system cells arises primarily from increased levels of conformationally altered wild-type P53. This could occur either by denaturation of wild-type P53 or by the presence of activating mutations (34,35).

Cellular distribution of P53.
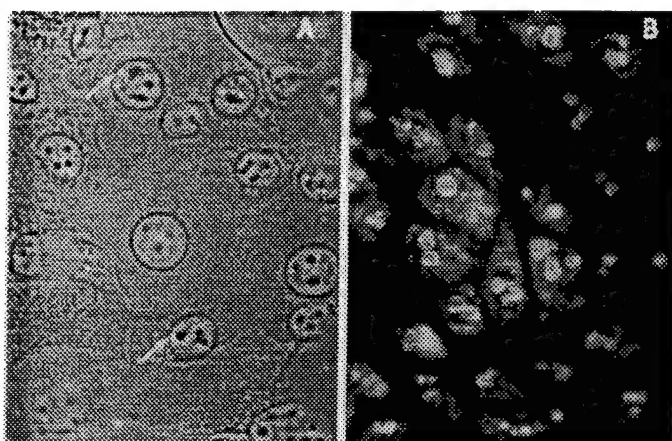
Figure 3. Distribution of P53 in nuclei and cytoplasm of confluent MCF10AT3b cells by immunofluorescence and confocal microscopy. Cells grown on coverslips were fixed in methanol-acetone (1:1, vol/vol) as described in Materials and methods. A, reactivity of P53 to pAb421 is restricted to nuclei of confluent MCF10AT3b cells that is visualized as punctate or stippled nuclei staining (indicated by arrows). B, reactivity of P53 to pAb240 is associated with staining of distinct large aggregates in both the nuclear and cytoplasmic compartments. Photomicrographs were made with a 40x objective.

Figure 4. A, the position of primer pairs, a⁺/ t⁻, and e⁺/ f⁻, are indicated. Reverse transcribed cDNA products amplified by using primer pairs a⁺ and t⁻ were digested with enzymes AvaII, BsmAI, BsmI, MaeIII or StuI as described in Materials and methods. B, SSCP analysis of *p53* gene and cDNAs amplified by the primer pair e⁺/ f⁻. Lane 1, wild-type *p53* encoded plasmid pC53-SN3; lane 2, human placental genomic DNA; lanes 3-5, genomic DNA from MCF10A, MCF10AneoT and MCF10AT3b, respectively; lanes 6-8, *p53* cDNAs amplified from MCF10A, MCF10AneoT and MCF10AT3b, respectively.

(reactive to pAb421 and pAb240 antibodies) in the nuclei and cytoplasm of MCF10AT3b cells. MCF10AT3b cells were chosen since they represented the most advanced serial xenograft passage of MCF10AT system cells, and metabolic labeling experiments have shown these cells to express significant amounts of conformationally altered P53 (Figs. 1 and 2). Results of immunofluorescence microscop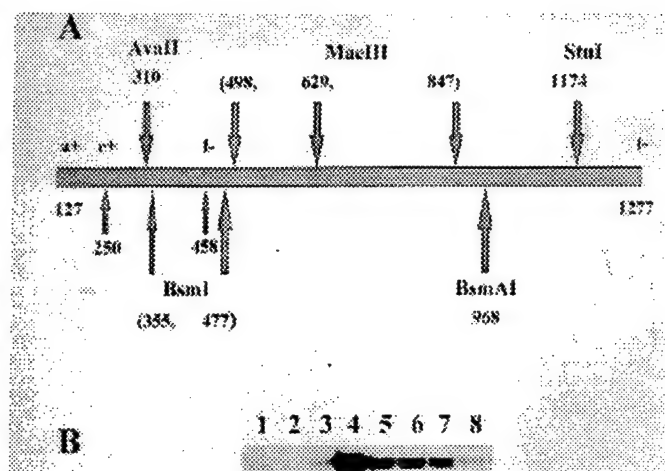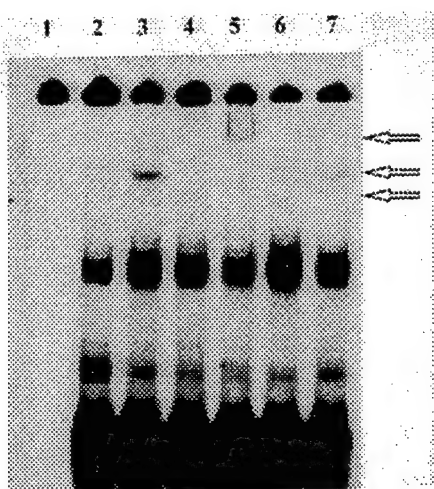y confirm the abundant presence of pAb240-reactive P53 in >95% of MCF10AT3b cells. Staining is often associated with large distinct aggregates in both the nuclear and cytoplasmic compartments (Fig. 3B). Similar accumulation of pAb240 reactive P53 has been reported in MCF-7 cells, suggesting a correlation between increasing accumulation of conformationally altered P53 and increasing potential for tumorigenicity (36). In contrast to pAb240 reactivity, pAb421 reactive protein is exclusively present in the nuclei of confluent MCF10AT3b cells; i.e., >90% of nuclei show punctate or granular staining (Fig. 3A). While pAb421 reactive P53 includes both native and conformationally altered forms in exponentially growing MCF10AT cells (Fig. 1), this reactivity is clearly altered in confluent cells possibly due to modifications that influence pAb421 immunoreactivity.

SSCP analysis of P53 mRNAs amplified from MCF10AT system cells. Since both accumulation of P53 and alteration in conformation as recognized by pAb240 could result from point mutations in the coding region of *p53*, *p53* transcripts amplified from MCF10AT system cells were analyzed for sequence variation by the SSCP method. Total cellular RNA from MCF10A and MCF10AT system cells was transcribed into cDNA using AMV reverse transcriptase and oligo (dT)₁₅. The resultant single stranded cDNA fragments were amplified by PCR as radiolabeled double stranded DNA fragments using a pair of oligonucleotide primers and [α-³²P]-dCTP. PCR amplified fragments from MCF10A and MCF10AT system

human wild-type *p53* cDNA encoded in the plasmid pC53-SN3 (30). Amplification of *p53* cDNA using primers a⁺ and t⁻ yielded a fragment with a nucleotide length of 1151 bp which was identical to that obtained from the wild-type *p53* cDNA, indicating that no major deletions had occurred in the coding regions. In order to analyze for conformational polymorphism arising from point mutations, the amplified cDNA fragments were subjected to restriction digestion with MaeIII, BsmI, StuI or AvaII to obtain overlapping fragments of suitable size for SSCP analysis. The positions of the primers and restriction enzymes used for SSCP analysis are illustrated in Fig. 4A. Restriction fragments derived from and including all of the sequences in exons 1-3 and 5-11 had identical mobilities regardless of whether they were prepared from *p53* cDNAs of MCF10A cells, MCF10AT system cells or the wild-type *p53* cDNA encoded in the plasmid pC53-SN3 (data not shown). However, the mobility of restriction fragments spanning exon 4 that were derived from control wild-type *p53* cDNA differed from those of similar fragments derived from MCF10A and MCF10AT cDNAs. These results were verified by SSCP analysis of exon 4 sequences directly amplified by PCR using primers e⁺ and f⁻ (base 250-480) (29). The mobilities of the exon 4 sequences from genomic DNAs of human placenta and MCF10A, MCF10AneoT or MCF10AT3b cells were identical to each other and to exon 4 sequences from MCF10A, MCF10AneoT or MCF10AT3b cDNAs but differed from those of exon 4 sequences of wild-type *p53* cDNA encoded in the plasmid pC53-SN3 (Fig. 4B). Thus, all MCF10A and MCF10AT system cells analyzed express only one allelic form of *p53*. Sequencing of exon 4 DNA confirmed that its sequence was indeed normal in the *p53* gene of MCF10A and MCF10AT system cells, and that the exon 4 alteration observed in pC53-SN3 p53 cDNA represented a previously characterized allelic polymorphism (CGC→CCC)

Figure 5. P53 from MCF10A cells exhibit sequence-specific DNA binding. Whole cell extracts were prepared from MCF10A cells as described in Materials and methods and assayed for sequence-specific DNA binding by electrophoretic mobility shift assay using the WAF1 P53 binding site as the oligonucleotide probe. MAbs pAb421 or pAb1801 were added as indicated, and the protein-DNA complexes were resolved on a native 6% polyacrylamide gel. Competitor oligonucleotides were added at molar excess; the vitamin D response element was the nonspecific competitor used. Lane 1, free WAF1 DNA probe; lane 2, binding in absence of antibodies; lane 3, binding in presence of pAb421; lane 4, binding in presence of pAb421 and 100X unlabeled WAF1 DNA; lane 5, binding in presence of pAb421 and pAb1801; lane 6, binding in presence of pAb1801 and lane 7, binding in presence of pAb1801 and 100X unlabeled nonspecific competitor.

Figure 6. Sequence-specific DNA binding activity of P53 from MCF10AT xenograft derived cell lines is defective but can be restored with pAb421. Whole cell extracts were prepared from MCF10AT xenografts and assayed for sequence-specific DNA binding by electrophoretic mobility shift assay as described in Materials and methods. MAbs pAb421 or pAb1801 were added as indicated, and the protein-DNA complexes were resolved on a native 6% polyacrylamide gel. Radioinert WAF1-P53 binding site and vitamin D response element added in molar excess were included as specific and nonspecific competitors, respectively. Lane 1, binding in presence of pAb421; lane 2, binding in presence of pAb1801; lane 3, binding in presence of pAb421 and 1801. *Binding in presence of 100-fold excess unlabeled specific competitor and **Binding in presence of 100-fold excess nonspecific competitor.

These results indicate that mutation in *p53* does not play a major role in progression in the MCF10AT model system. Instead, they suggest that changes in the balance between normal and altered conformation of wild-type P53 might provide a mechanistic basis for altered cell division.

To further examine this possibility we analyzed the relationship between levels of pAb240-reactive P53 and P53 capacity for site-specific DNA binding and transcriptional activation.

Analysis of DNA binding function of P53 expressed in MCF10AT system cells. The ability of wild-type P53 to cause G1 arrest *in vivo* is believed to require sequence-specific binding to DNA. Wild-type P53, but not mutant P53 (alterations in the DNA binding domain), binds *in vitro* to sequences matching the consensus 5'-(Pu)$_3$ C(A/T)(A/T) G(Py)$_3$-3' (8). To detect the presence of proteins with capacity to bind the P53 recognition site in the promoter of the WAF-1 gene (17), whole cell extracts of proteins from MCF10A, MCF10AneoT, MCF10AT1, MCF10AT2b, MCF10AT3b and MCF10AT3c cells were tested for binding to a double stranded oligonucleotide containing this site by electrophoretic mobility shift assay. Proteins in whole cell extracts from MCF10A cells gave a low but detectable level of complex formation with the P53 binding site (Fig. 5, lane 2). Addition of either pAb421 or pAb1801 to binding reactions enhanced formation of protein:DNA complexes, although pAb421 was much more efficient in forming a 'supershifted' complex (compare Fig. 5, lane 3 and lane 6). This suggested that both

recognition site in DNA, but that pAb421 is much more efficient in stabilizing the P53:DNA complex. This was confirmed by observation of an additional decrease in the mobility (but not the amount) of the protein:DNA complex when both pAb1801 and pAb421 were present in the binding reaction (Fig. 5, lane 5). Specificity was confirmed by determining that unlabeled oligonucleotides containing the P53 binding site competed effectively with radiolabeled P53 in the formation of the pAb421:P53:DNA complex (Fig. 5, lane 4) while a nonspecific oligonucleotide competitor containing the vitamin D response element had no effect on complex formation (Fig. 5, lane 7). Protein in extracts from MCF10AneoT cells was similar to protein from MCF10A cells in its capacity to form P53:DNA complexes (data not shown). However, proteins in extracts from MCF10AT xenograft derived cell lines did not form detectable complexes with the WAF-1 P53 binding site (data not shown) unless pAb421 was also present in the binding mixture (Fig. 6, lane 1). pAb1801 had no stabilizing effect on P53 binding (Fig. 6, lane 2). These results indicate that in both MCF10A and MCF10AneoT cells, a portion of native P53 is dependent on pAb421 for complex formation with the P53 binding site and that this portion is increased in cell lines derived from MCF10AT xenografts where all P53:DNA complex formation requires the presence of pAb421. Since the ratio of conformationally altered P53:normal P53 is much higher in cells of MCF10AT xenograft derived lines than in MCF10A and MCF10AneoT cells, these results imply an inverse relationship between availability of native P53 for DNA
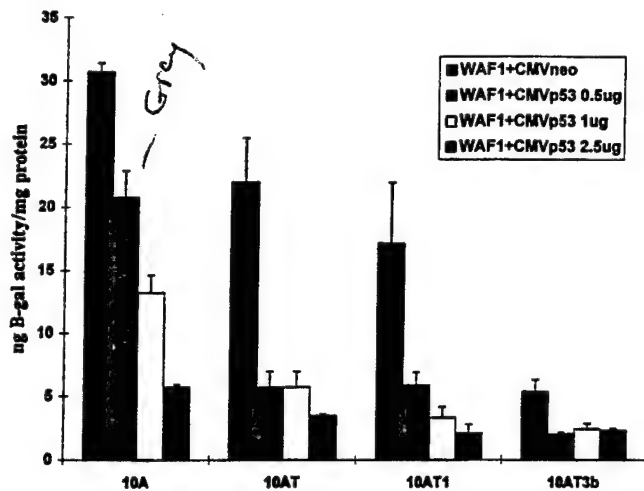
Figure 7. Functionality of P53 by reporter gene expression from a transiently transfected WAF1/ßgal construct in MCF10A and MCF10AT system cells. Cells were transfected with pWAF1/ßgal alone (5 µg) or in combination with pC53-SN3 (0.5-2.5 µg), an expression vector for wild-type P53 under the control of CMV promoter. The total amount of DNA in all samples were maintained at 10 µg with pCMV-neo as carrier DNA. Cell lysates prepared 28 h after transfection were analyzed for ß-gal (reporter) activity by ELISA. Results obtained from three independent experiments are summarized and graphically represented. Values are expressed as mean ± SD. Cotransfection of cells with pSVCAT and pWAF1/ßgal yielded comparable levels of CAT activity confirming that the results were not due to differences in transfection efficiency or cell viability (data not shown).
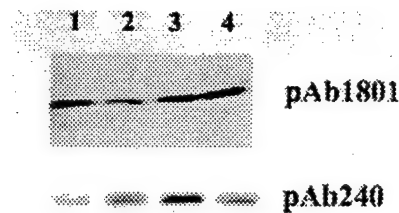

Figure 8. Immunological reactivity to mAbs pAb1801 and pAb240 of P53 from cell lysates of pC53-SN3 and pWAF1/ßgal co-transfected MCF10A and MCF10AT system cells. 28 h following transfection, cell lysates equivalent to 50 µg protein were immunoprecipitated with pAb1801 or pAb240 and precipitated proteins subjected to Western blot analysis with a polyclonal sheep anti-P53 antibody, Ab-7. Lane 1, MCF10A; lane 2, MCF10AneoT; lane 3, MCF10AT1 and lane 4, MCF10AT3b.

In this regard, it is of interest to note that pAb421 has been reported to activate the DNA binding function of P53 by mediating an allosteric change in its carboxyl-terminal regulatory domain (38).

Evaluation of functional status of P53 in the MCF10AT system. To determine whether the differences in capacity for formation of P53 complexes *in vitro* with the P53 recognition sequence in the WAF-1 promoter were related to P53 function as a transcription factor *in vivo*, MCF10A, MCF10AneoT, MCF10AT1, and MCF10AT3b cells were transfected with the WAF-1 ß-galactosidase expression vector, pWAF1/ß-gal. As shown in Fig. 7, a significant decrease in the ability of endogenous P53 to transactivate ß-gal expression from the WAF-1 promoter was observed in all MCF10AT system cells as compared to MCF10A cells. The capacity for ß-gal expression appeared to decrease relative to the number of transplant generations of the xenografts from which the cells were derived (compare MCF10AT1 and MCF10AT3b data in Fig. 7). The observed differences in ß-gal expression are not related to variations in transfection efficiency or cell viability as MCF10A and MCF10AT3b cells cotransfected with pWAF1/ßgal and pSVCAT yielded approximately similar CAT activities (data not shown). Thus, although the MCF10AT system cells express higher levels of total P53 than MCF10A cells, the ability of this P53 to function as a transcription factor is significantly reduced, presumably because of its existence in a conformationally altered state with reduced DNA binding capacity.

To determine whether increasing the levels of wild-type P53 in MCF10AT system cells could 'rescue' their capacity for

MCF10A and MCF10AT system cells were cotransfected with pWAF1/ßgal and various amounts of the wild-type P53 expression vector, pC53-SN3 (30). The results presented in Fig. 7 demonstrate that introduction of exogenous wild-type P53 did not enhance reporter activity over that mediated by endogenous P53 in any of the cell lines. In fact, measurable ß-gal activity was reduced in all cells in a dose dependent manner. Nevertheless, the data show the same inverse relationship between level of P53 mediated reporter gene activation and level of conformationally altered P53 relative to native P53, i.e., comparison of cells co-transfected with pC53-SN3 and pWAF1/ßgal showed that MCF10A cells had the highest level of P53-mediated reporter activity and MCF10AT3b cells the lowest (Fig. 7). They also indicate that levels of wild-type P53 are not limiting since introduction of exogenous wild-type P53 fails to enhance ß-gal expression from the WAF1 promoter.

It should be noted that inhibition of reporter gene expression occurred independently of any transcription factor depletion by the transfected CMV promoter, since all cells received an equivalent amount of this promoter in the form of pC53-SN3 or pCMVneo. Further, it was not due to loss of cell viability, which was only observed with levels of pC53-SN3 >5 µg. The observed differences in reporter gene activity were not related to variations in transfection or expression efficiency of pC53-SN3. Western blot analysis of cell lysates (50 µg protein) prepared from transfected cells revealed similar levels of pAb1801-reactive P53 (Fig. 8).

One possible explanation for the suppressive effect of increased wild-type P53 expression in MCF10 cells is induction of endogenous WAF-1 which down-regulates its own expression and could also down-regulate the response of the WAF-1 reporter plasmid. Alternatively, overexpression of P53 could predispose to increased ratios of conformationally altered:native P53. To examine this possibility, proteins were immunoprecipitated from cell lysates of pC53-SN3 co-transfected MCF10A and MCF10AT system cells with pAb240. Lysates from MCF10AT system cells still contained a higher concentration of P53 recognized by pAb240 than did lysates from MCF10A cells (Fig. 8). Thus, despite increased expression of exogenous wild-type P53, the pAb240-reactive conformationally altered P53 remains the predominant form in

a mixture of endogenous and exogenous P53 that has undergone the same conformational alteration. This would suggest that conformationally altered wild-type P53 is not only functionally defective but may also able to interfere with the function of native wild-type P53 by sequestering it in heteromeric complexes. An alternate possibility is that other proteins or factors in the cellular milieu of MCF10AT system cells are conducive for inducing exogenous P53 to adopt a conformationally altered state that has a 'mutant' immunological phenotype.

Results in literature are not consistent regarding the prognostic role and pathogenetic involvement of P53 in early human breast cancer. While all of the studies reported thus far have examined structure and function of P53 synthesized *in vitro*, our findings with cell lines from the MCF10AT xenograft model for early breast cancer substantiate the existence of mechanisms that modulate the DNA binding function of P53 through effects on protein conformation that are independent of genetic alterations of *p53*. Although previous studies have described P53 proteins capable of reversibly assuming wild-type and 'mutant' conformations (39-41), our study is the first to provide evidence that conformationally altered wild-type P53 is functionally defective in transcriptional activation *in vivo*, a property that is essential for growth suppressive function of P53. Our results suggest that in MCF10AT xenografts and probably in a subset of breast tumors that show overexpression of wild-type P53, factors exist that favor the abnormal stabilization of wild-type P53 in a conformationally altered state which is defective in P53-mediated functions and interferes with regulation of proliferation, apoptosis and response to chemotherapy (42). While the nature of molecular forces that render P53 inactive in the MCF10AT xenograft model remains to be established, several mechanisms have been suggested that may potentially modulate P53 structure and function. In some tumors, latency of P53 has been shown to be maintained through retention of P53 in the cytoplasm, and activation results in transportation to the nucleus. The heat shock protein Hsp84 (43) and the C-terminal domain of P53 (44) have been suggested to play a role in cytoplasmic sequestration and nuclear transportation. Both of these mechanisms may be contributing to inactivation of P53 in exponentially growing MCF10AT derived cell lines, since our immunofluorescence studies indicate abnormal accumulation of conformationally altered P53 in nuclei and cytoplasm.

Other mechanisms that have been suggested to render non-mutated wild-type P53 inactive *in vivo* include overexpression of zinc chelators such as metallothionein (MT) (45). In this regard, it is of interest to note that overexpression of MT is frequently observed in breast cancers carrying wild-type *p53* alleles (46,47). Another important mechanism for P53 regulation has been reported to result from redox regulation and metal binding. Redox modulators that reversibly perturb the wild-type phenotype of P53 can influence the biological activity of P53 by modulating DNA binding through effects on protein conformation (48). Similarly, P53 protein conformation and activity can be modulated through phosphorylation. Although phosphorylation at the C-terminus is not a prerequisite for conferring DNA binding capacity, it represents the most physiologically relevant mechanism by which the

conformation of P53 may be altered to confer DNA binding activity. In fact, mutation of a C-terminal serine residue of murine P53 has been shown to eliminate its tumor suppressive activity in mammalian cells, suggesting that phosphorylation of this residue is required for activation of P53 tumor suppression function (49). The accumulation of pAb240-reactive P53 in cytoplasm and nuclear compartments of MCF10AT cells, suggest that wild-type P53 inactivation may be occurring via one or more of these mechanisms.

In summary, our results clearly indicate that *p53* mutations are not necessary to account for *p53*-mediated changes in growth and morphology that occur in the early preneoplastic stages of breast tumor progression in the MCF10AT xenograft model. Rather, they indicate that stable changes in wild-type P53 conformation and function play a major role in breast cancer development. The availability of the MCF10AT xenograft model should provide an opportunity to further elucidate some mechanisms by which P53 function is altered and the consequences of these alterations in early stages of breast cancer which are technically difficult to examine in human tissues.

Acknowledgments

References

1. Momand J, Zambetti GP, Olson DC, George DL and Levine AJ: The mdm2 oncogene product forms a complex with the p53 protein and inhibits p53-mediated transactivation. Cell 69: 1237-1245, 1992.
2. Vogelstein B, Fearon ER, Hamilton SR, Kern SE, Preisinger AC, Leppert M, Nakamura Y, White R, Smits AM and Bos JL: Genetic alterations during colorectal tumor development. N Engl J Med 319: 525-532, 1988.
3. Bennett WP, Hollstein MC, Metcalf RA, Welsh JA, Zhu SM, Kusters I, Resau JH, Trump BF, Lane DP and Harris CC: P53 mutation and protein accumulation during multistage human esophageal carcinogenesis. Cancer Res 52: 6092-6097, 1992.
4. Sugimoto K, Toyoshima H, Sakai R, Miyagawa K, Hagiwara K, Hirai H, Ishikawa F and Takaku F: Mutations of the p53 gene in lymphoid leukemia. Blood 77: 1153-1156, 1991.
5. Hollstein M, Rice K, Greenblatt MS, Soussi T, Fuchs R, Sorlie T, Hovig E, Smith-Sorensen B, Montesano R and Harris CC: Database of p53 gene somatic mutations in human tumors and cell lines. Nucleic Acids Res 22 (Suppl.): 3551-3555, 1994.
6. Fields S and Jang SK: Presence of a potent transcription activating sequence in the p53 protein. Science 249: 1046-1049, 1990.
7. Pietenpol JA, Tokino T, Thiagalingam S, El-Deiry WS, Kinzler KW and Vogelstein B: Sequence-specific transcriptional activation is essential for growth suppression by p53. Proc Natl Acad Sci USA 91: 1998-2002, 1994.
8. Kern SE, Kinzler KW, Bruskin A, Jarosz D, Friedman P, Prives C

9. El-Deiry WS, Kern SE, Pietenpol JA, Kinzler KW and Vogelstein B: Definition of a consensus binding site for p53. Nat Genet 1: 45-49, 1992.

10. Funk WD, Pak DT, Karas RH, Wright WE and Shay JW: A transcriptionally active DNA-binding site for human p53 protein complexes. Mol Cell Biol 12: 2866-2871, 1992.

11. Zambetti GP, Bargonetti J, Walker K, Prives C and Levine AJ: Wild-type p53 mediates positive regulation of gene expression through a specific DNA sequence element. Gene Dev 6: 1143-1152, 1992.

12. Farmer G, Bargonetti J, Zhu H, Friedman P, Prywes R and Prives C: Wild-type p53 activates transcription in vitro. Nature 358: 83-86, 1992.

13. Kern SE, Pietenpol JA, Thiagalingam S, Seymour A, Kinzler KW and Vogelstein B: Oncogenic forms of p53 inhibit p53-regulated gene expression. Science 256: 827-830, 1992.

14. Weintraub H, Hauschka S and Tapscott SJ: The MCK enhancer contains a p53 responsive element. Proc Natl Acad Sci USA 88: 4570-4571, 1991.

15. Barak Y, Juven T, Haffner R and Oren M: mdm2 expression is induced by wild-type p53 activity. EMBO J 12: 461-468, 1993.

16. Kastan MB, Zhan Q, El-Deiry WS, Carrier F, Jacks T, Walsh WV, Plunkett BS, Vogelstein B and Fornace AJ Jr: A mammalian cell cycle checkpoint pathway utilizing p53 and GADD45 is defective in ataxia-telangiectasia. Cell 71: 587-597, 1992.

17. El-Deiry WS, Tokino T, Velculescu VE, Levy DB, Parsons R, Trent JM, Lin D, Mercer WE, Kinzler KW and Vogelstein B: WAF1, a potential mediator of p53 tumor suppression. Cell 75: 817-825, 1993.

18. Deb SP, Munoz RM, Brown DR, Subler MA and Deb S: Wild-type human p53 activates the human epidermal growth factor receptor promoter. Oncogene 9: 1341-1349, 1994.

19. Okamoto K and Beach D: Cyclin G is a transcriptional target of the p53 tumor suppressor protein. EMBO J 13: 4816-4822, 1994.

20. Martinez J, Georgoff I, Martinez J and Levine AJ: Cellular localization and cell cycle regulation by a temperature-sensitive p53 protein. Gene Dev 5: 151-159, 1991.

21. Yonish-Rouach E, Resnitzky D, Lotem J, Sachs L, Kimchi A and Oren M: Wild-type p53 induces apoptosis of myeloid leukemic cells that is inhibited by interleukin-6. Nature 352: 345-347, 1991.

22. Lowe SW, Schmitt EM, Smith SW, Osborne BA and Jacks T: p53 is required for radiation-induced apoptosis in mouse thymocytes. Nature 362: 847-849, 1993.

23. Clarke AR, Purdie CA, Harrison DJ, Morris RG, Bird CC, Hooper ML and Wyllie AH: Thymocyte apoptosis induced by p53-dependent and independent pathways. Nature 362: 849-852, 1993.

24. Basolo F, Elliott J, Tait L, Chen-XQ, Maloney T, Russo IH, Pauley R, Momiki S, Caamano J, Klein-Szanto AJ and Russo J: Transformation of human breast epithelial cells by c-Ha-ras oncogene. Mol Carcinogen 4: 25-35, 1991.

25. Miller FR, Soule HD, Tait L, Pauley RJ, Wolman SR, Dawson PJ and Heppner GH: Xenograft model of progressive human proliferative breast disease. J Natl Cancer Inst 85: 1725-1732, 1993.

26. Dawson PJ, Wolman SR, Tait L, Heppner GH and Miller FR: MCF10AT: a model for the evolution of cancer from proliferative breast disease. Am J Pathol 148: 313-319, 1996.

27. Harlow E, Crawford LV, Pim DC and Williamson NM: Monoclonal antibodies specific for simian virus 40 tumor antigens. J Virol 39: 861-869, 1981.

28. Gannon JV, Greaves R, Iggo R and Lane DP: Activating mutations in p53 produce a common conformation effects: a monoclonal antibody specific for mutant form. EMBO J 9: 1595-1602, 1990.

29. Locus HUMTP53B, Accession M14695.

30. Baker SJ, Markowitz S, Fearon ER, Willson JK and Vogelstein B: Suppression of human colorectal carcinoma cell growth by wild-type p53. Science 249: 912-915, 1990.

31. Bradford MM: A rapid and sensitive method for the quantitation of microgram quantities of protein utilizing the principle of protein-dye binding. Anal Biochem 72: 248-254, 1976.

32. Uchida M, Ozono K and Pike JW: Activation of the human osteocalcin gene by 24R, 25-di(OH)vitamin D3 occurs through the vitamin D receptor and the vitamin D responsive element. J Bone Miner Res 9: 1981-1987, 1994.

33. Graham FL and van der Eb AJ: A new technique for the assay of infectivity of human adenovirus 5 DNA. Virology 52: 456-467, 1973.

34. Stephen CW and Lane DP: Mutant conformation of p53: precise epitope mapping using a filamentous phage epitope library. J Mol Biol 225: 577-583, 1992.

35. Finlay CA, Hinds PW, Tan TH, Eliyahu D, Oren M and Levine AJ: Activating mutations for transformation by p53 produce a gene product that forms an hsc70-p53 complex with an altered half-life. Mol Cell Biol 8: 531-539, 1988.

36. Bartek J, Iggo R, Gannon J and Lane DP: Genetic and immuno-chemical analysis of mutant p53 in human breast cancer cell lines. Oncogene 5: 893-899, 1990.

37. Matlashewski GJ, Tuck S, Pim D, Lamb P, Schneider J and Crawford LV: Primary structure polymorphism at amino acid 72 of human p53. Mol Cell Biol 7: 961-963, 1987.

38. Hupp TR, Meek DW, Midgley CA and Lane DP: Regulation of the specific DNA binding function of p53. Cell 71: 875-886, 1992.

39. Zhu YM, Bradbury DA and Russell NH: Wild-type p53 is required for apoptosis induced by growth factor deprivation in factor-dependent leukemic cells. Br J Cancer 69: 468-472, 1994.

40. Milner J: A conformation hypothesis for the suppression and promoter functions of p53 in cell growth control and in cancer. Proc R Soc Lond (Biol) 245: 139-145, 1991.

41. Hainaut P, Butcher S and Milner J: Temperature sensitivity for conformation is an intrinsic property of wild-type p53. Br J Cancer 71: 227-231, 1995.

42. Levine AJ: P53, the cellular gatekeeper for growth and division. Cell 88: 323-331, 1997.

43. Sepehrnia B, Paz IB, Das-Gupta G and Momand J: Heat shock protein 84 forms a complex with mutant p53 protein predominantly within a cytoplasmic compartment of the cell. J Biol Chem 271: 15084-15090, 1996.

44. Ostermeyer AG, Runko E, Winkfield B, Ahn B and Moll UM: Cytoplasmically sequestered wild-type p53 protein in neuro-blastoma is relocated to the nucleus by a C-terminal peptide. Proc Natl Acad Sci USA 93: 15190-15194, 1996.

45. Hainaut P and Milner J: A structural role for metal ions in the 'wild-type' conformation of the tumor suppressor protein p53. Cancer Res 53: 1739-1742, 1993.

46. Oyama T, Take H, Hikino T, Nino Y and Nakajima T: Immuno-histochemical expression of metallothionein in invasive breast cancer in relation to proliferative activity, histology and prognosis. Oncology 53: 112-117, 1996.

47. Goulding H, Jasani B, Pereira H, Reid A, Galea M, Bell JA, Elston CW, Robertson JF, Blamey RW, Nicholson RA, Schmid KW and Ellis IO: Metallothionein expression in human breast cancer. Br J Cancer 72: 968-972, 1995.

48. Hainaut P and Milner J: Redox modulators of p53 conformation and sequence-specific DNA binding in vitro. Cancer Res 53: 4469-4473, 1993.

49. Milne DM, Palmer RH and Meek DW: Mutation of the casein kinase II phosphorylation site abolishes the anti-proliferative activity of p53. Nucleic Acids Res 20: 5565-5570, 1992.

Environmental Estrogen Stimulation of Growth and Estrogen Receptor Function in Preneoplastic and Cancerous Human Breast Cell Lines.

P.V.M. Shekhar[1,2,3], J. Werdell[1] and V.S Basrur[1].

[1]Breast Cancer Program, Karmanos Cancer Institute; [2]Department of Pathology, Wayne State University School of Medicine, Detroit, MI 48201.

Running Title: Environmental Estrogen Stimulation of Human Breast Cells

Key words: Xenoestrogens, DDT, PCB, Estrogen receptor-mediated regulation

[3]To whom correspondence should be addressed:

P.V.M. Shekhar
Breast Cancer Program
Karmanos Cancer Institute
110 E. Warren Avenue
Detroit, MI 48201
Tel: (313) 833-0715, Ex. 2326/2259
Fax: (313) 831-7518
E-mail: shekharm@kci.wayne.edu

Abbreviations used: Estrogen receptor (ER), Estradiol (E_2), Estrogen response element (ERE), Polychlorinated biphenyls (PCB), DMSO (dimethyl sulfoxide), Colony forming efficiency (CFE), Chloramphenicol acetyl transferase (CAT), Diethylstilbesterol (DES)

In press. J. Nat. Cancer Inst.

1

Abstract

Background: DDT and PCBs, which are widespread in the ecosystem, can mimic estrogen-mediated cell activities. Thus they can potentially interfere with many physiological processes. We compared the effects of organochlorines belonging to the DDT and PCB families, alone and in combination, for their ability to influence the estrogen receptor-mediated activities in preneoplastic breast epithelial cells and breast cancer cells. *Methods*: Multiple assay systems requiring functional estrogen receptor were employed to test estrogen-like activity of organochlorine ligands. Two-sided statistical tests were used to compare the data. *Results*: p,p'-DDT, the predominant form of DDT in the environment, is a more potent estrogen than o,p'-DDT ($P=0.0001$), although it is less effective than o,p'-DDT in inhibiting the binding of estradiol (natural estrogen) to estrogen receptor. Among the PCBs, Heptachlor is estrogenic (in both growth and transient reporter assays; $P=0.001$), whereas Aroclor 1221 and 1254, both individually and in combination, are only weakly estrogenic. *Conclusion:* p,p'-DDT is the most effective organochlorine in regulating estrogen receptor-mediated cellular responses. In estrogen receptor-positive breast cancer cells, DDT evokes responses by itself and enhances the responses in collaboration with estradiol or other organochlorines.

Epidemiological studies imply that hormones, genetic factors and environmental agents are important determinants in breast carcinogenesis. A wide variety of pollutants in the ecosystem have the ability to mimic the actions of steroid hormones in the body. Principal concern is centered around chemicals that can mimic the actions of estrogens, termed "environmental estrogens" or "xenoestrogens", since they have the ability to interfere with several physiological processes that are normally estrogen-regulated which could result in alterations in reproduction and susceptibility to cancer (1-10). Although there is great concern over the role of xenoestrogens in the development of breast cancer there are little data to support their role. Estrogen hormones are potent mitogens for breast epithelial and uterine cells whose hormone responsiveness is mediated by the estrogen receptor (ER). The mechanism by which estrogens affect proliferation of certain target cells is not fully understood (11,12). Several lines of evidence indicate that they can induce expression of cell cycle regulatory genes directly (13-18), suggesting a primary role for ER in regulating cell cycle progression.

Organochlorines are lipophilic compounds that accumulate and persist in human adipose tissue, reaching levels 200-300 times higher than those observed in serum (19-21). Well known examples of organochlorines are the pesticide DDT, 2,2-bis (p-chlorophenyl)-1,1,1-trichloroethane, its metabolite DDE (1,1-dichloro-2,2-bis (p-chlorophenyl) ethylene; Ref. 19-24) and PCBs (polychlorinated biphenyls; Ref. 19-23,25). To date, DDT has been shown to induce carcinogenesis of the liver, lymphatic tissue and lung in rats and mice (20,21,26,27) but not mammary cancer. At a molecular level, DDT can induce cytochrome p450 containing enzymes in humans, thus potentially affecting steroid metabolism ((20,21,26,27). p,p'-DDT, the predominant form of DDT has been considered nonestrogenic (28), whereas o,p'-DDT and its

3

isomer, o,p'-DDE, are estrogenic (24,29,30). o,p'-DDT has been shown to promote growth of rat

mammary tumors (31,32) and bind to the ER of rat and human mammary tumors (33,34) and

human uterine tumors (34). Similarly, Aroclor 1221, a mixture of polychlorinated biphenyls that

is rich in o-chlorobiphenyl, has been reported to be estrogenic whereas Aroclor 1254 is

nonestrogenic (35). In the present study we have compared the effects of closely related

organochlorines belonging to the DDT (p,p'-DDT and o,p'-DDT) and PCB (Aroclor 1221,

Aroclor 1254 and Heptachlor) families of pesticides singly and in mixtures for estrogenicity and

ER-mediated properties in two cell systems of human breast cancer: ER^+ preneoplastic breast

epithelial cells (MCF10AT system cells) and ER^+ breast carcinoma (MCF-7 cells).

Materials and Methods

Preneoplastic breast epithelial cell model system

The MCF10AT system is a xenograft model of early human breast cancer progression (36).

MCF10AneoT cells are T24 Ha-ras transformed cells derived from MCF10A human breast

epithelial cells (37). MCF10A cells do not form persistent lesions in immunedeficient mice (36),

whereas MCF10AneoT cells do (36). MCF10AneoT and lines derived by alternating in vivo

transplantation and in vitro culture (MCF10ATn) are collectively known as the MCF10AT

system (38). The lesions formed by lines of the MCF10AT system are composed of a

heterogeneous spectrum of ductular tissues with a range of morphology that includes mild

hyperplasia, atypical hyperplasia, carcinoma in situ (CIS), moderately differentiated carcinoma,

and undifferentiated carcinoma, as well as histologically normal ducts (36,38). Thus, the

4

MCF10AT system provides a transplantable, xenograft model of human proliferative breast disease with proven neoplastic potential.

Cell lines and cell culture

These studies utilized MCF10A, MCF10AneoT and MCF10AT3c, a third transplant generation of the MCF10AT xenograft model for human proliferative breast disease. MCF10A cells are ER⁻ and were used in some experiments to determine specificity of xenoestrogens for ER-mediated pathways. MCF10AneoT cells and transplant generations derived from MCF10AneoT express functional ER (39). MCF10A and MCF10AT cells were maintained in phenol red-free DMEM/F-12 medium with 0.1 μg/ml cholera toxin, 10 μg/ml insulin, 0.5 μg/ml hydrocortisone, 0.02 μg/ml epidermal growth factor, 100 i.u./ml penicillin, 100 μg/ml streptomycin, and 2.5% horse serum. The human breast carcinoma cell line, MCF-7, was maintained in DMEM/F-12 medium supplemented with 10 μg/ml insulin and 5% donor calf serum. Charcoal-stripped serum was not used in cultures of MCF-7 or MCF10A/MCF10AT cells since it reduced the proliferative capacity and/or viability of MCF10A/MCF10AT and MCF-7 cells, possibly due to removal of essential growth factors (40). However, since the studies examined estrogenicity of pesticides, the only sera used routinely were those which were unable to support growth of the ER⁺ cell line, MCF-7, indicating absence of biologically significant levels of 17 β-estradiol (E_2) or other estrogenic compounds.

Cell proliferation assay

To assess growth effects of DDT and PCB compounds, cell number was estimated at the end of a 10-day treatment. Cells were seeded at 5×10^4 (MCF-7) or 1×10^4 (MCF10AneoT or

5

MCF10AT3c) cells in 25 cm^2 flasks. Cells were plated in the appropriate medium as described

before and on the following day, treatments were begun with a change of medium twice a week.

Treatment consisted of vehicle (ethanol or DMSO at 0.01%), E$_2$ (1 or 10 nM), o,p'-DDT, p,p'-

DDT, Heptachlor, and Aroclors 1221 and 1254. All PCB compounds were tested individually at

1 or 10 μM; p,p'-DDT was tested at 0.01, 0.1, 1 and 10 μM concentrations. The influence of

combinations of o,p'-DDT/p,p'-DDT and Aroclor 1221/1254 on cell proliferation was tested at

0.1, 1 and 10 μM concentrations. The pure antiestrogen ICI 182,780, a gift from A. Wakeling

(Zeneca Pharmaceuticals, Cheshire, U.K.) was included in treatment with E$_2$ or xenoestrogens at

100-fold molar excess of the ligand tested. At the end of 10 days, monolayers were washed with

saline and lysed in 0.5 ml 0.01 M Hepes buffer/1.5 mM MgCl$_2$ plus two drops of ZAP reagent

(Acros, New Jersey) for 5 min. The nuclei released were counted in a Coulter Counter (Coulter

Electronics). All cell counts were done from triplicate flasks and results expressed as the mean ±

S.E from three independent experiments.

Growth in soft agar

 4 x 10^4 MCF10AT3c cells were seeded in 2 ml of 0.3% agar in phenol red-free DMEM/F-12

supplemented medium. This suspension was layered over 1 ml of 0.9% agar medium base layer

in 35-mm dishes (Costar) and overlaid with 2 ml of phenol red-free DMEM/F-12 medium

containing E$_2$ (1 or 10 nM), or 1 or 10 μM of the individual xenoestrogen (o,p'-DDT, p,p'-DDT,

Heptachlor, Aroclor 1221 or Aroclor 1254). Control dishes were treated with an equivalent

concentration of vehicle (ethanol or DMSO to final concentration of 0.01%). All dishes were

incubated at 37°C in 5% CO$_2$:95% O$_2$ for 3 weeks with twice-weekly media changes and

6

hormone supplementation. All cultures were examined 24 h after plating and cell aggregates that might bias final results were marked. Plates with more than 10 aggregates were discarded. Colony forming efficiency (CFE) was calculated by dividing the number of colonies larger than 50 μm (sized using a calibrated ocular grid) by the number of cells seeded. Ten microscopic fields were counted to calculate the total number of colonies/well for the whole well; reported values are the average count from triplicate wells. The numbers of colonies in different size ranges [50-100 μm, 100-200 μm, 200-300 μm and >300 μm] was calculated in the same manner.

ER Binding assay

MCF-7 cells were grown in monolayer culture in phenol red-free medium with 5% donor calf serum as described before. Cells were allowed to grow through two doublings to deplete steroid hormone levels in the cells. Cells were then harvested, pelleted and homogenized in 8-volumes of buffer (10 mM Tris-HCl, 2 mM DTT, 1 mM EDTA, 10% (v/v) glycerol, 0.5 M NaCl, pH 7.4) at 4°C. Cell homogenates were centrifuged at 105,000xg for 1 h at 4°C, and resulting high speed cytosols were stored in aliquots at -70°C. The ability of xenoestrogens to compete with E_2 for binding to ER was determined in single point competition assays by the standard dextran-coated charcoal method (41). Cytosolic protein (100 μg) was incubated with 2 nM 2,4,6,7 [^{3}H]17 β-estradiol (110 Ci/mmol, Amersham Corp., Arlington Heights, IL) and increasing amounts of unlabeled DES (1-1000 fold excess) or various xenoestrogens (10-1000 fold excess). Reactions were incubated at 4°C for 18 h. Bound and free radiolabel were separated by the addition of dextran-coated charcoal followed by centrifugation. The amount of specifically bound tracer was

expressed as percent of maximal specific binding. Protein assays were performed on the cytosols by the Bradford method (42).

Transient Transfection Assay using ERE-TK-CAT construct

Reporter plasmid construct

Estrogenicity of organochlorine compounds was assessed by measuring their effect on transient expression of the bacterial chloramphenicol acetyltransferase (CAT) reporter gene in JA-12, a plasmid with CAT expression regulated by tandem estrogen response elements (ERE) upstream of a minimal thymidine kinase (TK) promoter construct, p-37TKCAT (43, 44).

Cell culture and transfection

MCF-7, MCF10A or MCF10AneoT cells (5 x 10^5/60 mm dish) were plated in phenol red-free media as described before and maintained for 18 h prior to transfection with 10 μg of JA-12 plasmid DNA using the calcium phosphate method (45). Six hours after transfection, cells were shocked with glycerol (3 min incubation with 15% glycerol for MCF10A/MCF10AneoT cells or 3 min incubation with 10% glycerol for MCF-7 cells), washed and cultured in phenol red-free DMEM/F-12 or Eagle's supplemented media containing E_2 (positive control), o,p'-DDT, p,p'-DDT, Heptachlor, Aroclor 1221, Aroclor 1254 and/or ICI 182,780 at indicated concentrations for 40 h. Control cultures were treated with vehicle, ethanol or DMSO, at a final concentration of 0.01%.

Chloramphenicol acetyl transferase (CAT) assay

Transfected cells were lysed with four cycles of freezing and thawing in 0.25 M Tris-HCl, pH 7.5. CAT assays were carried out with reaction mixtures containing 100 μg of supernatant

8

protein and 0.1 μCi of ^{14}C-chloramphenicol (40-60 mCi/mmol, ICN Radiochemicals, Irvine, CA; Ref. 46). The assay tubes were incubated for 4 h at 37°C. Acetylated chloramphenicol was separated by thin layer chromatography and quantitated by liquid scintillation counting. The lacZ reporter plasmid pCH110 (Pharmacia, Piscataway, NJ) was cotransfected in some experiments to monitor transfection efficiency and assayed according to the manufacturer's protocol. β-galactoside standard and o-nitrophenyl β-galactoside were purchased from Boehringer Mannheim (Indianapolis, IN).

pS2 gene expression and its regulation by o,p'-DDT and p,p'-DDT

MCF-7 and MCF10AT3c cells were grown for 2 days in 75 cm^2 culture flasks in phenol red-free media as described before followed by a change to the same medium but containing the appropriate ligand additions for a further 96 h in the case of MCF10AT3c cells, or 24 h in the case of MCF-7 cells. Total cellular RNA was prepared from the cells and 20μg aliquots of RNA from MCF-7 cells and 40 μg aliquots of RNA from MCF10AT3c cells were subjected to Northern blot analysis in 1.5% agarose-formaldehyde gels. The nylon membranes were hybridized with ^{32}P-labeled cDNA for PS2 (gift from Dr. P. Chambon, INSERM, Strasbourg, France). Membranes were washed with 0.5X SSC (1XSSC = 0.15 M NaCl and 0.015 M sodium citrate, pH 7.0) and subjected to autoradiography. Loading was checked by reprobing the blot with 36B4 cDNA (47). Results were quantitated with a densitometer (Molecular Dynamics, Model 300A), and the 36B4 band intensities were used to normalize for equal sample loading.

Data analysis

9

With the exception of the binding experiment, data were analyzed with an analysis of variance. In cell proliferation assays, cell counts were transformed using the natural logarithm. Specific differences between treatments were examined using the Student's *t*-test. Bonferroni's technique was used to compensate for multiple comparisons, and *t*-statistics less than 0.01 were considered significant. For the binding experiment, we fit linear regressions for each treatment. A *t*-test was used to compare the slope for DES, o,p'-DDT, p,p'-DDT, Heptachlor, Aroclor 1221 or Aroclor 1254, and Dexamethasone (control).

Results

Effect of DDT and PCB derivatives on growth of ER+ human preneoplastic and breast cancer cells

We monitored the effects of xenoestrogens on cellular proliferation of ER^+ MCF-7, MCF10AneoT and MCF10AT3c cells (39; Shekhar PVM, Chen M.L., Werdell, J, Heppner, GH, Miller, Christman, JK, manuscript submitted). Contrary to previous reports (28), results presented in Figure 1 show that at equivalent doses, p,p'-DDT is more potent than o,p'-DDT at stimulating proliferation of MCF-7 cells. At a concentration of 10 μM, p,p'-DDT is approximately two times more effective than o,p'-DDT. Added individually, although concentrations of 0.01 and 0.1 μM p,p'-DDT stimulate significant increase in growth over that of cultures treated with vehicle only (p=0.0001 as determined by the *t* test), a significant dose dependent induction of growth with either o,p'-DDT or p,p'-DDT is observed only at concentrations > 1 μM (p=0.0001). However, when MCF-7 cells are exposed to combinations of

10

o,p'- and p,p'-DDT, doses as low as 0.1 μM of each compound are sufficient to elicit cellular proliferation to the same extent as 10 μM of p,p'-DDT added singly (Table 1). The measured cumulative effects of o,p'-DDT and p,p'-DDT on growth are not significantly different from those obtained with each isomer separately as determined by student t test. This suggests that the cumulative effect of the two DDT isomers is additive. The majority of growth stimulation induced by p,p'-DDT is mediated through the ER-dependent pathway since the proliferative effect is abolished by 100-fold molar excess of pure antiestrogen, ICI 182,780. We found that concentrations of 10 μM of the PCBs, Aroclor 1221 and Aroclor 1254, induced significant increase in cell yields over that of control cultures of MCF-7 cells (p=0.001) when used individually (Table 2). However, mixtures of Aroclor 1221 and 1254, even at concentrations as high as 10 μM, failed to elicit a cumulative effect on growth of MCF-7 cells (Table 2). Similarly, the PCB, Heptachlor, also caused a modest increase over control of MCF-7 cell growth (p=0.001; Table 2). We have not been able to demonstrate reproducibly the effects of E_2 or any of the organochlorines on monolayer growth of MCF10AneoT or MCF10AT3c cells.

Effect of DDTs and PCBs on anchorage independent growth of MCF10AT3c cells

It has been previously shown that monolayer growth of MCF10A cells and MCF10A cells rendered ER$^+$ after stable transfection with an ER expression plasmid is not enhanced by addition of E_2 to the growth medium (48). MCF10A cells do not form colonies in soft agar (49). However, both transfection with T24 Ha-ras (37) and successive transplant passage in nude mice result in enhanced capacity for anchorage independent growth. Under the conditions of assay utilized in our experiments, in the absence of E_2, MCF10AT3c cells had a colony forming

11

efficiency (CFE) of 25% and approximately 40% of these colonies had a diameter >100 μm; none had a diameter >200 μm. The CFE of MCF10AT3c cells showed a dramatic increase following exposure to physiological concentrations of E_2 (Fig. 1). E_2 treatment also enhanced the rate of growth in soft agar with ~ 7% of colonies larger than 200 μm. Exposure of cells to o,p'-DDT, p,p'-DDT and Heptachlor also induced increases in CFE and proliferative effects (Fig. 1), whereas Aroclor 1221 and 1254 exerted only a modest increase over that of control (data not shown). No colonies over 200 μm were found in o,p'-DDT-treated plates. Although p,p'-DDT and Heptachlor enhanced colony growth, formation of colonies > 300 μm was realized only with E_2 or p,p'-DDT (Fig. 1).

Regulation of reporter gene expression from a transiently transfected ERETKCAT construct in MCF-7 and MCF10AneoT cells

Although we have not been able to demonstrate effects of xenoestrogens and E_2 on monolayer growth of MCF10AT system cells, we tested whether binding of DDT or PCB derivatives to ER would cause induction of expression of estrogen-sensitive genes. MCF-7 and MCF10AneoT cells were transiently transfected with an exogenous estrogen-sensitive gene, ERETKCAT, and assayed for the regulatory effects of organochlorines on CAT gene expression. Results of CAT expression in MCF-7 cells are shown in Tables 3 and 4, and are consistent with those obtained for MCF-7 cell proliferation assays depicted in Tables 1 and 2. Data of Table 3 confirm that at equivalent doses, p,p'-DDT is significantly more effective than o,p'-DDT in regulating transcription from a minimal ERETKCAT plasmid (p=0.0001), and that concentrations of 10 μM of p,p'-DDT are required to invoke inductive effects similar to E_2 (p=0.0001). Mixtures of o,p'-

12

DDT and p,p'-DDT induced synergistic effects on ER-mediated CAT gene expression at 100-fold lower doses than those elicited by either isomer alone (p=0.0001; Table 3). Table 3 also shows that p,p'-DDT can not only synergize with o,p'-DDT but is also able to cooperate synergistically with E_2 (at 10^{-11}M or 10^{-10}M) to induce ER-mediated CAT gene expression (p=0.0001). The regulatory effects on CAT gene expression are completely abolished with the estrogen antagonist, ICI 182,780 (Table 1). Results of Table 4 show that although the PCB, Heptachlor, is as effective as p,p'-DDT in regulating transcription of the CAT gene, it does not cooperate synergistically with E_2; in fact the expression of CAT gene is lower than that observed in the presence of E_2 or Heptachlor alone (Table 4). These data indicate differences in mechanisms of interaction between p,p'-DDT and Heptachlor with E_2 in the cell system used. While a synergism between p,p'-DDT and E_2 for ER and the two EREs in the ERETKCAT construct is observed (Table 3), Heptachlor and E_2 appear to compete rather than cooperate for these binding sites (Table. 4). Aroclors 1221 and 1254 are unable to stimulate ER-driven CAT gene expression from the minimal ERETKCAT plasmid (Table. 4).

Table 5 shows that the pattern of xenoestrogen-mediated regulation of CAT gene expression in preneoplastic MCF10AneoT cells is overall similar to that observed in breast cancer MCF-7 cells (Tables 3 and 4) with some cell type differences. At equivalent doses, Heptachlor, o,p'-DDT and p,p'-DDT appear to be more efficient in regulating CAT gene expression in MCF10AneoT cells than in MCF-7 cells (Table 5). The effects of these chlorinated hydrocarbons on CAT gene expression are dependent on the presence of a functional ER since similar transfection assays performed in ER-negative MCF10A cells do not show ligand-dependent regulation of CAT gene expression (data not shown). Furthermore, xenoestrogen-mediated increases in CAT gene

13

expression are completely abolished by 100-fold molar excess of the pure antiestrogen ICI

182,780 (Table 5). Co-transfection with pCH110, which expresses β-galactosidase activity at a

constant level regardless of E_2 or xenoestrogen concentration, confirmed that these results are not

due to differences in transfection efficiency or cell viability (data not shown).

Regulation of pS2 gene expression in preneoplastic MCF10AT3c and breast cancer MCF-7 cells

In order to test whether o,p'-DDT and p,p'-DDT can regulate expression of an endogenous

estrogen-regulated gene, expression of pS2 was examined (50). 36B4 was chosen as a control

gene as its expression is not modulated by estrogen and to ensure equal loading of RNA samples

(46). Densitometric analysis of pS2 mRNA levels relative to 36B4 message from MCF-7 cells

showed that like E_2 which induced ~4-fold higher levels of pS2 mRNA, both o,p'- and p,p'-DDT

enhanced approximately 3- and 4-fold higher levels of pS2 mRNA (Fig. 2), respectively, when

compared to untreated cells which had no detectable pS2 mRNA (data not shown). Although,

DDT-mediated regulation of pS2 mRNA resulted in induction effects similar to that of E_2, it

must be noted that 10 μM o,p'-DDT or p,p'-DDT are required to evoke pS2 stimulation compared

to 1 nM E_2 (Fig. 2). Treatment of MCF-7 cells with a mixture of o,p'-DDT and p,p'-DDT at 100-

fold lower doses (0.1 μM of each ligand) caused ~ 10-fold enhancement of pS2 transcription

relative to untreated cells (Fig. 2). Similar enhancements in pS2 message levels (~9-fold) were

observed when MCF-7 cells were exposed to a mixture of p,p'-DDT (0.1 μM) and E_2 (1 nM)

(Fig. 2). Expression of pS2 was examined in MCF10AT3c cells rather than in MCF10AneoT

cells since a greater number of MCF10AT3c cells are ER^+ as compared to MCF10AneoT cells

14

(Shekhar PVM, Chen ML, Werdell, J, Heppner, GH, Miller, FR, Christman, JK, manuscript submitted). In contrast to MCF-7 cells that showed a rapid increase in accumulation of pS2 transcripts following exposure to E_2 or DDT, induction of pS2 mRNA in MCF10AT3c cells occurred more slowly. Levels of pS2 mRNA were very low in MCF10AT3c cells treated with E_2 or DDT for 24 h (data not shown); however, pS2 levels rose following exposure of the cells for 4 days (Fig. 2). Although the kinetics of pS2 induction differed greatly in MCF-7 and MCF10AT3c cells, pS2 gene expression was stimulated by E_2 and p,p'-DDT ~4-fold relative to untreated cells (which had undetectable pS2 signal, data not shown) in both cell lines. However, unlike MCF-7 cells, treatment of MCF10AT3c cells with mixtures of o,p'-DDT and p,p'-DDT (0.1 μM of each ligand) induced pS2 mRNA at a level intermediate between induced levels with either p,p'-DDT or o,p'-DDT alone (~2-fold; Fig. 2). Addition of antiestrogen, ICI 182,780, at 100-fold molar excess of E_2 or p,p'-DDT to treated MCF-7 or MCF10AT3c cells caused a substantial reduction (~60%) in the levels of pS2 transcripts relative to cells treated with E_2 or p,p'-DDT alone (Fig. 2).

Ligand Binding to Estrogen Receptor

Since the effects of estrogen are mediated by the binding to its intracellular receptor, we tested the binding ability of DDT and PCB compounds to ER in a single point competitive binding assay. ER prepared from MCF-7 cells was incubated with [^{3}H]17β-estradiol and the degree of inhibition of binding was determined in the presence of increasing amounts of DDT or PCB compounds. Among the xenoestrogens tested, only o,p'-DDT competed with estradiol binding to ER (p=0.03). Approximately 40% inhibition of binding was effected by 500-fold molar excess of

15

o,p'-DDT, whereas p,p'-DDT (p=0.35) and Aroclor 1221 (p=0.48) caused minimal (< 20%) inhibition at similar concentrations (Fig. 3). Heptachlor, Aroclor 1254 and dexamethasone had no effect on $[^3H]E_2$ binding (Fig. 3).

Discussion

The above studies show that among a series of DDT and PCB compounds tested, the DDT isomer, p,p'-DDT is the most effective organochlorine in regulating ER-mediated cellular responses in our models of human preneoplastic and breast cancer cells. Besides establishing estrogenicity of p,p'-DDT, we show for the first time that the two isomers of DDT, o,p'-DDT and p,p'-DDT, can cooperate to induce ER-mediated processes: viz., increase in cell proliferation, and transactivation of exogenous (from a minimal ERETKCAT plasmid) and endogenous estrogen-regulated (pS2) genes. We also show for the first time that whereas p,p'-DDT can synergistically collaborate with E_2 to induce ER-mediated increase in CAT gene expression, Heptachlor, an estrogenic PCB, exhibits a competitive interaction with E_2 with the resultant signal being less than those generated by Heptachlor or E_2 alone. Used individually, concentrations of 10 μM of the DDT isomers are required for induction of ER-mediated increases in cell proliferation and CAT gene expression; however, effective concentrations that generate similar magnitudes of ER-mediated cellular responses are dramatically reduced 10-100-fold when mixtures of the two DDT isomers are used. Although our data show o,p'-DDT, p,p'-DDT and Heptachlor to have estrogenic properties, none of these compounds compete effectively with $[^3H]-E_2$ as DES. Consistent with previous reports, our data from competition assays in in vitro cell free system

16

show o,p'-DDT to be most efficient in inhibiting binding of $[^3H]$-E_2 (33,34), although functional

assays using cultured cells show a stronger p,p'-DDT-mediated estrogenic effect. Further,

whereas xenoestrogens exert pleiotropic effects on cell growth and differentiation via

deregulation of signal transduction pathways, the bulk of the growth response induced by these

xenobiotics is abolished by the pure antiestrogen, ICI 182,780.

DDT isomers are estrogenic in the two systems tested: preneoplastic and breast cancer cells.

However, a major difference was observed, viz., a lack of cooperation between these derivatives

in the induction of pS2 expression in the preneoplastic breast epithelial cells. Regulation of pS2

gene expression in MCF10AT3c cells by o,p'-DDT and p,p'-DDT can be explained by a direct

competition between the two isomers for binding to the ER, suggesting that both isomers of DDT

induce pS2 transcription, but at different rates, so that the final levels of pS2 mRNA measured

represent the average of the two isomers. This variation in estrogenic response of MCF10AT3c

cells may be ascribed to differences in cell type or to differences in ER levels in the two cell

lines. Similar differences in synergistic interactions between E_2 and 3,4,3',4',-tetrachlorobiphenyl

on pS2 synthesis have been attributed to variations in cell type of two human breast cancer cells

that express high levels of ER: MCF-7 vs ZR-75-1 (51). Another difference observed in our two

human breast cell systems is the lack of correlation between estrogenicity of Heptachlor and

absence of growth stimulation in MCF-7 cells; whereas in MCF10AT cells, Heptachlor is a

potent stimulator of both CAT gene expression and colony growth. It is becoming increasingly

clear that estrogenic properties (activity and potency) of organochlorines are greatly influenced

by the assay system, cell type, level of ER (endogenous or exogenous), number of EREs in the

reporter construct, and sensitivity of the assay used. This disparity in estrogenicity of various

xenobiotics measured by different assays compel the inclusion of common standards, both positive and negative, to substantiate assays that may provide results most relevant to assessing cancer risk in humans.

Although many xenoestrogens are less potent than biological estrogens, and do not produce mammary gland neoplasms in the bioassay rodent models, their ability to promote growth and proliferation of high risk breast epithelial cells has not been investigated. The daily exposure from xenoestrogenic pesticides such as DDT, dieldrin, endosulfan, and methoxychlor is approximately 2.5 μg/day (10,52). Serum concentration of DDT in women range from 2 to 15 nM (53-56), and a recent report from Zava *et al* (57) using an *in vitro* cell culture system have shown that the concentration of o,p'-DDT required to half-saturate ER is about 1000-fold higher than the reported leves of DDT in serum (53-56). While these data would suggest DDT and other xenoestrogens to influence estrogen-mediated cellular responses only minimally, xenoestrogens are still cause for concern due to their persistence in the environment, resistance to enzymatic or chemical degradation, sequestration and storage by adipose tissues and long half-life (7). In fact, the levels of xenoestrogens, particularly those of DDT, detected in adipose tissue of human breast cancer are nearly 1000-fold higher than their serum levels and correlate with the concentrations required for in vitro stimulation of cells, suggesting that the doses (1-10 μM) are indeed physiologically relevant (53-58). A detailed comparison of organochlorine pesticide residues in samples of maternal blood, milk, subcutaneous fat and umbilical cord collected showed the presence of a variety of organochlorines (59). The major pesticide residues detected in all samples were p,p'-DDT and p,p'-DDE with small amounts of o,p'-DDT and significantly smaller amounts of β-hexachlorocyclohexane and dieldrin (59). Since the ban on usage of DDT

18

and restricted usage of PCBs in the United States, exposures to these compounds have been so drastically reduced that they have been considered to pose a negligible health risk. However, the adverse effects of these organochlorines could be overlooked if attention is paid only to tissue levels since through cooperation with other xenoestrogens or endogenous weak estrogens as our data and previous reports (60) show, these organochlorines could produce significant estrogenic effects. About 40% of all cancers in women are hormonally mediated (61) and epidemiologic evidence suggest that a major determinant of nongenetic breast cancer risk is total cumulative exposure to estrogen (62,63). Recent reports on ER-mediated cellular responses of organochlorines in human breast cancer cell lines necessitate the evaluation of the role of xenoestrogens in vivo in breast carcinogenesis (60,64). A detailed follow-up of breast cancer patients with high levels of DDT and other xenoestrogens, and of patients with ER⁺ breast tumors who fail to respond to endocrine intervention therapies are crucial to establish whether xenoestrogens contribute to breast cancer risk and incidence.

Acknowledgements

4427).

References

1. Hunter DJ, Kelsey KT Pesticide residues and breast cancer: the harvest of a silent spring. J Natl Cancer Inst 1993;85:598-9.

2. Coiborn T, Vom Saal FS, Soto AM Developmental effects of endocrine-disrupting chemicals in wildlife and humans. Environ Health Perspect 1993;101:378-384.

3. Rennie J Malignant mimicry. Sci Amer 1993;269:15-16.

4. Sharpe RM, Skakkebaek NF Are estrogens involved in falling sperm counts and disorders of the male reproductive tract? Lancet 1993;341:1392-1395.

5. Sumpter JP, Jobling S Male sexual development in "a sea of oestrogen". Lancet 1993;342:124-125.

6. Davis DL, Bradlow HL, Wolff M, Woodruff T, Hoel DG, Anton-Culver H Medical hypothesis: xenoestrogens as preventable causes of breast cancer. Environ Health Perspect 1993;101:372-377.

7. Stone R Environmental estrogens stir debate. Science 1994;265:308-310.

8. Safe SH Dietary and environmental estrogens and antiestrogens and their possible role in human disease. Environ Sci Pollut Res 1994;1:29-33.

9. Fagin D Estrogen link. Newsday 1994 (28 Dec), A7-A9.

10. Safe SH Environmental and dietary estrogens and human health: is there a problem? Environ Health Perspect 1995;103:346-351.

11. Davidson NE , Lippman ME The role of estrogens in growth regulation of breast cancer. Crit Rev Oncogenesis 1989;1:89-111.

12. Weisz A, Bresciani P Estrogen regulation of proto-oncogene coding for nuclear proteins. Crit Rev. Oncogenesis 1993;4:361-368.

13. Weisz A, Rosales R Identification of an estrogen response element upstream of the human *c-fos* gene that binds the estrogen receptor and the AP-1 transcription factor. Nucleic Acids Res 1990;18:5097-5106.

14. Hyder SM, Stancel GM, Nawaz Z, McDonnell, DP, Loose-Mitchell DS Identification of an estrogen response element in the 3'-flanking region of the murine *c-fos* protooncogene. J Biol Chem 1992;267:18047-54.

15. Dubik D, Shiu RP Mechanism of estrogen activation of *c-myc* oncogene expression. Oncogene 1992;7:1587-94.

16. Cicatiello L, Ambrosino C, Coletta B, Scalona M, Sica V, Bresciani F, Weisz A J Transcriptional activation of *jun* and actin genes by estrogen during mitogenic stimulation of rat uterine cells. Steroid Biochem Mol Biol 1992;41:523-8.

17. Cicatiello L, Sica V, Bresciani F, Weisz A. Identification of a specific pattern of "immediate-early" gene activation induced by estrogen during mitogenic stimulation of rat uterine cells. Receptor 1993;3:17-30.

18. Hyder SM, Nawaz Z, Chiappetta C, Yokoyama K, Stancel GM The proto-oncogene *c-jun* contains an unusual estrogen-inducible enhancer within the coding sequence. J Biol Chem 1995;270:8506-13.

19. Jensen AA Environmental and occupational chemicals. In: Bennet PN, editor. Drugs and

21

Human Lactation. New York: Elsevier Sci Publ, 1988:551-73.

20.   Kutz FW, Wood PH, Bottimore DP Organochlorine pesticides and polychlorinated biphenyls in human adipose tissue. Rev Environ Contam Toxicol 1991;120:1-87.

21.   Wolff MS Occupationally derived chemicals in breast milk. Am J Ind Med 1983;4:259-81.

22.   Mussalo-Rauhamaa H Partitioning and levels of neutral organochlorine compounds in human serum, blood cells, and adipose and liver tissue. Sci Total Environ 1991;103:159-175.

23.   Rogan WJ, Gladen BC, McKinney JD, et al Polychlorinated biphenyls (PCBS) and dichloro-diphenyl dichloroethene (DDE) in human milk: effects of maternal factors and previous lactation. Am J Public Health 1986;76:172-7.

24.   Levine R Recognized and possible effects of pesticides in humans. In: Hayes WJ Jr, Laws ER Jr, editors. Handbook of Pesticide Toxicology, Vol 1, General Principles. San Diego:Academic Press, 1991, 275-360.

25.   Safe S Toxicology, structure-function relationship, and human and environmental health impacts of polychlorinated biphenyls: progress and problems. Environ Health Perspect 1992;100:259-268.

26.   International Agency for Research on Cancer: Overall Evaluations of Carcinogenicity: an Update of IARC Monographs Volumes 1 to 42. Geneva: WHO, 1987, 186-187.

27.   Smith AG Chlorinated hydrocarbon insecticides. In: Hayes WJ Jr. Laws ER Jr, editors. Handbook of Pesticide Toxicology, Vol 2, Classes of Pesticides. San Diego: Academic Press, 1991,731-915.

28.   Welch RM, Levin W, Conney AH Estrogenic action of DDT and its analogs. Toxicol Appl Pharmacol 1969;14:358-367.

29.   Kupfer D, Bulger WH Estrogenic properties of DDT and its analogs. In: McLachlan J, editor. Estrogens in the Environment. New York: Elsevier, 1980,239-263.

30.   Bulger WH, Kupfer D Estrogenic action of DDT analogs. Am J Ind Med 1983;4:163-173.

31.   Scribner JD, Mottet NK DDT acceleration of mammary gland tumors induced in the male Sprague-Dawley rat by 2-acetamidophenanthrene. Carcinogenesis 1981;2:1235-1239.

32.   Robinson AK, Sirbasku DA, Stancel GM DDT supports growth of an estrogen responsive tumor. Toxicol Lett 1985;27:109-113.

33.   Mason RR, Schulte GJ Interaction of o,p'-DDT with the estrogen-binding protein (EBP) of DMBA-induced rat mammary tumors. Res Commun Chem Pathol Pharmacol 1981; 33:119-128.

34.   Kupfer D, Bulger WH Interaction of o,p'-DDT with the estrogen-binding protein (EBP) in human mammary and uterine tumors. Res Commun Chem Pathol Pharmcol 1977;16:451-462.

35.   Soto, AM, Lin TM, Justicia H, Silvia RM, Sonnenscheim C. An "in culture" bioassay to access the estrogenicity of xenobiotics (E. screen). In: Colbom T, Clemens C, editors. Chemically induced alterations in sexual and functional development: the wild-life/human connection. Advances in modern environmental toxicology, Vol. 21. Princeton, NJ:Princeton Scientific Publishing, 1992, 107-112.

36. Miller FR, Soule HD, Tait, L, Pauley RJ, Wolman, SR, Dawson, PJ, Heppner GH Xenograft model of human proliferative breast disease. J Natl Caner Inst 1993;85:1725-1732.

37. Basolo F, Elliott J, Tait L, Chen-XQ, Maloney T, Russo IH, Pauley R, Momiki S, Caamano J, Klein-Szanto AJ, Russo J Transformation of human breast epithelial cells by *c-Ha-ras oncogene*. Mol Carcinogen 1991;4:25-35.

38. Dawson PJ, Wolman SR, Tait L, Heppner GH, Miller, FR MCF10AT: A model for the evolution of cancer from proliferative breast disease. Am J Pathol 1996;148:313-319.

39. Shekhar PVM, Chen, ML, Werdell, J, Heppner, GH, Miller, FR, Christman JK Activation of the endogenous estrogen receptor gene in MCF10AT system cells, a potential factor for neoplastic progression of MCF10AT xenografts. Proc Amer Assoc Cancer Res 1995;36:255.

40. Wiese TE, Kral LG, Dennis KE, Butler WB, Brooks SC Optimization of estrogen growth response in MCF-7 cells. In Vitro Cell Dev Biol 1992;28A:595-602.

41. Green B, Leake RE Steroid Hormones: A practical approach. IRL Press Ltd., Oxford, U.K., 1987.

42. Bradford MM A rapid and sensitive method for the quantitation of microgram quantities of protein utilizing the principle of protein-dye binding. Anal Biochem 1976;72:248-254.

43. VanderKuur JA, Hafner MS, Christman JK, Brooks SC Effects of estradiol-17β analogues on activation of estrogen response element regulated chloramphenicol acetyltransferase expression. Biochemistry 1993:32:7016-7021.

44. Strahle U, , Schmid W, and Schutz G Synergistic action of the glucocorticoid receptor

with transcription factors. EMBO J 1988;7:3389-3395.

45. Graham F, van der Eb A A new technique for the assay of infectivity of human adenovirus 5 DNA. Virology 1973;52:456-467.

46. Gorman CM, Moffat LF, Howard BH Recombinant genome which express chloramphenicol acetyltransferase in mammalian cells. Mol Cell Biol 1982;2:1044-1051.

47. Brown AMC, Jeltsch JM, Roberts M, Chambon P Activation of pS2 gene transcription is a primary response to estrogen in the human breast cancer cell line MCF-7. Proc Natl Acad Sci USA 1984;81:6344-6348.

48. Pilat MJ, Christman JK, Brooks SC Characaterization of the estrogen receptor transfected MCF10A breast cell line 139B6. Breast Cancer Res Treat 1996;37:253-266.

49. Soule HD, Maloney TM, Wolman SR, Peterson WD, Brenz R, McGrath CM, Russo J, Pauley RJ, Jones RF, Brooks SC Isolation and characterization of a spontaneously immortalized human breast epithelial cell line, MCF-10. Cancer Res 1990;50:6075-6086.

50. Masiakowski P, Breathnach R, Bloch J, Gannon F, Krust A, Chambon P Cloning of cDNA sequences of hormone-regulated genes from the MCF-7 human breast cancer cell line. Nucleic Acids Res 1982;10:7895-7903.

51. Nesaretnam K, Corcoran D, Dils RR, Darbre P 3,4,3',4'-Tetrachlorobiphenyl acts as an estrogen *in vitro* and *in vivo*. Mol Endocrin 1996;10: 923-936.

52. Safe SH Do environmental estrogens play a role in development of breast cancer in women and male reproductive problems? Hum Ecol Risk Assess 1995;1:17-23.

53. MacMahon B Pesticide residues and breast cancer? J Natl Cancer Inst 1994;86:572-573.

54. Dewailly E, Dodin S, Verreault R, Ayotte P, Sauve L, Morin J, Brisson J High organochlorine body burden in women with estrogen-receptor positive breast cancer. J Natl Cancer Inst 1994;86:232-234.

55. Krieger N, Wolff MS, Hiatt RA, Rivera M, Vogelman J, Orentreich N Breast cancer and serum organochlorines: a prospective study among white, black, and Asian women. J Natl Cancer Inst 1994;86:589-599.

56. Djordjevic MV, Hoffman D, Fran J, Fan J, Prokopczyk B, Citron ML, *et al* Assessment of chlorinated pesticides and polychlorinated biphenyls in adipose breast tissue using a supercritical fluid extraction method. Carcinogenesis 1994;15:2581-2585.

57. Zava DT, Blen M, Duwe G Estrogenic activity of natural and synthetic estrogens in human breast cancer cells in culture. Environ Health Perspect 1997;105:637-645.

58. Wolff MS, Toniolo PG, Lee EW, Rivera M, Dubin N Blood levels of organochlorine residues and risk of breast cancer. J Natl Cancer Inst 1993;85:648-651.

59. Kanja LW, Skaarc JU, Ojwang SBO and Maitai CK A comparison of organochlorine pesticide residues in maternal adipose tissue, maternal blood, cord blood and human milk from mother/infant pairs. Arch Environ Contam Toxicol 1992;22:21-24.

60. Soto AM, Chung KL, Sonnenschein C The pesticides endosulfan, toxaphene, and dieldrin have estrogenic effects on human estrogen-sensitive cells. Environ Health Perspect 1994;102:380-383.

61. Henderson BE, Ross RK, Pike MC Toward the primary prevention of cancers. Science 1991;254:131-8.

62. Lipworth L Epidemiology of breast cancer. Eur J Cancer Prevention 1995;4:7-30.

63. Miller WR General review: endocrine therapy for breast cancer: biological rationale and current progress. J Steroid Biochem Mol Biol 1990;37: 467-480.

64. Steimetz R, Young PCM, Caperell-Grant A, Gize EA, Madhukar BV, Ben-Jonathan N *et al* Novel estrogen action of the pesticide residue β-hexachlorocyclohexane in human breast cancer cells. Cancer Res 1996;56:5403-9.

Fig. 1. Effects of DDT and PCBs on anchorage independent growth of MCF10AT3c cells. Total number of colonies represent colonies larger than 50 μm in diameter. Colonies were estimated according to their size: small, medium, large and very large: 50-100 μm, 100-200 μm, 200-300 μm and > 300 μm in diameter, respectively. Control wells received additions of vehicle, ethanol or DMSO at final concentration of 0.01%. Since no difference in colony size or numbers were observed between the two vehicles, results are shown under one group. Treatments included E_2 (1 nM or 10 nM), o,p'-DDT (10 μM), p,p'-DDT (10 μM) and Heptachlor (10 μ M). Colony forming efficiency was calculated by dividing the number of colonies larger than 50 μm (sized using a calibrated ocular grid) by the number of cells seeded. Ten microscopic fields were counted to calculate the total number of colonies/well for the whole well, and average of 3 wells for each treatment was calculated. The numbers of colonies in different size ranges [50-100 μm, 100-200 μm, 200-300 μm and >300 μm] was calculated in the same manner. Results are expressed as mean ± S.D. of 3 experiments. Where bars are not seen, deviations were too small for visual display.

Fig.2. Regulation by o,p'-DDT and p,p'-DDT of pS2 mRNA in preneoplastic MCF10AT3c and MCF-7 human breast cancer cells. Total cellular RNA isolated at 96 h from MCF10AT3c (40 μg) and at 24 h from MCF-7 (20 μg) cells following treatment with E_2 (E; 1 nM), o,p'-DDT (op; 10 μM), p,p'-DDT (pp; 10 μM) or mixtures of p,p'-DDT and o,p'-DDT (pp+op; 0.1 μM of each ligand) or p,p'-DDT (0.1 μM) and E_2 (1 nM) were subjected to Northern blot analysis as described in Materials and Methods. ICI 182,780 was added at 100-fold molar excess of E_2 or p,p'-DDT. Blots were probed for expression of pS2, an estrogen-regulated gene, (top row) and

28

for 36B4 mRNA a non-estrogen regulated gene (bottom row) to ensure equal RNA loading. Results were quantitated by densitometric scanning, and the pS2 signals were normalized to 36B4 signals.

Fig. 3. Binding of DDT isomers and PCBs to estrogen receptor from MCF-7 human breast cancer cells.

2 nM 2,4,6,7-[^{3}H]17β-estradiol was incubated with cytosol prepared from MCF-7 cells and the indicated molar excess of DES, o,p'-DDT, p,p'-DDT, Aroclor 1221, Aroclor 1254, Heptachlor (Hep) or dexamethasone (DX) in a single point competitive binding assay as described in Materials and Methods. Among all the xenoestrogens tested, only o,p'-DDT competed with [^{3}H]-estradiol binding to estrogen receptor (p=0.03).

Table **1**. Effect of o,p'-DDT and p,p'-DDT on growth of MCF-7 human breast cancer cells.

Compound (Concentration)	Cell number x 10^{-5} $\pm$ S.E.
None	2.27 ± 0.2
Estradiol (1 nM)	$4.87 \pm 0.2^*$
Estradiol (1 nM) + ICI 182,780 (100 nM)	2.64 ± 0.1
o,p'-DDT (1 μM)	$3.02 \pm 0.5^*$
(10 μM)	$3.79 \pm 0.3^*$
p.p'-DDT (0.01 μM)	$2.75 \pm 0.5^*$
(0.1 μM)	$2.88 \pm 0.5^*$
(1 μM)	$3.90 \pm 0.04^*$
(10 μM)	$6.42 \pm 0.4^*$
p,p'-DDT + o'p-DDT (0.1 μM each)	$6.69 \pm 0.2^*$
p,p'-DDT + o,p'-DDT (1 μM each)	$7.06 \pm 0.2^*$
p,p-DDT + o,p'-DDT (1 μM each) + ICI 182,780 (100 μM)	2.81 ± 0.1

Results obtained from three independent experiments performed in triplicate are expressed as mean $\pm$ S.E. As no differences in cell numbers were observed in control cultures exposed to ethanol or DMSO, results are grouped together. *Indicates doses of compounds that increased cell number significantly over the hormoneless control (p=0.0001). Cumulative effects of mixtures of o,p'-DDT and p,p'-DDT are additive (p=0.01). Co-transfection with pCH110 which expresses β-galactosidase activity at a constant level regardless of estradiol or xenoestrogen concentration confirmed that the results are not due to differences in transfection efficiency or cell viability (data not shown).

Table **2**. Effect of PCBs on estrogen-stimulated growth of MCF-7 human breast cancer cells.

Compound (Concentration)	Cell number x 10^{-5} $\pm$ S.E.
None	1.48 ± 0.2
Estradiol (1 nM)	4.24 ± 0.5*
Estradiol (1 nM) + ICI 182,780 (100 nM)	1.40 ± 0.1
Heptachlor (10 μM)	1.90 ± 0.1*
Aroclor 1221 (10 μM)	2.58 ± 0.3*
Aroclor 1254 (10 μM)	2.21 ± 0.1*
Aroclor 1221 + 1254	
(0.1 μM each)	2.75 ± 0.3
(1 μM each)	2.20 ± 0.2
(10 μM each)	2.84 ± 0.2

Effects of all three PCBs on growth of MCF-7 cells were tested at 1 and 10 μM, however, results at only 10 μM are shown. Results obtained from three independent experiments performed in triplicate are expressed as mean $\pm$ S.E. As no differences in cell numbers were observed in control cultures exposed to ethanol or DMSO, results are grouped together. *Indicates compounds that enhanced cell yields significantly over the hormoneless control cultures (p=0.001). Mixtures of Aroclors 1221 and 1254 did not elicit significant cumulative effects on cell growth at any of the three concentrations tested. Co-transfection with pCH110 which expresses β-galactosidase activity at a constant level regardless of estradiol or xenoestrogen concentration confirmed that the results are not due to differences in transfection efficiency or cell viability (data not shown).

Table **3**. Regulation of CAT gene expression by a mixture of o,p'-DDT and p,p'-DDT, and p,p'-DDT and 17 β-estradiol in ERETKCAT transfected MCF-7 cells.

Compound (Concentration)	% CAT conversion ± S.D.
None	1.9 ± 0.2
Estradiol $(10^{-11}$ M$)$	$6.8 \pm 2.1^*$
$(10^{-10}$ M$)$	$14.3 \pm 3.2^*$
$(10^{-9}$ M$)$	$33.3 \pm 4.6^*$
Estradiol $(10^{-9}$ M$)$ + ICI 182,780 $(10^{-7}$ M$)$	1.4 ± 0.3
o,p'-DDT $(10^{-6}$ M$)$	2.2 ± 0.3
$(10^{-5}$ M$)$	$8.5 \pm 0.7^*$
p.p'-DDT $(10^{-8}$ M$)$	1.2 ± 0.2
$(10^{-7}$ M$)$	$4.5 \pm 0.3^*$
$(10^{-6}$ M$)$	$22.8 \pm 3.0^*$
$(10^{-5}$ M$)$	$35.1 \pm 5.8^*$
p,p'-DDT $(10^{-5}$ M$)$ + ICI 182,780 $(10^{-3}$ M$)$	3.6 ± 0.2
o,p'-DDT + p,p'-DDT $(10^{-7}$ M each$)$	$47.6 \pm 5.7^*$
o,p'-DDT + p,p'-DDT $(10^{-6}$ M each$)$	$50.9 \pm 7.8^*$
o,p-DDT + p,p'-DDT $(10^{-6}$ M each$)$ + ICI 182,780 $(10^{-4}$ M$)$	4.7 ± 0.4
Estradiol $(10^{-11}$M$)$ + p,p'-DDT $(10^{-6}$ M$)$	$50.2 \pm 6.9^*$
Estradiol $(10^{-10}$M$)$ + p,p'-DDT $(10^{-6}$ M$)$	$61.9 \pm 10.6^*$

Results obtained from three independent transfections are expressed as mean $\pm$ S.D. *Indicates doses of compounds that increased CAT expression significantly over the hormoneless control transfections (p=0.0001). CAT expression for mixtures of o,p'-DDT and p,p'-DDT or estradiol and p,p'-DDT were significantly different from CAT expressions observed with the individual compounds using the student t test analysis (p=0.001). Co-transfection with pCH110 which expresses β-galactosidase activity at a constant level regardless of estradiol or xenoestrogen concentration confirmed that the results are not due to differences in transfection efficiency or cell viability (data not shown).

Table **4**. Regulation of CAT gene expression by PCBs from ERETKCAT transfected MCF-7 breast cancer cells.

Compound (Concentration)	% CAT conversion ± S.D.
None	1.7 ± 0.2
Estradiol (1 nM)	$33.3 \pm 5.8^*$
Estradiol (1 nM) + ICI 182,780 (100 nM)	1.0 ± 0.2
Aroclor 1221 (1 µM)	1.5 ± 0.3
(10 µM)	1.2 ± 0.4
Aroclor 1254 (1 µM)	1.3 ± 0.2
(10 µM)	2.9 ± 0.2
Heptachlor (10 µM)	$39.2 \pm 6.8^*$
Heptachlor (10 µM) + Estradiol (1 nM)	22.4 ± 4.5

Results obtained from three independent transfections are expressed as mean $\pm$ S.D. *Indicates compounds that increased CAT expression significantly over the hormoneless control transfections (p=0.0001). Co-transfection with pCH110 which expresses β-galactosidase activity at a constant level regardless of E_2 or xenoestrogen concentration confirmed that the results are not due to differences in transfection efficiency or cell viability (data not shown).

Table **5.** Regulation of CAT gene expression by DDT and PCBs from ERETKCAT transfected MCF10AneoT cells.

Compound (Concentration)	% CAT conversion ± S.D.
None	8.5 ± 2.4
Estradiol (1 nM)	$19.5 \pm 1.3^*$
Estradiol (1 nM) + ICI 182,780 (100 nM)	8.6 ± 1.8
o,p'-DDT (1 µM)	$12.2 \pm 1.2^*$
(10 µM)	$17.4 \pm 1.8^*$
o,p'-DDT (10 µM) + ICI 182,780 (1 mM)	10.9 ± 1.8
p,p'-DDT (1 µM)	$17.1 \pm 4.1^*$
(10 µM)	$27.6 \pm 1.4^*$
p,p'-DDT (10 µM) + ICI 182,780 (1 mM)	9.2 ± 2.3
Aroclor 1221 (1 µM)	11.8 ± 1.2
(10 µM)	$13.2 \pm 2.0^*$
Aroclor 1254 (1 µM)	10.5 ± 2.3
(10 µM)	11.2 ± 3.1
Heptachlor (1 µM)	$23.8 \pm 3.0^*$
(10 µM)	$40.0 \pm 5.4^*$
Heptachlor (10 µM) + ICI 182,780 (1 mM)	13.4 ± 2.2

Results obtained from three independent transfections are expressed as mean ± S.D.
*All compounds, except Aroclor 1254, increased CAT expression significantly over the hormoneless control transfections (p=0.001). Co-transfection with pCH110 which expresses β-galactosidase activity at a constant level regardless of E_2 or xenoestrogen concentration confirmed that the results are not due to differences in transfection efficiency or cell viability (data not shown).
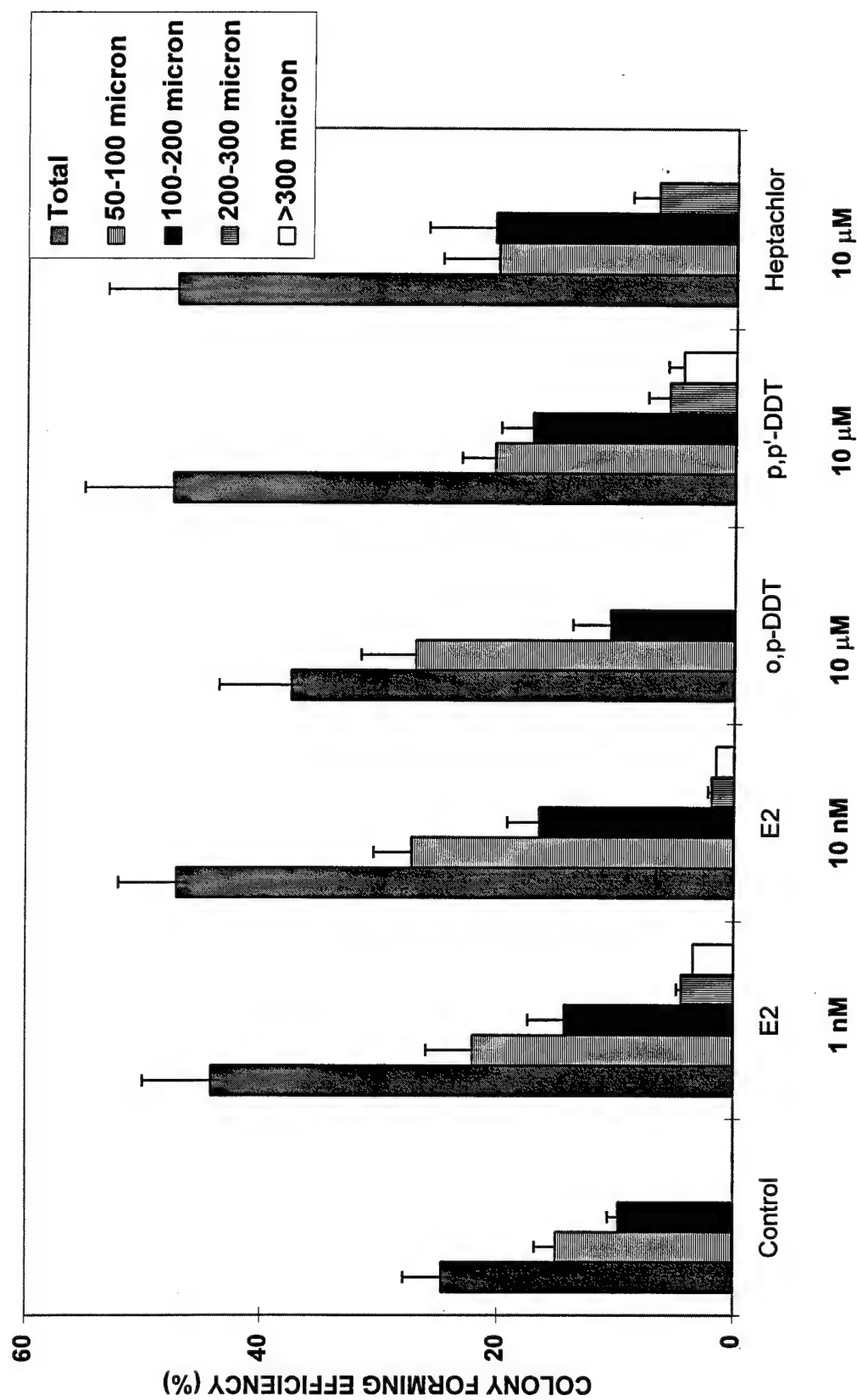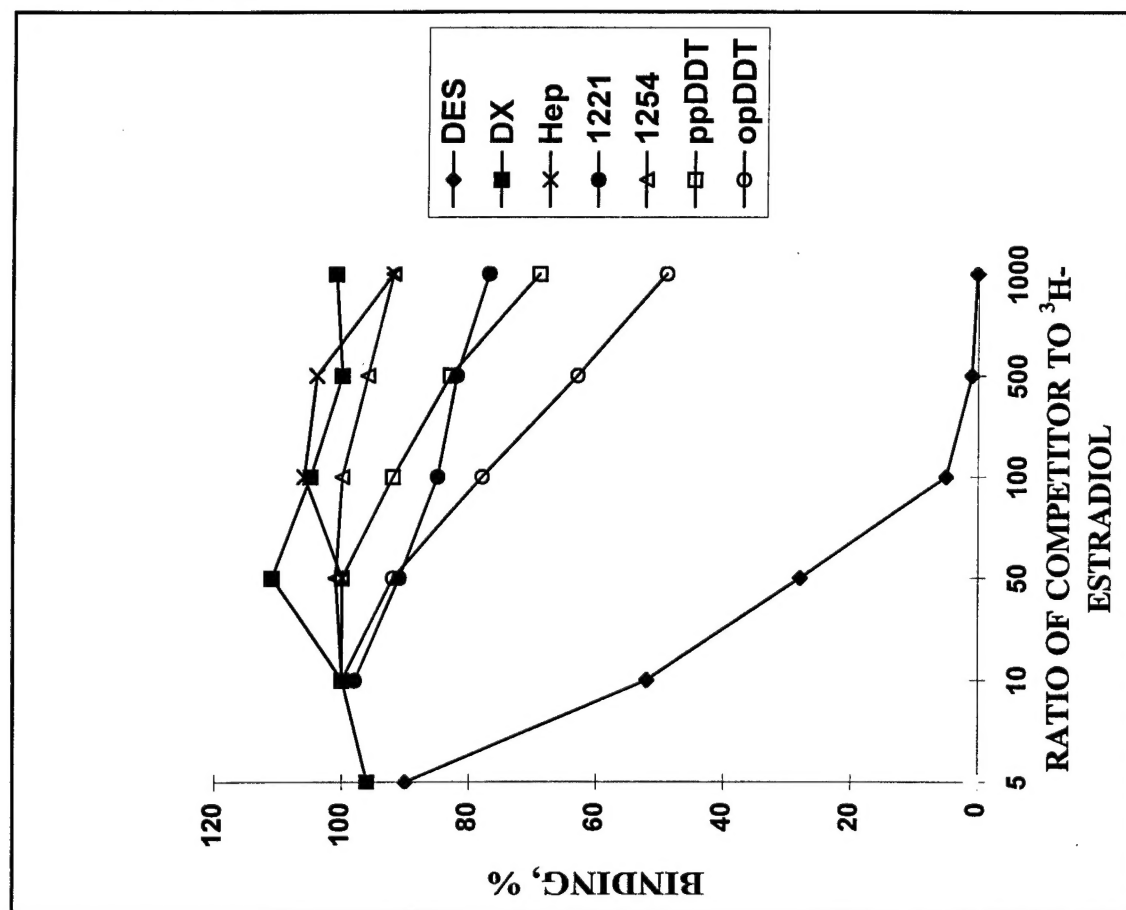
34

Sheet1 Chart 1

Figure 1

Figure 2

September 15, 1997

Barnett S. Kramer, M.D., M.P.H.
Editor-in-Chief
Journal of the National Cancer Institute

Dear Dr. Kramer:

Enclosed are the revised copies of the manuscript entitled "Environmental Estrogen Stimulation of Growth and Estrogen Receptor Function in Preneoplastic and Cancerous Human Breast Cell Lines" by P.V.M. Shekhar, J. Werdell and V.S. Basrur.

Response to reviewers' comments:

Reviewer #1

1. Levels of DDT in serum and breast tissue are now included to indicate the physiologic relevance of the concentrations of xenoestrogens used in *in vitro* assays. (page 18).
2. Information on the relative affinities of DDT and the PCBs used in our assays for the Arylhydrocarbon receptor are not available.
3. ERETKCAT: Abbreviation for this term is expanded on Page 8.
4. We do not have *in vivo* data, but these assays have been planned and will soon be started.
5. Actual numbers showing an increase in breast cancer and exposure to environmental agents are not available.
6. Concentration of organochlorines in serum and breast adipose tissue are included on page 18.
7. Structural similarity: The molecular structures of DDT and PCB compounds tested in our assays are structurally very different from estradiol. Despite their structural diversity these compounds and other xenoestrogens have the capacity at some concentration to bind to ER and initiate or inhibit estrogen-like actions. Recently Cunningham *et al* (Environ Health Perspect, 105:665; 1997) have demonstrated the presence of a lipophilic 2D region in estradiol and some xenoestrogens, that is absent in nonestrogens as well as in phytoestrogens. Cunningham *et al* have suggested that this lipophilic region may affect binding to specific receptors. However, o,p'-DDE was shown to lack this 2D biophore. Other compounds used in our study were not included in their investigation. As the authors of this study point out, this 2D biophore is not expected to provide a unifying principle that accounts for the action of estrogens, although some insight into their mechanism of action may be derived. Due to lack of information on the compounds used in our study, this information has not been included in the text.
8. The positive control used in all our assays is estradiol. p-nonyl phenol, a plasticizer known to be a potent estrogen was also positive in all our assays, but these data are not shown.

110 East Warren Avenue
Detroit, Michigan 48201-1379

(313) 833-0710
(313) 831-8714 Fax

Michigan Cancer Foundation

The Detroit Medical Center

Wayne State University

Meyer L. Prentis
Comprehensive Cancer Center
of Metropolitan Detroit

NCI
CCC

The antiestrogen, ICI 182,780, was always included to test for ERr-mediated specificity. The ability of the compounds to influence transcription of reporter gene from a ERETKCAT vector has been tested in ER-negative line, viz., the parental MCF10A line (page 14).

Results

8. All compounds were tested at 10^{-8}, 10^{-7}, 10^{-6} and 10^{-5}M in our assays. Data at all these concentrations are not shown for PCBs and o,p'-DDT as these compounds did not elicit estrogenic effects over that of control below 10^{-6}M, and some of these compounds evoked a significant effect only at 10^{-5}M.

Discussion

9. Page 18. Although many xenoestrogens are less potent than biological estrogens, and do not produce mammary gland neoplasms in the bioassay rodent models, their ability to promote growth and proliferation of high risk breast epithelial cells has not been investigated. The effects of xenoestrogens on tumor growth must be established *in vivo*, to establish the direct relevance of *in vitro* assays in predicting human disease.

9. An additional reference has been included as suggested (page 19). Factors that influence estrogenicity of compounds measured by transient reporter assays are included on page 18.

Reviewer #2

3. Figs. 1,2,4, 5 and 6 have been reformatted in tabular form, Tables 1-5, for simplicity.

5. All compounds were tested at 10^{-8}, 10^{-7}, 10^{-6} and 10^{-5}M in our assays. Data at all these concentrations are not shown for PCBs and o,p'-DDT as these compounds did not elicit estrogenic effects over that of control below 10^{-6}M, and some of these compounds evoked a significant effect only at 10^{-5}M.

6. Statistical analysis of data are done as suggested.

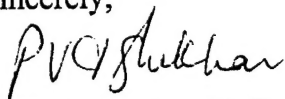7. We do not have animal data, but these assays will soon be started.

Statistical Reviewer

1. Spelling for Heptachlor has been corrected. Corrections for "PCBs are not pesticides" have been made as suggested.

3. Statistical comparisons are added for all of the measured responses (pages 11, 13, 16). With regard to relative binding affinities for ER, our data concur with previous reports in that o,p'-DDT is more than 1000-times less effective than estradiol for binding to ER. Statistical analysis of binding data presented in this manuscript show that the PCBs, Heptachlor, Aroclor1221, and Aroclor 1254, and p,p'-DDT have no affinity or only minimal affinity to compete with estradiol for binding to ER at 1000-fold higher concentrations than estradiol.

4. Statistical analysis of data have been done to evaluate the significance of estrogenic response and to determine whether mixtures of compounds elicit cumulative effects.

5. We have found that the doses of estradiol required to saturate estrogen receptor assays vary from 10^{-9} to 10^{-7}M. Factors that influence receptor concentration include extent of depletion of steroid in the culture media, extent and rate of downregulation of estrogen receptor by estrogen/xenoestrogen, variation in the timing of nuclear ER accumulation, alterations in steroid metabolism caused by estrogen/xenoestrogen, cumulative effects of

estrogen/xenoestrogen mixtures on any of these steps, etc. One or more of these factors may explain the lack of dose dependent response of estradiol or mixtures of DDT isomers at the concentrations used in our assays.

7. Probable reasons that may account for disparate results on estrogenicity of various compounds are included on page 18.

8. Reference summarizing results from Soto et al is included as suggested (Ref. #60, page 26).

9. The abbreviation for ERE is defined on page 8.

Sincerely,

P.V.M. Shekhar, Ph.D.
Breast Cancer Program and
Department of Pathology
Karmanos Cancer Institute
Wayne State University
Detroit, MI 48201

Tel: (313) 833-0715, Ex. 2326
Fax: (313) 831-7518
E mail: shekharm@kci.wayne.edu